(12) INTERNATIONAL APPLICATION PUBLISHED UNDER THE PATENT COOPERATION TREATY (PCT)

(19) World Intellectual Property Organization
International Bureau

(43) International Publication Date
06 August 2020 (06.08.2020)

WIPO | PCT

(10) International Publication Number
WO 2020/159441 A1

(51) International Patent Classification:
C07D 213/56 (2006.01) *A61K 38/05* (2006.01)
C07K 5/06 (2006.01) *A61K 38/06* (2006.01)
C07K 5/08 (2006.01) *A61P 35/00* (2006.01)
A61K 31/4402 (2006.01)

(21) International Application Number:
PCT/SG2020/050040

(22) International Filing Date:
29 January 2020 (29.01.2020)

(25) Filing Language: English

(26) Publication Language: English

(30) Priority Data:
10201900927V 31 January 2019 (31.01.2019) SG

(71) Applicant: **AGENCY FOR SCIENCE, TECHNOLOGY AND RESEARCH** [SG/SG]; 1 Fusionopolis Way, #20-10, Connexis North Tower, Singapore 138632 (SG).

(72) Inventors: **ZENG, Huaqiang**; c/o Institute of Bioengineering and Nanotechnology, 31 Biopolis Way, Singapore 138669 (SG). **ZENG, Fei**; c/o Institute of Bioengineering and Nanotechnology, 31 Biopolis Way, Singapore 138669 (SG).

(74) Agent: **DAVIES COLLISON CAVE ASIA PTE. LTD.**; 10 Collyer Quay #07-01, Ocean Financial Centre, Singapore 049315 (SG).

(81) Designated States *(unless otherwise indicated, for every kind of national protection available)*: AE, AG, AL, AM, AO, AT, AU, AZ, BA, BB, BG, BH, BN, BR, BW, BY, BZ, CA, CH, CL, CN, CO, CR, CU, CZ, DE, DJ, DK, DM, DO, DZ, EC, EE, EG, ES, FI, GB, GD, GE, GH, GM, GT, HN, HR, HU, ID, IL, IN, IR, IS, JO, JP, KE, KG, KH, KN, KP, KR, KW, KZ, LA, LC, LK, LR, LS, LU, LY, MA, MD, ME, MG, MK, MN, MW, MX, MY, MZ, NA, NG, NI, NO, NZ, OM, PA, PE, PG, PH, PL, PT, QA, RO, RS, RU, RW, SA, SC, SD, SE, SG, SK, SL, ST, SV, SY, TH, TJ, TM, TN, TR, TT, TZ, UA, UG, US, UZ, VC, VN, WS, ZA, ZM, ZW.

(84) Designated States *(unless otherwise indicated, for every kind of regional protection available)*: ARIPO (BW, GH, GM, KE, LR, LS, MW, MZ, NA, RW, SD, SL, ST, SZ, TZ, UG, ZM, ZW), Eurasian (AM, AZ, BY, KG, KZ, RU, TJ, TM), European (AL, AT, BE, BG, CH, CY, CZ, DE, DK, EE, ES, FI, FR, GB, GR, HR, HU, IE, IS, IT, LT, LU, LV, MC, MK, MT, NL, NO, PL, PT, RO, RS, SE, SI, SK, SM, TR), OAPI (BF, BJ, CF, CG, CI, CM, GA, GN, GQ, GW, KM, ML, MR, NE, SN, TD, TG).

Declarations under Rule 4.17:
— *of inventorship (Rule 4.17(iv))*

Published:
— *with international search report (Art. 21(3))*
— *in black and white; the international application as filed contained color or greyscale and is available for download from PATENTSCOPE*

(54) **Title:** COMPOUNDS FOR USE AS PROTON CHANNELS AND METHODS THEREOF

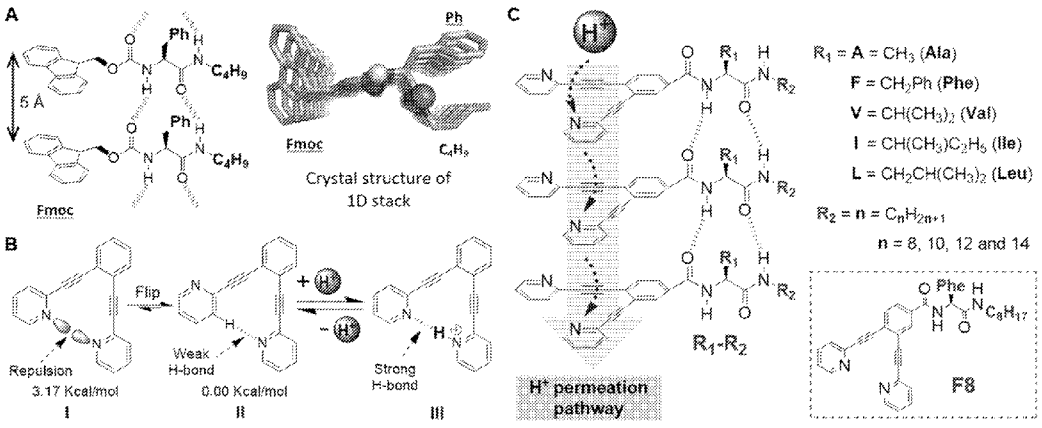

Figure 1

(57) **Abstract:** The present disclosure relates generally to compounds or a salt, solvate, stereoisomer and prodrug thereof for forming synthetic membrane channels. The present disclosure also relates to methods of synthesizing the compounds, methods of forming the synthetic membrane channels and methods of use thereof. In particular, the synthetic membrane channels are synthetic proton channels in a lipid membrane.

WO 2020/159441 A1

COMPOUNDS FOR USE AS PROTON CHANNELS AND METHODS THEREOF

FIELD

The present disclosure relates generally to compounds for forming synthetic membrane channels. The present disclosure also relates to methods of synthesizing the compounds and methods of forming the synthetic membrane channels.

BACKGROUND

Rapidly dividing cancer cells derive their main source of energy from glycolysis, a metabolic process that generates large quantities of unwanted protons in the form of lactic acid. Subsequent proton expulsion results in a significant transmembrane proton gradient between cytosolic and extracellular environments (pH_i and pH_e, respectively) in tumor cells, but not in blood and normal tissue cells. In tumor cells, pH_e mostly ranges from 6.5 to 6.8 and could reach as low as 6.1, with pHi maintained at around a physiological pH of 7.4.

This asymmetric living environment in tumor cells has been used in various anticancer strategies. By far the most widely utilization of the acidic tumor pH_e in cancer treatment is in designing advanced tumor-specific delivery techniques. While neutralizing the more acidic extracellular environment using bicarbonate or disrupting transmembrane pH control by inhibiting cellular proton-regulating mechanisms have been suggested as potential therapeutic strategies for cancer intervention, these two approaches have been met with limited success. On the one hand, oral bicarbonate administration does inhibit spontaneous tumor metastases but exerts no predictable effect on primary tumor growth and may result in metabolic alkalosis. On the other hand, there exist many evolved mechanisms for regulating pH_i/pH_e under conditions of acid over-loading via the use of carbonic anhydrases, vacuolar ATPases, monocarboxylate transporters, Na^+/H^+ exchangers and HCO^{3-}/Cl^- exchangers, each undesirably having many different isoforms and expression levels that depend on cancer types. This suggests that inhibiting the function of any single or a few of these proton-sequestering proteins may not lead to preferred anticancer outcomes with wide applicability in cancers having high genetic heterogeneity. Similar to other types of chemotherapy agents, rapid development of drug resistance among cancer cells to these inhibitors are also inevitable.

Since the first report of synthetic ion channel by Tabushi in 1982, artificially created membrane transporters over the past four decades are predominantly designed for transporting inorganic cations or anions, with much less on molecular species such as water, amino acids, and glucose. As for proton transport, an interesting strategy by nature utilizes fatty acids as proton ionophores via a flip-flop mechanism, a process that can be boosted by carboxylate-stabilizing molecules. Recently, a photo-responsive proton carrier derived from boronic acid was reported for regulating transmembrane proton transfer kinetics. Other representative proton carriers include 2,4-dinitrophenol, niclosamide and FCCP.

Despite availability of diverse proton carriers, synthetic proton channels with high selectivity still remain unexplored and also challenging to develop at present. In fact, all known channels capable of proton conduction also transport water or ions. To be more precise or somewhat awkward, proton conduction often is the "by-product" of synthetic channels designed for water or ion transport. This is in sharp contrast to high selectivity seen in the homotetrameric influenza Matrix-2 (M2) proton channel, shuttling protons, not ions (Na^+ and K^+) and even water molecules, through the channel. The permeability of M2 channel to protons vs Na^+ or K^+ ions was determined to be 10.

Accordingly, there is a need to develop synthetic proton-selective channels which are desirable in bio-medical applications, for example by targeting the asymmetric living environment in tumor cells as an anti-cancer therapy.

SUMMARY OF THE INVENTION

The present invention discloses a compound of Formula (I), or a salt, solvate, stereoisomer and prodrug thereof for forming a proton channel in a lipid membrane:

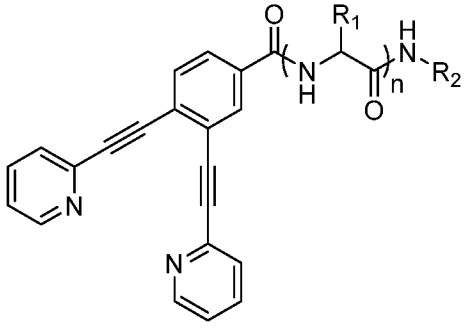

(I)

wherein R_1 is optionally substituted alkyl, optionally substituted alkenyl or optionally substituted alkynyl, optionally substituted arylalkyl, optionally substituted heteroarylalkyl, optionally substituted aryl, optionally substituted heteroaryl;

R_2 is an optionally substituted alkyl, optionally substituted alkenyl or optionally substituted alkynyl; and

n is an integer selected from 1 to 5.

In some embodiments, R_1 is optionally substituted alkyl, optionally substituted arylalkyl or optionally substituted heteroarylalkyl.

In some embodiments, R_2 is optionally substituted C_5-C_{18} alkyl.

In some embodiments, n is 1.

In some embodiment, the compounds of Formula (I) are selected from:

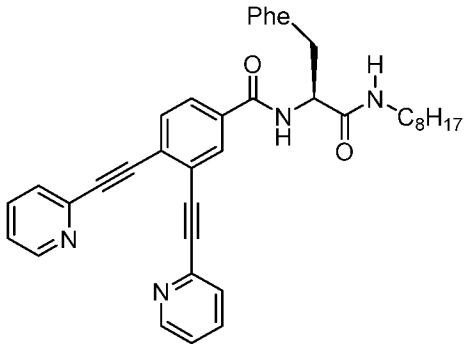

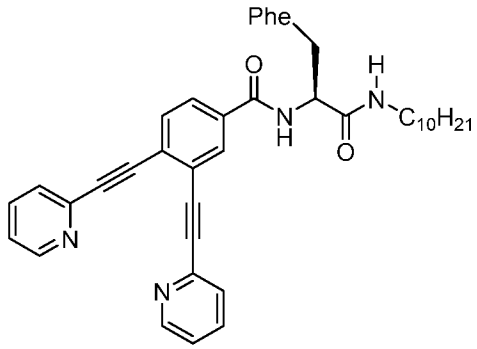

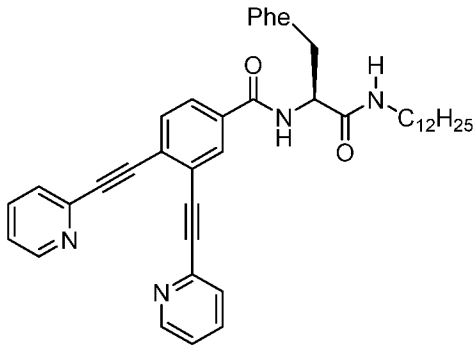

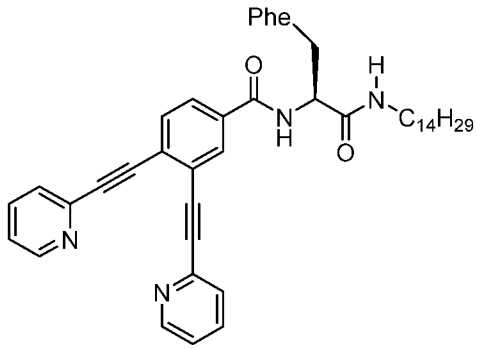

The present invention also discloses an assembly of two or more compounds of Formula (I) or a salt, solvate, stereoisomer and prodrug thereof, wherein the assembly of compounds is capable of forming a proton channel in a lipid membrane.

In some embodiments, the assembly comprises at least 6 compounds of Formula (I).

The present invention also discloses a combination comprising:

a) a lipid membrane; and

b) an assembly of two or more compounds of Formula (I) or a salt, solvate, stereoisomer and prodrug thereof;

wherein the assembly of compounds is capable of forming a proton channel in the lipid membrane.

In some embodiment, the lipid membrane is a phospholipid bilayer.

The present invention also discloses a method of forming a proton channel in a lipid membrane, including the step of contacting the lipid membrane with two or more compounds of Formula (I) or a salt, solvate, stereoisomer and prodrug thereof.

The present invention also discloses a method of modulating a flow of protons through a lipid membrane, including the steps of:

a) providing a proton channel, the proton channel comprising an assembly of two or more compounds of Formula (I) or a salt, solvate, stereoisomer and prodrug thereof; and

b) imposing a proton gradient or membrane potential across the lipid membrane.

The present invention also discloses a pharmaceutical composition comprising an effective amount of a compound of Formula (I) or a pharmaceutically acceptable salt, solvate or prodrug thereof.

The present invention also discloses a method of treating cancer, comprising administering a therapeutically effective amount of compound of Formula (I) or a pharmaceutically acceptable salt, solvate or prodrug thereof to a subject in need, for a sufficient time and under conditions to treat the subject.

The present invention also discloses a compound of Formula (I) or a pharmaceutically acceptable salt, solvate or prodrug thereof for use as a medicament in treating cancer in a subject in need thereof.

The present invention also discloses a use of a therapeutically effective amount of a compound of Formula (I) or a pharmaceutically acceptable salt, solvate or prodrug thereof in the manufacture of a medicament for treating cancer in a subject in need thereof.

In some embodiments, the cancer is selected from breast cancer, cervix adenocarcinoma, colorectal carcinoma, epidermoid carcinoma, glioblastoma, hepatocellular carcinoma, kidney carcinoma, lung cancer, neuroblastoma, ovarian carcinoma, prostate carcinoma, prostate adenocarcinoma, renal cell adenocarcinoma and small cell lung carcinoma.

BRIEF DESCRIPTION OF THE DRAWINGS

Some embodiments of the present invention will now be described by way of non-limiting example only, with reference to the accompanying drawings in which:

Figure 1 illustrates the molecular design of compound of Formula (I) and the proton permeation pathway;

Figure 2 illustrates LUV-based lipid bilayer experiments for elucidating proton transport activity and selectivity;

Figure 3 illustrates the evaluation of *in vivo* anticancer efficacy, systemic toxicity and hemolytic activities of an example of compound of Formula (I) (F8);

Figure 4 illustrates a computationally optimized packing arrangement of an example of compound of Formula (I) (F8) and a proton transport plot;

Figure 5 illustrates a proton transport curve of examples of compound of Formula (I) compared to comparator (sF8);

Figure 6 illustrates ^{1}H NMR-based determination of pKa values of F8 (DMSO-d_6 at room temperature);

Figure 7 illustrates a proton transport curve of example of compound of Formula (I) compared to comparator (F8-ester);

Figure 8 illustrates EC_{50} determination for compounds of Formula (I) in the absence of cholesterol;

Figure 9 illustrates molecular dynamics simulation results of F8 in POPC (1-palmitoyl-2-oleoyl-glycero-3-phosphocholine) membrane;

Figure 10 illustrates EC_{50} determination for gramicidin A (gA);

Figure 11 illustrates EC_{50} determination for compounds of Formula (I) using cholesterol-containing LUVs;

Figure 12 illustrates ion transport curves for gA and F14 at different conditions; and

Figure 13 illustrates a LUV-based assay for determining proton transport selectivity.

DETAILED DESCRIPTION

"Alkyl" refers to monovalent alkyl groups which may be straight chained or branched and preferably have from 1 to 10 carbon atoms or more preferably 1 to 6 carbon atoms. Examples of such alkyl groups include methyl, ethyl, *n*-propyl, *iso*-propyl, *n*-butyl, *iso*-butyl, *n*-hexyl, and the like.

"Alkenyl" refers to a monovalent alkenyl group which may be straight chained or branched and preferably have from 2 to 10 carbon atoms and more preferably 2 to 6 carbon atoms and have at least 1 and preferably from 1-2, carbon to carbon, double bonds. Examples include ethenyl (-$CH{=}CH_2$), *n*-propenyl (-$CH_2CH{=}CH_2$), *iso*-propenyl (-$C(CH_3){=}CH_2$), but-2-enyl (-$CH_2CH{=}CHCH_3$), and the like.

"Alkynyl" refers to alkynyl groups preferably having from 2 to 10 carbon atoms and more preferably 2 to 6 carbon atoms and having at least 1, and preferably from 1-2, carbon to carbon, triple bonds. Examples of alkynyl groups include ethynyl (-C≡CH), propargyl (-$CH_2C{\equiv}$ CH), pent-2-ynyl (-$CH_2C{\equiv}CCH_2$-CH_3), and the like.

"Aryl" refers to an unsaturated aromatic carbocyclic group having a single ring (eg. phenyl) or multiple condensed rings (eg. naphthyl or anthryl), preferably having from 6 to 14 carbon atoms. Examples of aryl groups include phenyl, naphthyl and the like.

"Heteroaryl" refers to a monovalent aromatic heterocyclic group which fulfils the Hückel criteria for aromaticity (ie. contains $4n + 2\ \pi$ electrons) and preferably has from 2 to 10 carbon atoms and 1 to 4 heteroatoms selected from oxygen, nitrogen, selenium, and sulfur within the ring (and includes oxides of sulfur, selenium and nitrogen). Such heteroaryl groups can

have a single ring (eg. pyridyl, pyrrolyl or N-oxides thereof or furyl) or multiple condensed rings (eg. indolizinyl, benzoimidazolyl, coumarinyl, quinolinyl, isoquinolinyl or benzothienyl).

Examples of heteroaryl groups include, but are not limited to, oxazole, pyrrole, imidazole, pyrazole, pyridine, pyrazine, pyrimidine, pyridazine, indolizine, isoindole, indole, indazole, purine, isoquinoline, quinoline, phthalazine, naphthylpyridine, quinoxaline, quinazoline, cinnoline, pteridine, carbazole, carboline, phenanthridine, acridine, phenanthroline, isothiazole, phenazine, isoxazole, isothiazole, phenoxazine, phenothiazine, thiazole, thiadiazoles, oxadiazole, oxatriazole, tetrazole, thiophene, benzo[b]thiophene, triazole, imidazopyridine and the like.

'Arylalkyl' refers to an alkyl group wherein the alkyl group is substituted by one or more aryl group as described above. The terms "heteroarylalkyl" is likewise defined.

In this specification "optionally substituted" is taken to mean that a group may or may not be further substituted or fused (so as to form a condensed polycyclic group) with one or more groups selected from hydroxyl, acyl, alkyl, alkoxy, alkenyl, alkenyloxy, alkynyl, alkynyloxy, amino, aminoacyl, thio, arylalkyl, arylalkoxy, aryl, aryloxy, carboxyl, acylamino, cyano, halogen, nitro, phosphono, sulfo, phosphorylamino, phosphinyl, heteroaryl, heteroarylalkyl, heteroaryloxy, heterocyclyl, heterocyclylalkyl, heterocyclyloxy, oxyacyl, oxime, oxime ether, hydrazone, oxyacylamino, oxysulfonylamino, aminoacyloxy, trihalomethyl, trialkylsilyl, pentafluoroethyl, trifluoromethoxy, difluoromethoxy, trifluoromethanethio, trifluoroethenyl, mono- and di-alkylamino, mono-and di-(substituted alkyl)amino, mono- and di-arylamino, mono- and di-heteroarylamino, mono- and di-heterocyclyl amino, and unsymmetric di-substituted amines having different substituents selected from alkyl, aryl, heteroaryl and heterocyclyl, and the like, and may also include a bond to a solid support material, (for example, substituted onto a polymer resin). For instance, an "optionally substituted amino" group may include amino acid and peptide residues.

By leveraging on the specific difference (i.e. transmembrane proton gradient) between cancer and normal cells, and the greater need for proton-overproducing cancer cells to expel cytosolic protons than normal cells, the inventors have found an alternative anticancer strategy based on a

unique class of compounds for forming synthetic proton channels with high activity and selectivity in promoting transmembrane proton flux. As is demonstrated herein, compounds of Formula (I) form proton channels which exhibit not only pH-dependent broad-spectrum *in vitro* anticancer activities with IC_{50} values of 2.22 – 10.28 μM against at least 20 types of cancer cell lines, but also *in vivo* efficacy with > 60% tumor volume reduction at a dose of 40 mg/kg of body weight. These potent *in vitro* and *in vivo* anticancer activities establish synthetic proton channels as an exciting and innovative cancer intervention strategy that can be broadly applied to kill various cancers, while limiting the potential for drug resistance.

Without wanting to be bound by theory, assisted further by the chloride concentration gradient across membrane, it is hypothesized that these proton channels may attain effective and general cancer killing by blocking proton efflux from the cytosolic region, or pumping protons from the more acidic extracellular environment back to the cytosolic region, or simply disrupting the cytosolic pH homeostasis. Accordingly, this proton channel-based therapeutics is applicable to anticancer treatment. Furthermore, since (1) these proton channels rely on the hydrophobic effect to localize and function in the hydrophobic membrane region with their self-assembled channel length spontaneously adjustable to match the membrane's hydrophobic thickness and (2) the cytoplasmic membrane is less mutable than DNAs/proteins, development of drug resistance through membrane mutation or efflux pumps to these membrane-targeting channel agents would be limited.

Accordingly, the present invention discloses a compound of Formula (I) or a salt, solvate, stereoisomer or prodrug thereof for forming a proton channel in a lipid membrane:

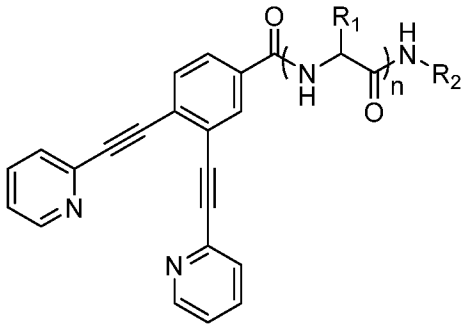

(I)

wherein R_1 is optionally substituted alkyl, optionally substituted alkenyl, optionally substituted alkynyl, optionally substituted arylalkyl, optionally substituted heteroarylalkyl, optionally substituted aryl or optionally substituted heteroaryl;

R_2 is an optionally substituted alkyl, optionally substituted alkenyl or optionally substituted alkynyl; and
n is an integer selected from 1 to 5.

In some embodiments, R_1 is optionally substituted alkyl, optionally substituted alkenyl, optionally substituted alkynyl, optionally substituted arylalkyl or optionally substituted heteroarylalkyl. In other embodiments, R_1 is optionally substituted alkyl, optionally substituted arylalkyl or optionally substituted heteroarylalkyl. In other embodiments, R_1 is optionally substituted C_1-C_6 alkyl, optionally substituted aryl(C_1-C_4)alkyl or optionally substituted heteroaryl(C_1-C_4)alkyl. In other embodiments, R_1 is C_1-C_6 alkyl, aryl(C_1-C_4)alkyl or heteroaryl(C_1-C_4)alkyl. In other embodiments, R_1 is selected from methyl, ethyl, propyl, iso-propyl, butyl, iso-butyl, tert-butyl, n-butyl, sec-butyl, phenylmethyl, phenylethyl or phenylpropyl.

In some embodiments, R_2 is an optionally substituted alkyl or optionally substituted alkenyl. In other embodiments, R_2 is an optionally substituted alkyl. In other embodiments, R_2 is optionally substituted C_5-C_{18} alkyl, optionally substituted C_5-C_{18} alkenyl or optionally substituted C_5-C_{18} alkynyl. In other embodiments, R_2 is optionally substituted C_5-C_{18} alkyl. In other embodiments, R_2 is C_5-C_{18} alkyl. In other embodiments, R_2 is C_6-C_{18} alkyl, C_6-C_{17} alkyl, C_6-C_{16} alkyl, C_6-C_{15} alkyl, C_6-C_{14} alkyl, C_7-C_{18} alkyl, C_7-C_{17} alkyl, C_7-C_{16} alkyl, C_7-C_{15} alkyl, C_7-C_{14} alkyl, C_8-C_{18} alkyl, C_8-C_{17} alkyl, C_8-C_{16} alkyl, C_8-C_{15} alkyl or C_8-C_{14} alkyl.

In some embodiments, n is an integer selected from 1 to 4. In other embodiments, n is an integer selected from 1 to 3. In other embodiments, n is 1.

In some embodiments, when R_2 is optionally substituted C_5-C_{18} alkyl, R_1 is optionally substituted C_1-C_6 alkyl, optionally substituted aryl(C_1-C_4)alkyl or optionally substituted heteroaryl(C_1-C_4)alkyl. In other embodiments, when R_2 is C_5-C_{18} alkyl, R_1 is C_1-C_6 alkyl, aryl(C_1-C_4)alkyl or heteroaryl(C_1-C_4)alkyl. In other embodiments, when R_2 is C_8-C_{14} alkyl, R_1 is selected from methyl, ethyl, propyl, iso-propyl, butyl, iso-butyl, tert-butyl, n-butyl, sec-butyl, phenylmethyl, phenylethyl or phenylpropyl.

Some examples of compound of Formula (I) are as follows:

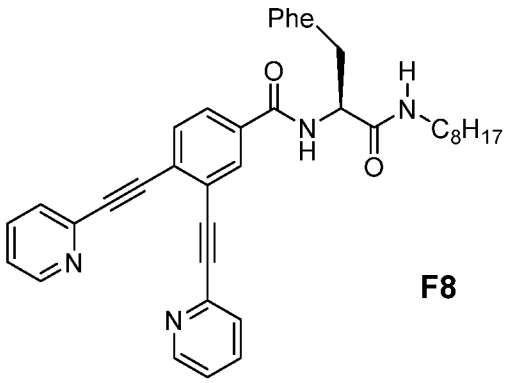

F8

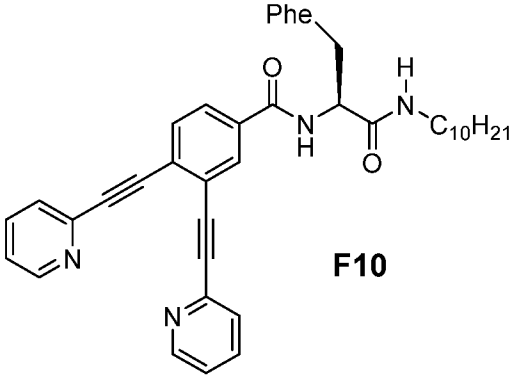

F10

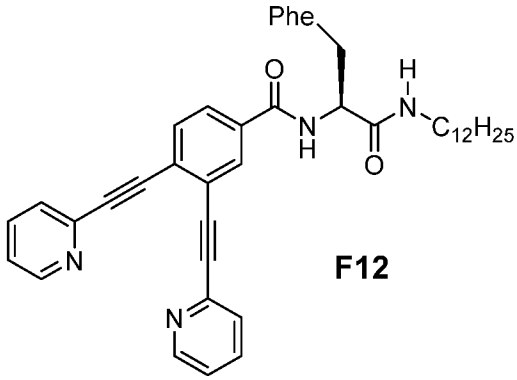

F12

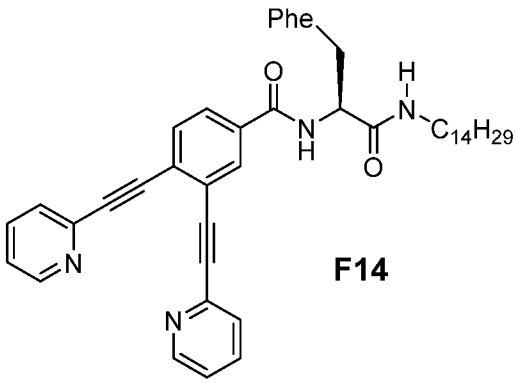

F14

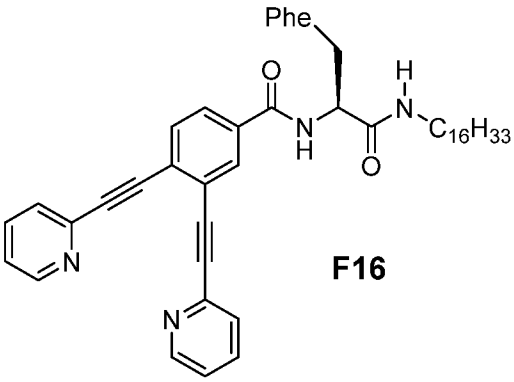

F16

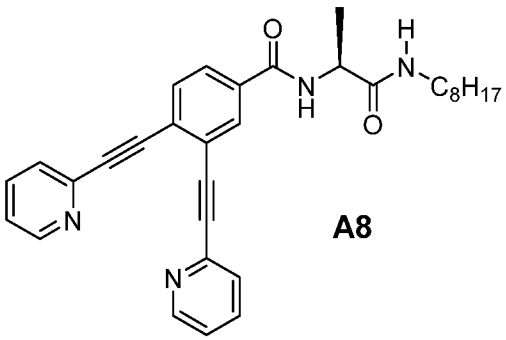

A8

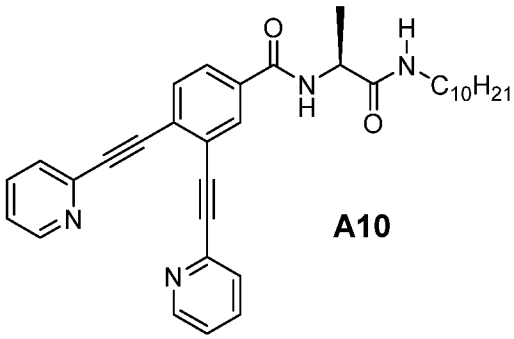

A10

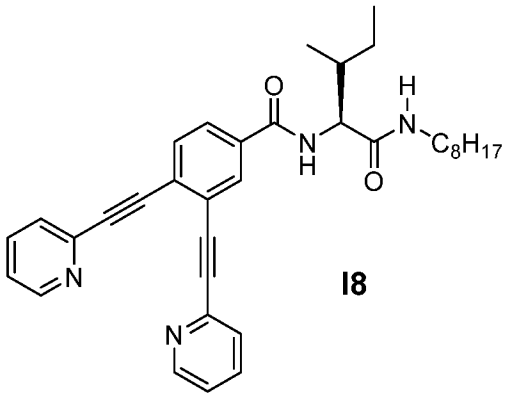

I8

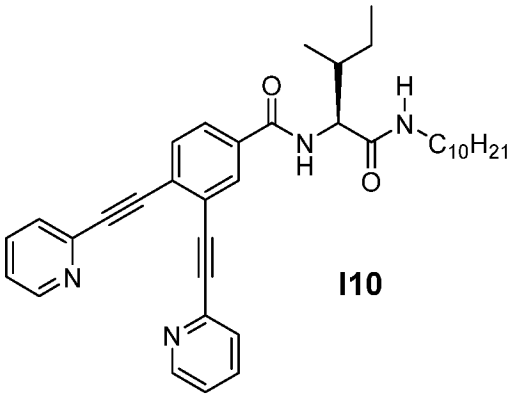

I10

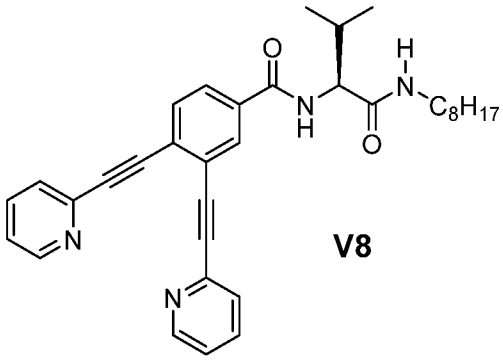

V8

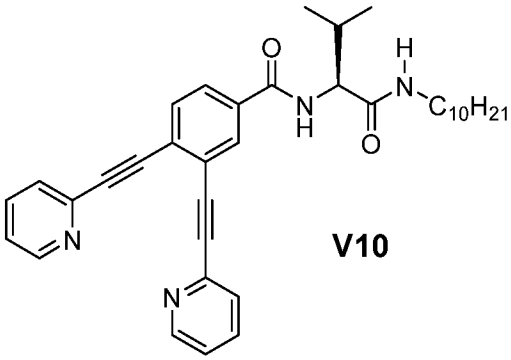

V10

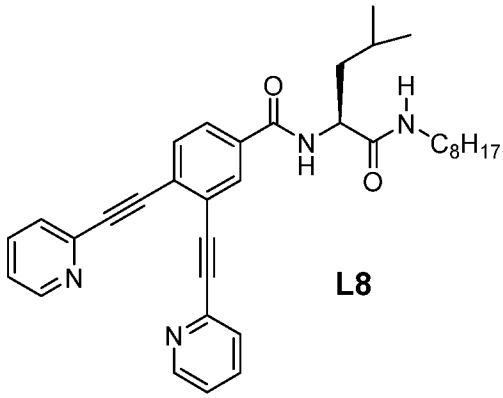

L8

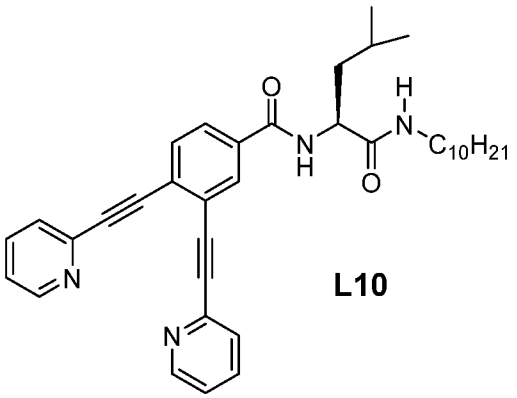

L10

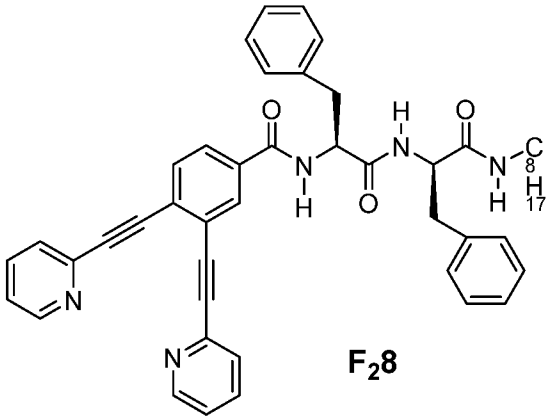

F_28

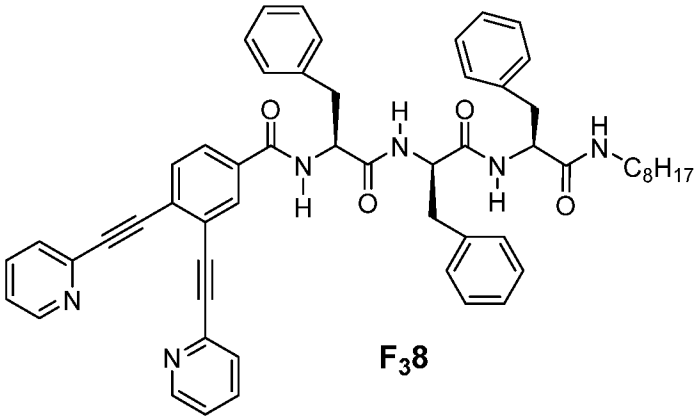

F_38

In some embodiment, the compounds of Formula (I) are selected from:

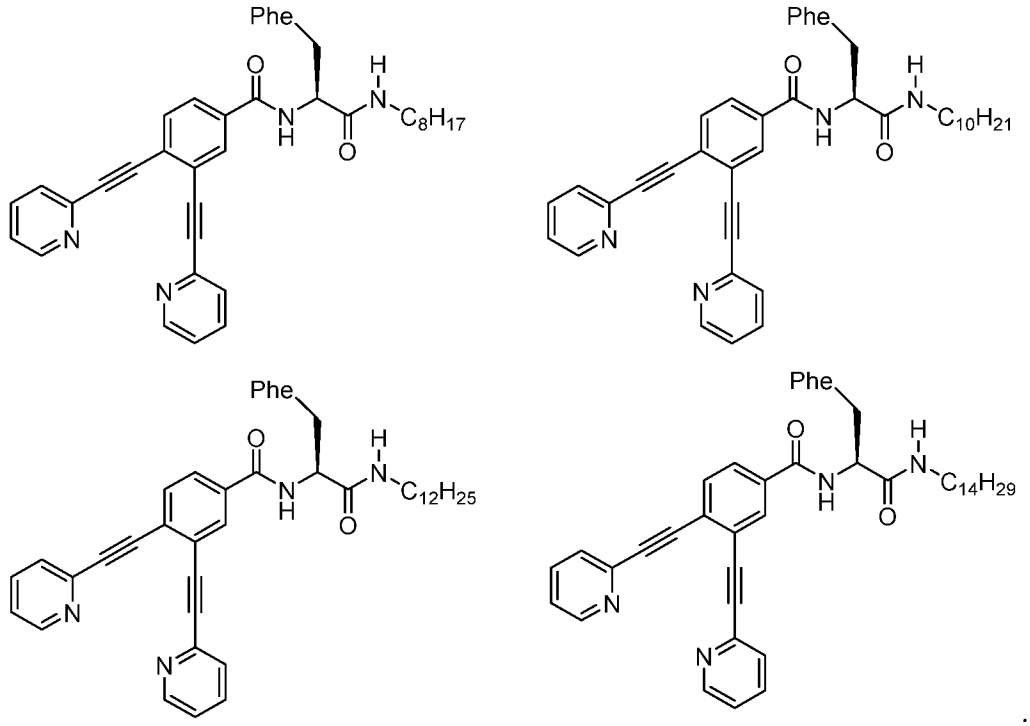

Figure 1 illustrates molecular design of compound of Formula (I) and the proton permeation pathway. (A) Columnar packing in the solid state that induces the same type of side chain to pack at the same side, with an inter-chain separation distance of ~5 Å. (B) A bipyridine-based molecular switch designed for efficient proton binding and releasing. (C) Structures of designed proton channels with diversifications at R_1 and R_2 positions for combinatorial identification of efficient and selective proton channels; a representative structure of channel F8 is also shown. In (C), one-dimensionally aligned bifurcated pyridine motifs serve as the proton permeation pathway for protons to cross the membrane.

Figure 2 illustrates large, unilamellar vesicles (LUV)-based lipid bilayer experiments for elucidating proton transport activity and selectivity. (**A**) Scheme of the HPTS assay, employing pH-sensitive HPTS for evaluating proton transport activities of proton channels. (**B**) Proton transport activities of **F8**, **F12** and **F14** and the corresponding EC_{50} values. (**C**) Insignificant variations in fractional transport activity in the presence of various extravesicular MCl salts suggest **F14** does not transport alkali metal ions M^+ (M = Li, Na, K, Rb and Cs). (**D**) Contrasting performances between gA and **F14** relative to blank in the absence of channels unambiguously confirms Na^+ ions do not permeate through **F14**. (**E**) Chloride-sensitive SPQ assay demonstrates that **F14** is not permeable to Cl^- anions; **IL8** (structure shown in plot) forms a chloride channel.

(**F**) The HPTS assay that points to no or low transport of Ca^{2+} and Mg^{2+} by **F14**. (**G**) Stopped-flow measurements suggest water molecules are not species transportable by **F14**. (**H**) Self-quenching CF-leakage assay indicates that **F14** is not permeable to CF dye and that the observed **F14**-mediated proton transport is not a result of membrane lysis. All fractional transport activities were determined over 5 min at 1.25 μM. $R_{H^+} = (I_{H^+} - I_0)/(I_{Triton} - I_0)$ wherein I_{H^+} and I_0 (background intensity) are the ratiometric values of I_{460}/I_{403} at t = 300 s before addition of triton, and I_{Triton} is the ratiometric value of I_{460}/I_{403} at t = 300 s right after addition of triton. HPTS = 8-hydroxy-pyrene-1,3,6-trisulfonic acid; CF = carboxyfluorescein; gA = gramicidin A.

Without wanting to be bound by theory, the inventors have found that compound Fmoc-Phe-C_4H_9 (Figure 1A) shows a strong tendency of amidated monopeptides to stack together via H-bonds into an orientationally fixed column that aligns the same type of side chains (e.g., **Fmoc**, **Ph** and **C_4H_9**) on the same side. The inventors have postulated that if this ordered structure can be modified to carry one-dimensionally packed proton-binding units, one could readily envision formation of a proton permeation pathway for facilitated selective proton transport across membrane. In designing proton-binding and transporting unit, structural simplicity and binding selectivity are considered two prime factors. To this end, the inventors have tested numerous groups and have found that the structurally simple pyridine group, having pKa of 5.2 and little affinity toward anions, appears to be a reasonably good match. Compared to the physiological pH of 7.4, this pKa value of 5.2 suggests that a pyridine group as a relay station might be able to quickly bind and release protons. To potentially enhance both transport activity and selectivity, a bifurcated scaffold derived from a diethynylbenzene motif for supporting two pyridine groups was designed (Figure 1B). In the absence of a proton, this bifurcated pyridine segment exists almost exclusively in the H-bonded conformation **II** state, which is more stable than **I** by 3.17 kcal/mol and is thus in a locked state. This locked state should prevent the efficient binding of the bifurcated pyridine unit by the biologically relevant cations (Na^+, K^+, Ca^{2+} and Mg^{2+}) and water molecules, not to mention anions such as Cl^-. In the presence of proton, this bi-pyridine segment will switch from conformation **II** to conformation **III**s (Figure 1B), allowing proton binding and subsequent release to the next binding motif. Such proton binding and releasing then continues along the one-dimensionally aligned H^+ permeation pathway lined up by the bifurcated pyridine segments (Figure 1C), eventually enabling proton hopping across membrane.

Advantageously, compounds of Formula (I) can be easily tuned at R_1 and/or R_2 positions for combinatorial optimization of channels' ion transport performance (Figure 1C). For example, a library of 10 channel molecules derived from five amine acids (**A**, **F**, **V**, **I** and **L**) at R_1 position and two straight alkyl chains (n-C_8H_{17} and n-$C_{10}H_{21}$) at R_2 position demonstrated that these compounds can form an assembly linked by H-bonding. Figure 4A presents top and side views of a computationally optimized tripartite ensemble (**F8**)$_3$ with three **F8** molecules all in conformation **II** state and another closely related ensemble (**F8**-p**F8**-**F8**) with the central **F8** protonated by one proton (conformation **III**). Structural comparison of these ensembles indicates a negligible structural perturbation by protonation in generating conformation **III** from **II**. Employing large unilamellar vesicles (LUVs) composed of egg yolk L-α-phosphatidylcholine (EYPC) as a cell membrane model system, the ion transport activities were evaluated using the LUVs containing a membrane-impermeant pH-sensitive fluorescent HPTS dye in the intravesicular region (Figure 2A and Figure 4B). At a final concentration of as low as 1.25 μM, proton channels comprising compounds of Formula (I) display fractional activities of 66 – 101%, presumably resulting from selective transport of protons. For example, channels comprising compounds of Formula (I) containing n-C_8H_{17} (at R_2) have higher transport activities than their corresponding analogs (n-$C_{10}H_{21}$ at R_2).

As is disclosed herein, the moiety at R_1 can contribute to the strength of the H-bond and accordingly influence the transport of proton across the channel. In some embodiments, R_1 is an amino acid side chain. In other embodiments, R_1 is selected from the following:

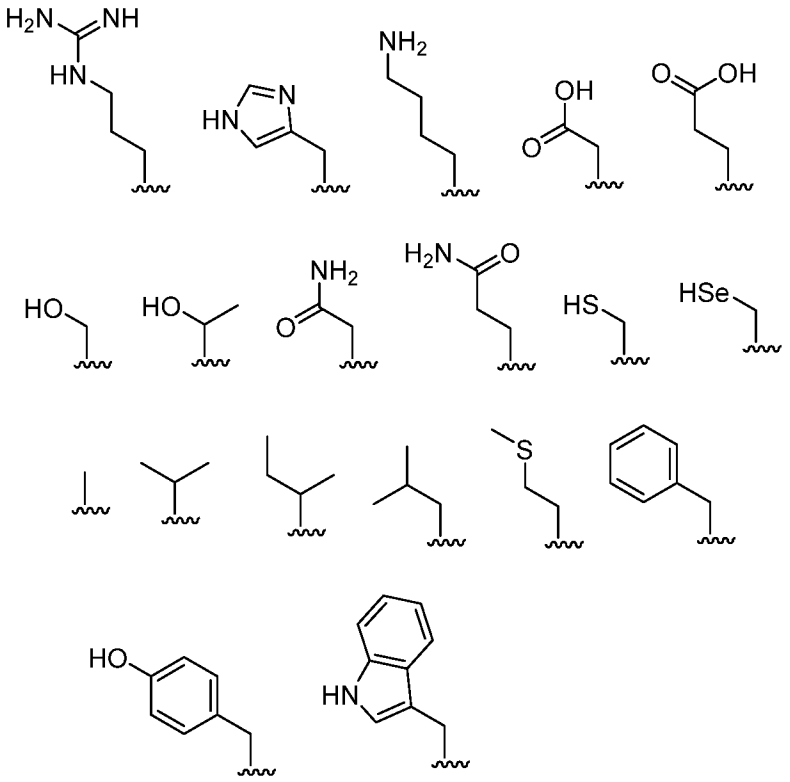

Figure 5 illustrates H^+ transport curves at a channel concentration of 1.25 μM using the HPTS assay, illustrating progressively attenuated transports in the order of **F8** < **sF8** < **F$_2$8** < **F$_3$8**. Compared to a fractional activity of 101% by more acidic **F8** (pKa = 1.59 in DMSO), a much lower activity of 36% by the more basic s**F8** (pKa = 4.19 in DMSO) suggests proton release to be the rate-limiting step in proton transport. That activity decreases with increase in peptidic chain length (101% for **F8**, 27% for **F$_2$8** and 25% for **F$_3$8**) is a clear indication of an important need for ring flipping of the bifurcated pyridin group to change from **II** to **III** for proton binding, and this ring flipping is expected to be more difficult in di/tripeptide-based proton channels with enhanced H-bonding interactions. This also demonstrates that the rate of transfer of proton across the lipid membrane can be controlled by varying n between 1 to 5.

Taking **F8** as an example, the ion transport activities of three closely related structures were examined, i.e., monopeptide s**F8** that carries a single pyridine group, dipeptide **F$_2$8** and tripeptide **F$_3$8** (Figure 5). Compared to a fractional activity of 101% by more acidic **F8** (pKa = 1.59 in DMSO, Figure 6), a much lower activity of 36% by the more basic s**F8** (pKa = 4.19 in DMSO) suggests proton release to be the rate-limiting step in proton transport. That activity decreases with increase in peptidic chain length (101% for **F8**, 27% for **F$_2$8** and 25% for **F$_3$8**) is a clear

indication of an important need for ring flipping of the bifurcated pyridinyl group to change from **II** to **III** for proton binding, and this ring flipping is believed to be more difficult in di/tripeptide-based proton channels with enhanced H-bonding interactions. As a comparator, **F8-ester** was generated by replacing one of the two amide groups of **F8** with an ester group (Figure 7). In Figure 7, ion transport activity of F8 and F8-ester was investigated at a final channel concentration of 1 μM. A huge difference in transport activity (95% for **F8** and 19% for **F8-ester** at 1 μM) confirms the importance of at least two amide bonds in forming stable H-bonded network to link molecules of **F8** into 1D channels for conducting transmembrane proton transport; i.e. n is at least 1.

F10 (96%) performs similar to **F8** (101%) at 1.25 μM; further increases in alkyl chain length leads to considerably boosted transport activity. More specifically, the fractional activities increase in the order of **F8** (88%) < **F12** (95%) < **F14** (101%) at 0.63 μM (Figure 2B). This may be due to the improved affinity for the hydrophobic region of the membrane with increased alkyl chain length (R_2). Using Hill Analysis, the EC_{50} values were determined to be 0.40 μM (**F8**), 0.41 μM (**F10**), 0.22 μM (**F12**), 0.17 μM (**F14**) (Figure 2B and Figure 8). The EC_{50} determination was based on using the ratiometric values of I460/I403 at different concentrations as a function of time. Given an interchain separation distance of 5 Å (Figure 1A) and a hydrophobic thickness of 28 Å for EYPC membrane which is supported by molecular dynamics simulation. In Figure 9, MD-simulated structures of $(\mathbf{F8})_6$ and $(\mathbf{F8})_7$ in POPC (1-palmitoyl-2-oleoyl-glycero-3-phosphocholine) membrane illustrates a better fit into the membrane by $(\mathbf{F8})_6$ than by $(\mathbf{F8})_7$. In $(\mathbf{F8})_7$, the 7th molecule curves up at the end and does not form any H-bond with the 6th molecule. In contrast, In $(\mathbf{F8})_6$, all the six molecules of **F8** form two H-bonds with the neighboring molecules, ordering the bifurcated pyridine groups to the same side to create a transmembrane pathway for facilitated proton conduction across membrane. In this regard, at least six molecules will be needed to form an H-bonded ensemble for fully spanning the hydrophobic membrane region. The EC_{50} value in terms of effective channel concentration for **F14** on a per compound basis therefore is ~28 nM. Compared to EC_{50} value of 2.3 nM (Figure 10) for gramicidin A, which has an estimated conductance of 1.1 x 10^{-17} A at pH 7, the proton-transporting activity of **F14** is estimated to be > 4.4 x 10^{-19} A (> 4% of that of gramicidin A, gA), a value that is comparable to 1.2 x 10^{-18} A for M2 channel. In LUVs containing 33 mol% cholesterol, these proton channels still remain very active, with EC_{50} values of 0.71 μM (**F8**), 2.06 μM (**F10**), 0.72 μM (**F12**), 0.68 μM (**F14**), respectively (Figure 11). The highest activities of 0.17 and 0.68 μM

for **F14** correspond to 0.54 mol% and 1.62 mol% relative to lipid or lipid+cholesterol, respectively.

Accordingly, the present invention also discloses an assembly of two or more compounds of Formula (I) or a salt, solvate, stereoisomer or prodrug thereof, wherein the assembly of compounds is capable of forming a proton channel in a lipid membrane.

In some embodiments, the assembly comprises at least 3, 4, 5, 6, 7 or 8 compounds of Formula (I). In other embodiments, the assembly comprises at least 6 compounds of Formula (I). In other embodiments, based on theoretical calculations of a typical hydrophobic membrane region of about 3.4 nm, the assembly comprises about 6 compounds of Formula (I). The assembly can comprise the same compounds of Formula (I); i.e. all the compounds have the same n, R_1 and R_2, or the assembly can comprise a mixture of compounds; i.e. the compounds have different , R_1 and/or R_2.

In some embodiments, the assembly is formed via H-bonds (hydrogen bonds). The H-bonds can be between amides moieties of adjacent compounds. Depending on the number of amide moieties in compound of Formula (I), the number of H-bonds between the compounds to form the assembly can vary. In this regard, in some embodiments, at least 2 H-bonds are present between 2 compounds of Formula (I). In other embodiments, the assembly is formed via π-π stacking. This can be present, if for example, a phenyl ring is present at R_1. Alternatively, this can be present from the stacking of diethynylbenzenylene moiety of adjacent compounds. In other embodiments, both H-bonds and π-π stacking are present.

As is clear from the disclosure, the proton is transported via the space between the bipyridinyl moieties. Accordingly, the assembly is arranged in a manner such that the bipyrindyl moieties of the at least 2 or more compounds are aligned. In some embodiments, the diethynylbenzenylene moiety of the at least 2 or more compounds are aligned or stacked. In other embodiments, the bipyridinyl moieties are aligned along a single axis. In other embodiments, the space between the bipyridinyl moieties are aligned along a single axis. For example, the bifurcated pyridine groups (bipyridinyl moieties) can be ordered to a same side to create a transmembrane pathway for facilitated proton conduction across membrane (Figure 1C).

In some embodiments, the two or more compounds in the assembly has the same stereochemistry. In other embodiments, the two or more compounds are of a single enantiomeric form. In other embodiments, the two or more compounds are of a S configuration. In other embodiments, the two or more compounds are of a R configuration. In this regard, the skilled person would understand that compounds of Formula (I) with either the R or S configuration can be used. In other embodiments, the two or more compounds are of a single diastereomeric form. Examples of compounds of Formula (I) with chiral centers are shown below:

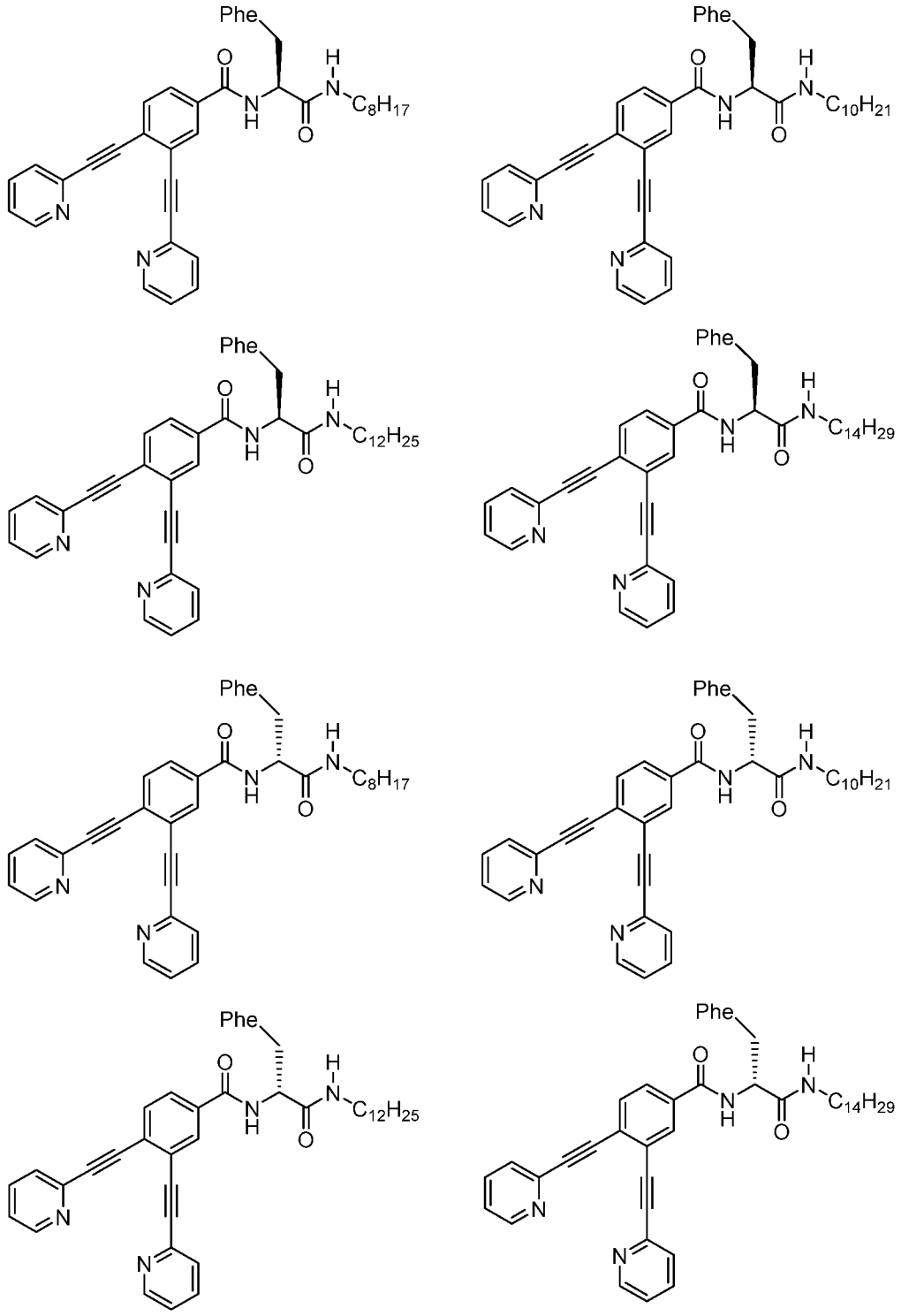

As used herein, 'EC_{50}' refers to the half maximal effective concentration, the concentration of a compound which induces a response halfway between the baseline and maximum after a specified exposure time.

In some embodiments, the assembly has an EC_{50} value of less than 2.5 μM. In other embodiments, the EC_{50} value is less than 2.2 μM, 2.1 μM, 2.0 μM, 1.8 μM, 1.6 μM, 1.4 μM, 1.2 μM, 1.0 μM, 0.9 μM, 0.8 μM, 0.7 μM, 0.6 μM, 0.5 μM, 0.4 μM, 0.3 μM or 0.2 μM.

As is disclosed herein, the anti-cancer effect is not adversely influenced when the compounds of Formula (I) are either provided as molecules or pre-formed as channels. Such channels can be pre-formed in solution or when in contact with a lipid membrane.

The present invention also discloses a combination comprising:

a) a lipid membrane; and

b) an assembly of two or more compounds of Formula (I) or a salt, solvate, stereoisomer or prodrug thereof;

wherein the assembly of compounds of Formula (I) forms a proton channel in the lipid membrane. In this regard, the proton channel is transverse and span across the lipid membrane.

In some embodiments, the lipid membrane is a phospholipid bilayer. In other embodiments, the lipid membrane further comprises cholesterol. In other embodiments, the lipid membrane is a large unilamellar vesicle or a cell membrane. Such lipid membrane can be synthetic or naturally occurring (tissue derived). Such lipids can be obtained, for example, from Avanti Polar Lipids Inc. Examples of phospholipid hydrophilic head groups includes, but not limited to, phosphate (PA), phosphocholine (PC), phosphoethanolamine (PE), phospho-(1'-rac-glycerol) (PG), phospho-(1'-myo-inositol) (PI) and phospho-L-serine (PS).

In some embodiments, the lipid membrane can be small unilamellar vesicles or large unilamellar vesicles. In other embodiments, the lipid membrane is large multilamellar vesicles. In other embodiments, the lipid membrane is a cell membrane.

The present invention also discloses a method of forming a proton channel in a lipid membrane, comprising contacting the lipid membrane with two or more compounds of Formula (I) or a salt, solvate, stereoisomer or prodrug thereof. In this regard, the proton channel is formed in situ at the lipid membrane upon contact. Alternatively, the method can comprise contacting the lipid membrane with the combination as disclosed herein. In this regard, the proton channel may be

pre-formed in the lipid membrane of the combination, and on addition, the lipid membranes can fuse and thereby transfer the proton channel to the lipid membrane of interest.

The observed transport activities in Figures 2A and B may be accounted for by four possible mechanisms, Na^+/H^+ antiport, H^+/Cl^- symport/, OH^-/Cl^- antiport or Na^+/OH^- symport. To discern these pathways, a series of LUV-based bilayer experiments on proton channel **F14** were performed (Figure 2C-F). First, using the HPTS assay shown in Figure 2C, replacement of extravesicular NaCl with MCl ($M^+ = Li^+$, K^+, Rb^+ and Cs^+) leads to no significant differences in transport activity among the five alkali metal ions (Figure 2C). These data suggest either the inability of **F14** to transport alkali metal ions or transport of these ions take place approximately to the same extent. The former conclusion can be unambiguously affirmed by a second set of LUV experiments, with intravesicular region containing HEPES (10 mM) at pH 7 and extravesicular region containing HEPES (10 mM) and M_2SO_4 (200 mM, $M^+ = Li^+$, Na^+, K^+, Rb^+ and Cs^+) at pH 7 (Figure 2D and Figure 12). The LUV contains 1 mM HPTS and is at pH 7.0, while external of the LUV is at 200 mM sulphate salt and pH 7.0. Under such a high ionic concentration gradient, **F14** at 10 μM barely causes any measurable ion transport of alkali ions with respect to the background signals, which is in sharp contrast with the gramicidin (gA) that results in a fractional activity of 110% at a 100-fold lower concentration of 0.1 μM in less than 25 s (Figure 3D; Hemolytic activities of **F8** toward rat red blood cells at concentrations of 0.03 – 60 μM.).

Differing from a highly active chloride channel **IL8** that induces substantial chloride influx into LUVs using a chloride-sensitive SPQ assay, the same assay reveals no chloride influx by **F14** (Figure 2E). Moreover, given that hydration energy of OH^- (460 kJ/mol) is much higher than that of chloride ion (378 kJ/mol) and that no chloride transport by **F14** was observed, it is unlikely for **F14** to bind and transport OH^- across membrane. From these investigations, it can be concluded that **F14**-mediated ion conduction does not occur through OH^-/Cl^- antiport or Na^+/OH^- symport pathways and, if needed, both Na^+ and Cl^- ions could cross membrane to maintain charge neutrality only through passive diffusion, not through proton channel **F14**.

To further differentiate between Na^+/H^+ antiport and H^+/Cl^- symport mechanisms, ion transport was evaluated in the absence of chloride anions with NaCl replaced with Na_2SO_4 (Figure 13). LUV-based assays with both intra- and extra-vesicular regions containing 50 mM Na_2SO_4 was

used for determining proton transport selectivity and possible transport species. Unlike the high activity of 101% by **F14** at 0.63 μM when NaCl was used (Figure 2B), **F14** in the presence of Na_2SO_4 produces very marginal activities of 5% and 8% after background subtraction and normalization at high concentrations of 5 μM and 12 μM, respectively. These comparative activity values clearly rule out any significant role played by Na^+, and support H^+/Cl^- symport pathway as the predominant mechanism, i.e., **F14**-mediated transport of H^+ ions is accompanied by a passive diffusion of Cl^- anions across membrane in order to maintain a charge neutrality of the system.

Another LUV scheme (Figure 2F) was designed with extravascular region containing metal chloride salts to elucidate whether **F14** could promote transport of Ca^{2+} ions as $CaSO_4$ is poorly soluble in water. In this scheme, Ca^{2+} influx will lead to efflux of intravesicular protons or influx of chloride anions in order to maintain charge neutrality, subsequently resulting in increase or no change in fluorescence intensity of HPTS, respectively. In contrary to these expectations, we observed sharply decreased fluorescence intensity by 44% (50 – 6%) for $CaCl_2$. This decrease can only be explained by **F14**-induced highly efficient transport of extravesicular protons into intravesicular region, accompanied by passive diffusion of membrane-permeable chlorides driven by the Cl^- concentration gradient. Even if **F14** can transport Ca^{2+}, this transport must be far slower than proton transport. This statement can be unequivocally proven by more significant decreases of 47% for $MgCl_2$ and 67% for NaCl, both of which cannot be transported by **F14**.

Stopped-flow measurements (a technique used to measure the water permeability of channel molecules) reveal good and no water permeation for gA and **F14** embedded in the lipid membrane at lipid:channel molar ratios of 500:1 and 168:1, respectively (Fig. 2G), demonstrating that **F14** does not transport water molecules either.

Accordingly, in some embodiments, the proton channel is a highly selective proton channel. In this regard, only protons are able to pass through the channel.

The present invention also discloses a method of modulating a flow of protons (hydrogen ions) through a lipid membrane, including the steps of:

a) providing a proton channel, the proton channel comprising an assembly of two or more compounds of Formula (I) or a salt, solvate, stereoisomer or prodrug thereof; and

b) imposing a proton gradient or membrane potential across the lipid membrane.

The proton gradient or membrane potential can be imposed by a pH difference, or can be imposed by a difference in salt content and/or concentration across the lipid membrane. For example, a difference in Cl^- concentration across the lipid membrane can impose a membrane potential such that proton is transported through the proton channel to maintain charge neutrality.

Carboxyfluorescein (CF)-leakage assay (λ_{ex} = 492 nm, λ_{em} = 517 nm, Fig. 2H) was employed to look into whether **F14** impairs the membrane integrity. For this purpose, CF dye was employed. CF dye consists of a mixture of two isomers of ~1 nm in size, with fluorescence mostly self-quenched at a high concentration (500 mM), As such, fluorescence intensity increases when CF molecules trapped inside LUVs get transported into extravesicular region. Results show that addition of **F14** at 10 μM causes only 7% increase in fluorescence, a value that is much lower than 97% increase caused by membrane-lysing melittin at 0.125 μM. These data are consistent with the inability of **F14** to form a pore in the membrane and further confirm that the observed **F14**-mediated proton transport is not a result of membrane lysis. In this regard, membrane integrity is maintained.

Using the CellTiter-Glo® Cell Viability Assay, the expected pH-dependent cancer-killing ability of these highly selective proton channels was verified on HepG2, a human liver cancer cell line. From IC_{50} values presented in Table 1, the anticancer activities of proton channels **F8**, **F10** and **F14** increase with decrease in pH of the cell growth medium. **F8** exhibits IC_{50} values of 4.35 μM and 2.39 μM at pH's of 7.4 and 6.5, respectively, and yet displays no significant cytotoxicity toward red blood cells. These high activities compare very favorably with the broadly effective anticancer agent Cisplatin, having IC_{50} value of 11.36 μM toward the same HepG2 cells (Table 2). If it is assumed that all **F8** molecules associate to form proton-conducting channels, each consisting of six molecules, the IC_{50} value in terms of effective channel concentration is calculated to be 0.40 μM at pH 6.5.

Table 1. IC_{50} values (μM) for Fn (n = 8 – 14) against HepG2 cancer cells at pH_e of 6.5 and 7.4[a]

pH	F8	F10	F12	F14
6.5	2.34 ± 0.29	2.50 ± 0.03	7.79 ± 0.15	22.24 ± 0.70
7.4	4.35 ± 0.01	4.61 ± 0.11	7.76 ± 0.08	54.43 ± 0.93

[a] Before cell viability assay, cancer cells were incubated in the presence of channel molecules at various concentrations in 5% CO_2 at 37°C for 48 h.

Table 2. IC_{50} values (μM) for F8 and Cisplatin toward 20 human cancer cell lines at pH_e of 6.5 and 7.4[a]

Human Cell Line	Human Cell Type	IC50 (μM)		
		F8		Cisplatin
		pH_e = 7.4	pH_e = 6.5	pH_e = 7.4
BT-474	Breast cancer	2.33 ± 0.06	2.47 ± 0.41	4.36 ± 0.11
HeLa	Cervix adenocarcinoma	10.16 ± 0.67	3.46 ± 0.17	15.91 ± 1.46
HCT 116	Colorectal carcinoma	5.60 ± 0.12	5.22 ± 0.14	40.60 ± 0.64
A-431	Epidermoid carcinoma	5.74 ± 0.10	6.03 ± 0.36	8.99 ± 2.46
U-87 MG	Glioblastoma	6.75 ± 0.33	7.46 ± 0.36	23.17 ± 0.81
HEPG2	Hepatocellular carcinoma	4.35 ± 0.89	2.39 ± 0.10	11.36 ± 0.82
HUH 7	Hepatocellular carcinoma	6.00 ± 0.79	5.28 ± 0.70	27.86 ± 1.32
A-498	Kidney carcinoma	4.95 ± 0.06	2.12 ± 0.65	24.50 ± 0.05
A549	Lung cancer cell	5.17 ± 0.09	5.01 ± 0.01	34.22 ± 0.94
SH-SY5Y	Neuroblastoma	5.78 ± 0.23	5.11 ± 0.03	5.18 ± 0.52
A2780	Ovarian carcinoma	6.19 ± 0.51	1.59 ± 0.02	34.93 ± 0.87
PC-3	Prostate adenocarcinoma	10.28 ± 1.05	5.80 ± 0.41	15.23 ± 0.86
DU 145	Prostate carcinoma	6.35 ± 1.12	5.45 ± 0.34	10.77 ± 0.68
786-O	Renal adenocarcinoma	5.41 ± 0.11	4.59 ± 0.15	23.81 ± 1.02
H69	Small cell lung carcinoma	2.66 ± 0.71	0.53 ± 0.22	45.54 ± 1.21
H69AR[b]		2.22 ± 0.26	2.40 ± 1.66	27.63 ± 0.97
PC-9	Lung cancer	5.77 ± 0.17	5.06 ± 0.83	N.D.
PC-9/GR[b]		2.81 ± 0.22	2.42 ± 0.13	N.D.
MCF-7	Breast cancer	6.57 ± 0.22 (13.74 ± 1.58)[c]	5.39 ± 0.19 (16.61 ± 2.08)[c]	N.D.
MCF-7/LCC2[b]		5.17 ± 0.26 (152.09 ± 19.26)[c]	4.56 ± 0.13 (169.40 ± 12.07)[c]	N.D.

[a] Before cell viability assay, cancer cells were incubated in the presence of channel molecules at various concentrations in 5% CO_2 at 37°C for 48 h. [b] Drug-resistant cell line. [c] IC_{50} values by Tamoxifen, a drug for treating breast cancers.

Using ALOGPS 2.1, the partition coefficient (log P) values of **F14, F12, F10** and **F8** were calculated to be 5.93, 6.94, 7.95 and 8.67 respectively, a trend that coincides with the anticancer trend. This suggests that the compound's solubility, not proton transport activity, should play a more predominant role in delivering high anticancer activity seen in **F8**.

As mentioned above, proton channel-mediated transport of H^+ ions is accompanied by a passive diffusion of membrane-permeable Cl^- anions, rather than less permeable Na^+/K^+ ions, across membrane in order to maintain a charge neutrality in the system. Since the Cl^- concentration in the extracellular environment is much higher than that in the cytosolic region in cancer cells, these proton channels can exert their anticancer activity at pH 7.4 (e.g., in the absence of proton concentration gradient with $pH_e = pH_i = 7.4$) by breaking down the proton homeostasis via the same mechanism, i.e., passive influx of Cl^- anions to accompany channel-mediated influx of H^+ ions with the Cl^- concentration gradient providing the driving forces for such co-transport of H^+ and Cl^- (Figure 2F). This mode of action indicates possible cytotoxicity of the proton channels to proton-overproducing cancer cells.

To investigate the broad applicability of proton channels in anticancer treatment, 14 types of cancers were studied (Table 2), covering 17 normal cancer cell lines and three drug-resistant cell lines (H69AR, PC-9/GR and MCF-7/LCC2). At pH_e 7.4, **F8** displays outstanding anticancer activities against all normal and drug-resistant cancer cell lines tested here, with IC_{50} values of 2.22 – 10.28 μM and a mean IC_{50} value of 5.40 μM. In comparison, IC_{50} values were determined to range from 4.36 to 45.54 μM with a mean value of 21.86 μM for Cisplatin, the first FDA-approved platinum compound for cancer treatment in 1978. In other words, on average, **F8** is more than 4 times as potent as Cisplatin in *in vitro* anticancer activity. The tested 16 cell lines are more susceptible to **F8** upon lowering the pH_e from 7.4 to 6.5, with IC_{50} values of 0.53 – 5.80 μM with a mean value of 4.02 μM. The mean value of 4.02 μM, when compared to a mean value of 5.83 μM for the same 16 cancer cell lines at pH_e 7.4, translates to an average of 31% increase in **F8**-mediated *in vitro* anticancer potency at pH_e 6.5.

A huge difference in anticancer activity toward normal (MCF-7) and drug-resistant (MCF-7/LCC2) breast cancer cell lines between **F8** and Tamoxifen was observed, which is a FDA-approved drug for treating breast cancers (Table 2). At pH_e 7.4, **F8** is twice as potent as Tamoxifen toward normal MCF-7 cell lines, and this difference in activity increases dramatically to 30 times in the case of drug-resistant MCF-7/LCC2 cell line. At pH_e of 6.5, the corresponding differences enlarge considerably, reaching 3- and 37-folds, respectively.

Interestingly, **F8** becomes even more potent against the drug-resistant cancer cell lines when compared to normal cancer cell lines. Particularly for lung cancer (PC-9 *vs* PC-9/GR), the

potency increases by more than 50%, with IC_{50} values decreasing from > 5 μM to < 3 μM. This may imply a more vulnerable nature of drug-resistant cancer cells to a disrupted proton homeostasis.

The *in vivo* anticancer activity of **F8** was investigated using nude mice bearing HCT116 (colorectal carcinoma) xenografts. Compared to vehicle mice, mice treated with **F8** at a dose of 40 mg/kg of mouse body weight every 2 or 3 days for 20 days showed substantial reduction in tumor onset and growth as well as significant tumor growth inhibition by 60% (Figure 3A; Tumor volume changes over time upon treatment with PBS, control vehicle and **F8** at 20 or 40 mg/kg of mouse body weight (n = 8) in nude mice bearing HCT116 xenografts), confirming that **F8** could operate *in vivo* as an antitumor agent.

Notably, mice treated with **F8** at 40 mg/kg at 20 days post-treatment exhibited insignificant difference in average body weight relative to those receiving the vehicle control (Figure 3B; The corresponding average body weight. $^{**}p < 0.01$.), suggesting **F8** is minimally toxic over the 20-day duration of treatment. The *in vivo* effects of **F8** in major organs was further examined. Mice were euthanized, and their kidneys, liver, spleen, heart, lungs, brain, and tumor were harvested, fixed with 3.7% formaldehyde, embedded with paraffin and sectioned, followed by staining with hematoxylin and eosin (H & E staining). Histology revealed no significant differences in these organs between vehicle and **F8**-treated mice (Figure 3C; H & E staining of liver, kidney, spleen, lung and heart sections from HCT116 xenografted nude mice (n = 8) at 20 days post-treatment), demonstrating that **F8** caused no adverse side effects in major organs.

Subsequent hematological analyses of the plasma collected from vehicle and **F8**-treated mice revealed biochemical indexes of blood (concentrations of chloride, potassium, sodium, urea, creatinine, alanine aminotransferase, aspartate aminotransferase and total bilirubin) to be comparable with each other and within the normal ranges (Table 3).

Figure 3D demonstrates that **F8** was essentially non-toxic to red blood cells at up to 60 μM at pH 7.4. Remarkably, cytotoxicity of **F8** toward red blood cells remained negligible at up to 60 μM of **F8** even when the pH was lowered to 6.5, suggesting either **F8** could not target red blood cells or red blood cells were less sensitive to a disruption in pH homeostasis than those rapidly dividing acid-overproducing cancer cells.

The present invention discloses a pharmaceutical composition comprising an effective amount of a compound of Formula (I) or a pharmaceutically acceptable salt, solvate or prodrug thereof.

In some embodiments, the pharmaceutical composition further comprises a lipid membrane. In this regard, the pharmaceutical composition comprises channels, which are pre-formed from the compounds of Formula (I).

The present invention also discloses a method of treating cancer, comprising administering a therapeutically effective amount of compound of Formula (I) or a pharmaceutically acceptable salt, solvate or prodrug thereof to a subject in need, for a sufficient time and under conditions to treat the subject.

The present invention also discloses a compound of Formula (I) or a pharmaceutically acceptable salt, solvate or prodrug thereof for use as a medicament in treating cancer in a subject in need thereof.

The present invention also discloses a use of a therapeutically effective amount of a compound of Formula (I) or a pharmaceutically acceptable salt, solvate or prodrug thereof in the manufacture of a medicament for treating cancer in a subject in need thereof.

In some embodiments, the cancer is selected from breast cancer, cervix adenocarcinoma, colorectal carcinoma, epidermoid carcinoma, glioblastoma, hepatocellular carcinoma, kidney carcinoma, lung cancer, neuroblastoma, ovarian carcinoma, prostate carcinoma, prostate adenocarcinoma, renal cell adenocarcinoma, small cell lung carcinoma.

The compound of the invention can be administered to a subject as a pharmaceutically acceptable salt thereof. Suitable pharmaceutically acceptable salts include, but are not limited to salts of pharmaceutically acceptable inorganic acids such as hydrochloric, sulphuric, phosphoric, nitric, carbonic, boric, sulfamic, and hydrobromic acids, or salts of pharmaceutically acceptable organic acids such as acetic, propionic, butyric, tartaric, maleic, hydroxymaleic, fumaric, maleic, citric, lactic, mucic, gluconic, benzoic, succinic, oxalic, phenylacetic, methanesulphonic,

toluenesulphonic, benezenesulphonic, salicyclic sulphanilic, aspartic, glutamic, edetic, stearic, palmitic, oleic, lauric, pantothenic, tannic, ascorbic and valeric acids.

Base salts include, but are not limited to, those formed with pharmaceutically acceptable cations, such as sodium, potassium, lithium, calcium, magnesium, ammonium and alkylammonium. In particular, the present invention includes within its scope cationic salts e.g. sodium or potassium salts, or alkyl esters (eg methyl, ethyl) of the phosphate group.

Basic nitrogen-containing groups may be quarternised with such agents as lower alkyl halide, such as methyl, ethyl, propyl, and butyl chlorides, bromides and iodides; dialkyl sulfates like dimethyl and diethyl sulfate; and others.

It will be appreciated that any compound that is a prodrug of the compound of formula (I) is also within the scope and spirit of the invention. Thus the compound of the invention can be administered to a subject in the form of a pharmaceutically acceptable pro-drug. The term "pro-drug" is used in its broadest sense and encompasses those derivatives that are converted *in vivo* to the compound of the invention. Such derivatives would readily occur to those skilled in the art. Other texts which generally describe prodrugs (and the preparation thereof) include: *Design of Prodrugs*, 1985, H. Bundgaard (Elsevier); *The Practice of Medicinal Chemistry*, 1996, Camille G. Wermuth *et al.*, Chapter 31 (Academic Press); and *A Textbook of Drug Design and Development*, 1991, Bundgaard *et al.*, Chapter 5, (Harwood Academic Publishers).

The compound of the invention may be in crystalline form either as the free compound or as a solvate (e.g. hydrate) and it is intended that both forms are within the scope of the present invention. Methods of solvation are generally known within the art.

Compounds described herein can comprise one or more asymmetric centers, and thus can exist in various isomeric forms, *e.g.,* enantiomers and/or diastereomers. For example, the compounds described herein can be in the form of an individual enantiomer, diastereomer or geometric isomer, or can be in the form of a mixture of stereoisomers, including racemic mixtures and mixtures enriched.in one or more stereoisomer. Isomers can be isolated from mixtures by methods known to those skilled in the art, including chiral high pressure liquid chromatography (HPLC) and the formation and crystallization of chiral salts; or preferred isomers can be prepared

by asymmetric syntheses. See, for example, Jacques *et al., Enantiomers, Racemates and Resolutions* (Wiley Interscience, New York, 1981); Wilen *et al., Tetrahedron* 33:2725 (1977); Eliel, *Stereochemistry of Carbon Compounds* (McGraw-Hill, NY, 1962); and Wilen, *Tables of Resolving Agents and Optical Resolutions* p. 268 (E.L. Eliel, Ed., Univ. of Notre Dame Press, Notre Dame, IN 1972). The invention additionally encompasses compounds described herein as individual isomers substantially free of other isomers, and alternatively, as mixtures of various isomers.

The compound of the invention, or a pharmaceutically acceptable salt, solvate, stereoisomer or prodrug thereof is administered to the patient in a therapeutically effective amount. As used herein, a therapeutically effective amount is intended to include at least partially attaining the desired effect, or delaying the onset of, or inhibiting the progression of, or halting or reversing altogether the onset or progression of macular degeneration.

As used herein, the term "effective amount" relates to an amount of compound which, when administered according to a desired dosing regimen, provides the desired therapeutic activity. Dosing may occur at intervals of minutes, hours, days, weeks, months or years or continuously over any one of these periods. Suitable dosages may lie within the range of about 0.1 ng per kg of body weight to 1 g per kg of body weight per dosage, such as is in the range of 1 mg to 1 g per kg of body weight per dosage. In one embodiment, the dosage may be in the range of 1 mg to 500 mg per kg of body weight per dosage. In another embodiment, the dosage may be in the range of 1 mg to 250 mg per kg of body weight per dosage. In yet another embodiment, the dosage may be in the range of 1 mg to 100 mg per kg of body weight per dosage, such as up to 50 mg per body weight per dosage.

Suitable dosage amounts and dosing regimens can be determined by the attending physician and may depend on the severity of the condition as well as the general age, health and weight of the patient to be treated.

The compound of the invention may be administered in a single dose or a series of doses. While it is possible for the active ingredient to be administered alone, it is preferable to present it as a composition, preferably as a pharmaceutical composition. The formulation of such compositions is well known to those skilled in the art. The composition may contain any suitable carriers,

diluents or excipients. These include all conventional solvents, dispersion media, fillers, solid carriers, coatings, antifungal and antibacterial agents, dermal penetration agents, surfactants, isotonic and absorption agents and the like. It will be understood that the compositions of the invention may also include other supplementary physiologically active agents.

The carrier must be pharmaceutically "acceptable" in the sense of being compatible with the other ingredients of the composition and not injurious to the patient. The compositions may conveniently be presented in unit dosage form and may be prepared by any methods well known in the art of pharmacy. Such methods include the step of bringing into association the active ingredient with the carrier which constitutes one or more accessory ingredients. In general, the compositions are prepared by uniformly and intimately bringing into association the active ingredient with liquid carriers or finely divided solid carriers or both, and then if necessary shaping the product.

For example, encapsulation of compounds of Formula (I) into pH-sensitive cancer-targeting nano-delivery vehicles may allow cancer-specific release of proton channels for enhanced anticancer efficacy and reduced cytotoxicity.

Injectables for such use can be prepared in conventional forms, either as a liquid solution or suspension or in a solid form suitable for preparation as a solution or suspension in a liquid prior to injection, or as an emulsion. Carriers can include, for example, water, saline (e.g., normal saline (NS), phosphate-buffered saline (PBS), balanced saline solution (BSS)), sodium lactate Ringer's solution, dextrose, glycerol, ethanol, and the like; and if desired, minor amounts of auxiliary substances, such as wetting or emulsifying agents, buffers, and the like can be added. Proper fluidity can be maintained, for example, by using a coating such as lecithin, by maintaining the required particle size in the case of dispersion and by using surfactants. By way of example, the compound, composition or combination can be dissolved in a pharmaceutically effective carrier and be injected into the vitreous of the eye with a fine gauge hollow bore needle (e.g., 30 gauge, 1/2 or 3/8 inch needle) using a temporal approach (e.g., about 3 to about 4 mm posterior to the limbus for human eye to avoid damaging the lens).

A person skilled in the art will appreciate that other means for injecting and/or administering the compound, composition or combinations to the vitreous of the eye can also be used. These other

means can include, for example, intravitreal medical delivery devices. These devices and methods can include, for example, intravitreal medicine delivery devices, and biodegradable polymer delivery members that are inserted in the eye for long term delivery of medicaments. These devices and methods can further include transscleral delivery devices.

Although intravitreal administration is likely to be a form of administration, the present invention also includes other modes of administration including topical or intravenous administration. For example, solutions or suspensions of the compound, composition or combinations of the invention may be formulated as eye drops, or as a membranous ocular patch, which is applied directly to the surface of the eye. Topical application typically involves administering the compound of the invention in an amount between 0.1 ng and 10 mg.

The compound or composition of the invention may also be suitable for intravenous administration. For example, a compound of formula (I) or a pharmaceutically acceptable salt, solvate or prodrug thereof may be administered intravenously at a dose of up to 50 mg/m^2.

The compound or composition of the invention may also be suitable for oral administration and may be presented as discrete units such as capsules, sachets or tablets each containing a predetermined amount of the active ingredient; as a powder or granules; as a solution or a suspension in an aqueous or non-aqueous liquid; or as an oil-in-water liquid emulsion or a water-in-oil liquid emulsion. The active ingredient may also be presented as a bolus, electuary or paste. In another embodiment, the compound of formula (I) or a pharmaceutically acceptable salt, solvate or prodrug is orally administerable.

A tablet may be made by compression or moulding, optionally with one or more accessory ingredients. Compressed tablets may be prepared by compressing in a suitable machine the active ingredient in a free-flowing form such as a powder or granules, optionally mixed with a binder (e.g inert diluent, preservative disintegrant (e.g. sodium starch glycolate, cross-linked polyvinyl pyrrolidone, cross-linked sodium carboxymethyl cellulose) surface-active or dispersing agent. Moulded tablets may be made by moulding in a suitable machine a mixture of the powdered compound moistened with an inert liquid diluent. The tablets may optionally be coated or scored and may be formulated so as to provide slow or controlled release of the active ingredient therein using, for example, hydroxypropylmethyl cellulose in varying proportions to

provide the desired release profile. Tablets may optionally be provided with an enteric coating, to provide release in parts of the gut other than the stomach.

The compound or composition of the invention may be suitable for topical administration in the mouth including lozenges comprising the active ingredient in a flavoured base, usually sucrose and acacia or tragacanth gum; pastilles comprising the active ingredient in an inert basis such as gelatine and glycerin, or sucrose and acacia gum; and mouthwashes comprising the active ingredient in a suitable liquid carrier.

The compound or composition of the invention may be suitable for topical administration to the skin may comprise the compounds dissolved or suspended in any suitable carrier or base and may be in the form of lotions, gel, creams, pastes, ointments and the like. Suitable carriers include mineral oil, propylene glycol, polyoxyethylene, polyoxypropylene, emulsifying wax, sorbitan monostearate, polysorbate 60, cetyl esters wax, cetearyl alcohol, 2-octyldodecanol, benzyl alcohol and water. Transdermal patches may also be used to administer the compounds of the invention.

The compound or composition of the invention may be suitable for parenteral administration include aqueous and non-aqueous isotonic sterile injection solutions which may contain anti-oxidants, buffers, bactericides and solutes which render the compound, composition or combination isotonic with the blood of the intended recipient; and aqueous and non-aqueous sterile suspensions which may include suspending agents and thickening agents. The compound, composition or combination may be presented in unit-dose or multi-dose sealed containers, for example, ampoules and vials, and may be stored in a freeze-dried (lyophilised) condition requiring only the addition of the sterile liquid carrier, for example water for injections, immediately prior to use. Extemporaneous injection solutions and suspensions may be prepared from sterile powders, granules and tablets of the kind previously described.

Preferred unit dosage composition or combinations are those containing a daily dose or unit, daily sub-dose, as herein above described, or an appropriate fraction thereof, of the active ingredient.

It should be understood that in addition to the active ingredients particularly mentioned above, the composition of this invention may include other agents conventional in the art having regard to the type of composition or combination in question, for example, those suitable for oral administration may include such further agents as binders, sweeteners, thickeners, flavouring agents disintegrating agents, coating agents, preservatives, lubricants and/or time delay agents. Suitable sweeteners include sucrose, lactose, glucose, aspartame or saccharine. Suitable disintegrating agents include cornstarch, methylcellulose, polyvinylpyrrolidone, xanthan gum, bentonite, alginic acid or agar. Suitable flavouring agents include peppermint oil, oil of wintergreen, cherry, orange or raspberry flavouring. Suitable coating agents include polymers or copolymers of acrylic acid and/or methacrylic acid and/or their esters, waxes, fatty alcohols, zein, shellac or gluten. Suitable preservatives include sodium benzoate, vitamin E, alpha-tocopherol, ascorbic acid, methyl paraben, propyl paraben or sodium bisulphite. Suitable lubricants include magnesium stearate, stearic acid, sodium oleate, sodium chloride or talc. Suitable time delay agents include glyceryl monostearate or glyceryl distearate.

Those skilled in the art will appreciate that the invention described herein is susceptible to variations and modifications other than those specifically described. It is to be understood that the invention includes all such variations and modifications which fall within the spirit and scope. The invention also includes all of the steps, features, compositions and compounds referred to or indicated in this specification, individually or collectively, and any and all combinations of any two or more of said steps or features.

As used in this application, the singular form "a," "an," and "the" include plural references unless the context clearly dictates otherwise. For example, the term "an agent" includes a plurality of agents, including mixtures thereof.

Throughout this specification and the claims which follow, unless the context requires otherwise, the word "comprise", and variations such as "comprises" and "comprising", will be understood to imply the inclusion of a stated integer or step or group of integers or steps but not the exclusion of any other integer or step or group of integers or steps.

The reference in this specification to any prior publication (or information derived from it), or to any matter which is known, is not, and should not be taken as an acknowledgment or admission

or any form of suggestion that that prior publication (or information derived from it) or known matter forms part of the common general knowledge in the field of endeavor to which this specification relates.

Certain embodiments of the invention will now be described with reference to the following examples which are intended for the purpose of illustration only and are not intended to limit the scope of the generality hereinbefore described.

EXAMPLES

The reference in this specification to any prior publication (or information derived from it), or to any matter which is known, is not, and should not be taken as an acknowledgment or admission or any form of suggestion that that prior publication (or information derived from it) or known matter forms part of the common general knowledge in the field of endeavor to which this specification relates.

Materials and Methods

All the reagents were obtained from commercial suppliers and used as received unless otherwise noted. Aqueous solutions were prepared from MilliQ water. The organic solutions from all liquid extractions were dried over anhydrous Na_2SO_4 for a minimum of 15 minutes before filtration. Flash column chromatography was performed using pre-coated 0.2 mm silica plates from Selecto Scientific. Chemical yield refers to pure isolated substances. ^1H and ^{13}C NMR spectra were recorded on either a Bruker ACF-400 spectrometer. The solvent signal of $CDCl_3$ was referenced at δ= 7.26 ppm. Coupling constants (J values) are reported in Hertz (Hz). ^1H NMR data are recorded in the order: chemical shift value, multiplicity (s, singlet; d, doublet; t, triplet; q, quartet; m, multiplet; br, broad), number of protons that gave rise to the signal and coupling constant, where applicable. ^{13}C spectra are proton-decoupled and recorded on Bruker ACF400 (400 MHz). The solvent, $CDCl_3$, was referenced at δ= 77 ppm. $CDCl_3$ (99.8%-Deuterated) was purchased from Aldrich and used without further purification. Mass spectra were acquired with Shimazu LCMS-2010EV.

Synthetic Scheme and Chemical Structures of Proton Channels

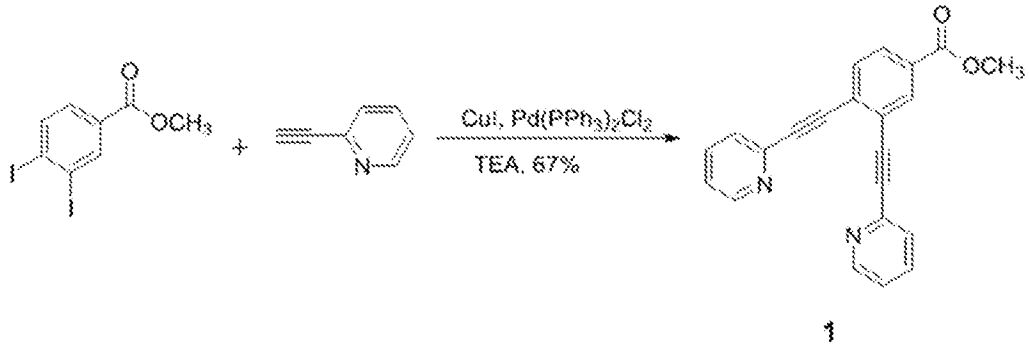

1

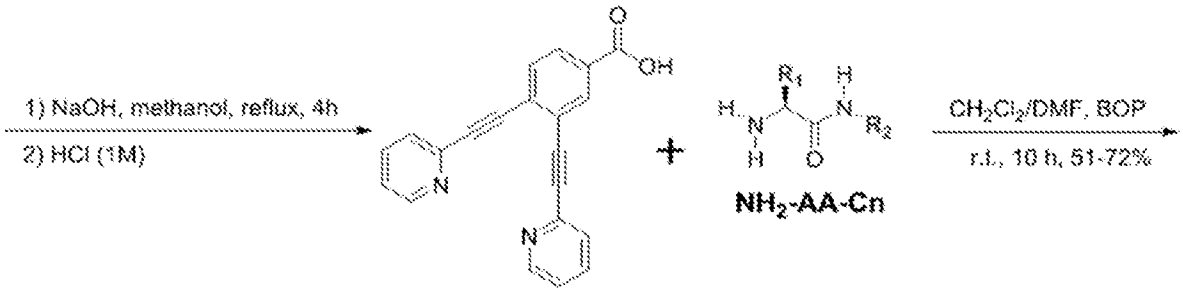

2

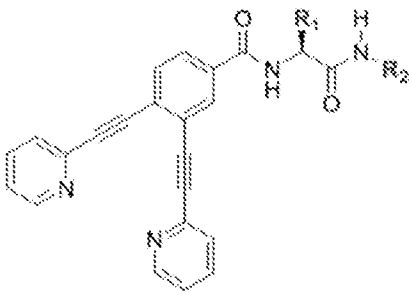

R_1 = CH_3 (**Ala = A**)
CH_2Ph (**Phe = F**)
$CH(CH_3)_2$ (**Val = V**)
$CH(CH_3)C_2H_5$ (**Ile = I**)
$CH_2CH(CH_3)_2$ (**Leu = L**)

R_2 = n-C_8H_{17} (**C8**)
n-$C_{10}H_{21}$ (**C10**)
n-$C_{12}H_{25}$ (**C12**)
n-$C_{14}H_{29}$ (**C14**)
n-$C_{16}H_{33}$ (**C16**)

Synthetic Scheme and Chemical Structure of sF8

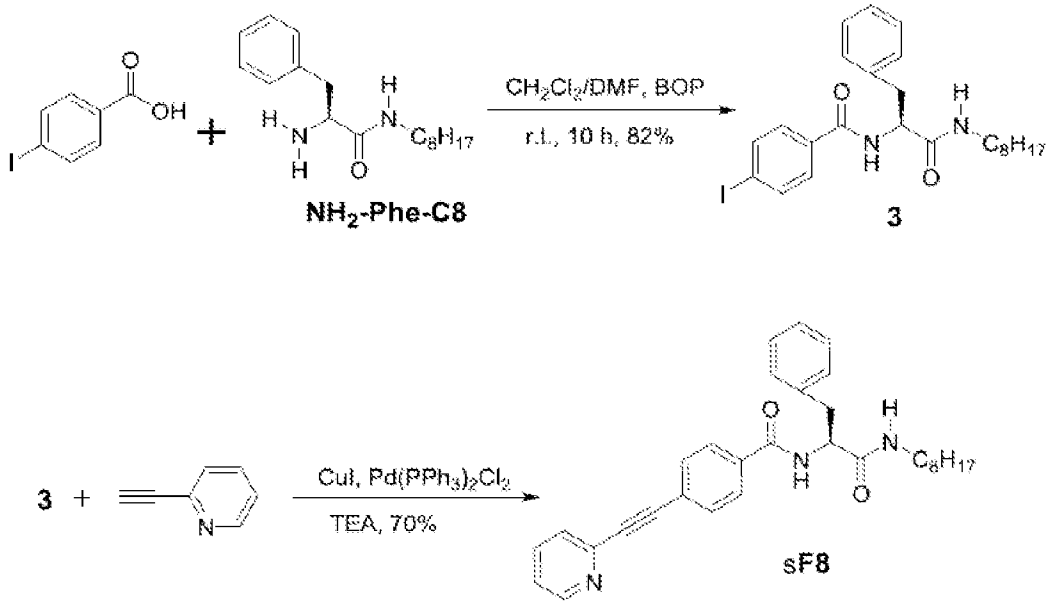

Synthetic Scheme and Chemical Structures of F28 and F38

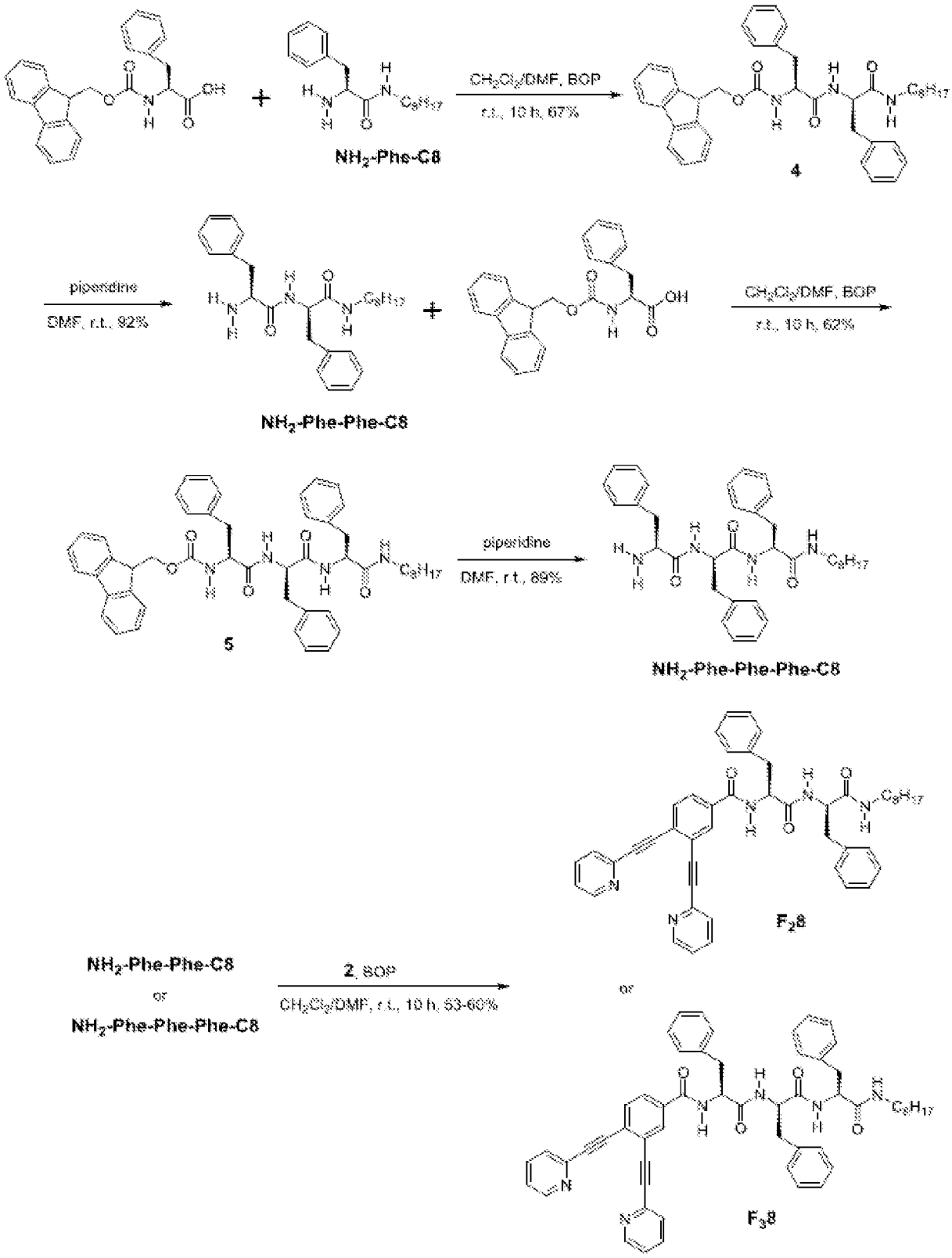

Synthetic Scheme and Chemical Structure of F8-ester

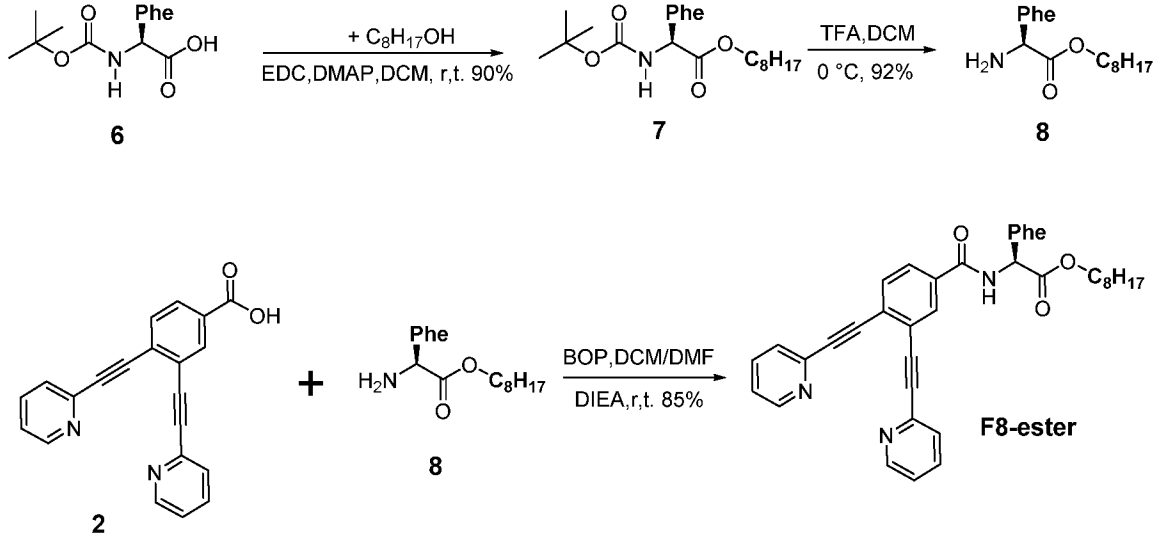

For synthesis of starting materials NH2-AA-Cn, see: Ren, C. L.; Ding, X.; Arundhati, R.; Shen, J.; Zhou, S.; Chen, F.; Li, S. F. Y.; Ren, H.; Yang, Y. Y.; Zeng , H. Q. ***Chem. Sci.*** **2018**, ***9***, 4044-4051.

1: In a 100 mL round-bottom flask charged with 3,4-diiodobenzoic acid methyl ester (3.88 g, 10 mmol), 2-ethynylpyridine (2.06 g, 20 mmol), $PdCl_2(PPh_3)_2$ (0.35 g, 10 mol%) and CuI (38 mg, 5 mol%) were dissolved in NEt_3 (60 mL). The reaction mixture was degassed through three freeze-pump-thaw cycles and heated to 50 °C under a nitrogen atmosphere and held there for 20 h. The resulting suspension was filtered off and the residue was purified by flash column chromatography (MeOH:CH_2Cl_2 = 1:50, v:v) to afford the pure compound **1** as a pale yellow solid. Yield: 2.3 g, 67%. ^{1}H NMR (400 MHz, $CDCl_3$) δ 8.68 – 8.59 (m, 2H), 8.31 – 8.24 (m, 1H), 7.99 (dd, *J* = 8.2, 1.7 Hz, 1H), 7.75 – 7.63 (m, 5H), 7.32 – 7.26 (m, 2H), 3.91 (s, 3H). ^{13}C NMR (101 MHz, $CDCl_3$) δ 165.71, 150.08, 150.03, 142.75, 142.63, 136.60, 133.40, 132.35, 132.09, 131.99, 130.27, 129.57, 129.35, 128.68, 128.56, 128.11, 127.85, 125.56, 123.57, 123.42, 95.30, 93.35, 87.14, 87.00, 52.57, 46.40. MS-ESI: calculated for $[M+H]^+$ ($C_{22}H_{15}O_2N_2$): *m/z* 339.11, found: *m/z* 339.25.

F8: 1 (1.69 g, 5 mmol) was dissolved in methanol (80 mL) to which 1M NaOH (22.5 mL, 22.5 mmol) was added. The mixture was heated under reflux for 1 hour and then the reaction solvent was removed in *vacuo* to yield a white solid, which was dissolved in water and neutralized with 1 M HCl (40 mL) to yield crude product **2,** which was directly used in the next step without further purification. **2** (324 mg, 1.0 mmol), **NH2-Phe-C8** (276 mg, 1.0 mmol) and BOP (486 mg,

1.1 mmol) were dissolved in 10 mL CH_2Cl_2/DMF (8:2, v:v) to which diisopropylamine (0.39 ml, 2.2 mmol) was added. The reaction mixture was stirred for 10 hours at room temperature. Solvent was removed in *vacuo* and the crude product was purified by flash column chromatography (MeOH:CH_2Cl_2 = 1:50, v:v) to afford the pure product **F8** as a yellow solid. Yield: 379 mg, 65%. ^{1}H NMR (400 MHz, $CDCl_3$) δ 8.70 – 8.52 (m, 2H), 8.00 (t, *J* = 4.5 Hz, 2H), 7.75 – 7.60 (m, 5H), 7.58 (d, *J* = 8.1 Hz, 1H), 7.32 – 7.26 (m, 5H), 7.20 (ddd, *J* = 6.9, 3.7, 1.4 Hz, 1H), 6.89 (t, *J* = 5.3 Hz, 1H), 4.98 (q, *J* = 7.5 Hz, 1H), 3.75 (s, 1H), 3.24 (d, *J* = 7.1 Hz, 2H), 3.18 – 2.99 (m, 2H), 1.36 (dt, *J* = 21.1, 6.9 Hz, 4H), 1.20 – 1.09 (m, 8H), 0.83 (t, *J* = 7.0 Hz, 3H). ^{13}C NMR (101 MHz, $CDCl_3$) δ 171.12, 165.59, 150.00, 149.84, 142.69, 142.63, 136.96, 136.58, 136.46, 133.80, 132.28, 131.04, 129.42, 128.55, 128.07, 128.04, 127.95, 127.57, 126.90, 125.41, 123.41, 123.36, 94.79, 93.21, 87.32, 87.20, 55.70, 46.32, 39.67, 38.78, 31.80, 29.24, 29.19, 26.88, 22.65, 14.13, 8.71. MS-ESI: calculated for $[M+Na]^+$ ($C_{38}H_{38}O_2N_4Na$): *m/z* 605.29, found: *m/z* 605.17.

Preparation of other compounds of Formula (I) follows the same synthetic procedure as F8.

F10: ^{1}H NMR (400 MHz, $CDCl_3$) δ 8.71 (s, 2H), 8.11 (s, 1H), 7.90 – 7.74 (m, 4H), 7.70 (d, *J* = 8.1 Hz, 1H), 7.54 (d, *J* = 6.9 Hz, 1H), 7.44 – 7.23 (m, 7H), 6.08 (s, 1H), 4.85 (dd, *J* = 14.4, 7.4 Hz, 1H), 3.57 (s, 1H), 3.41 – 3.00 (m, 4H), 1.58 – 1.05 (m, 16H), 0.90 (dd, *J* = 8.9, 4.9 Hz, 3H). ^{13}C NMR (101 MHz, $CDCl_3$) δ 170.62, 165.34, 149.53, 149.05, 142.24, 141.83, 137.61, 137.04, 136.88, 134.02, 132.59, 131.11, 129.40, 128.74, 128.29, 128.08, 127.90, 127.08, 125.29, 123.57, 94.38, 92.36, 88.68, 87.86, 55.75, 39.70, 38.91, 31.92, 31.66, 29.73, 29.66, 29.59, 29.55, 29.35, 29.28, 26.85, 22.72, 14.18. MS-ESI: calculated for $[M+H]^+$ ($C_{40}H_{43}O_2N_4$): *m/z* 611.33, found: *m/z* 611.28.

F12: ^{1}H NMR (400 MHz, $CDCl_3$) δ 8.74 – 8.58 (m, 2H), 8.06 (d, *J* = 1.6 Hz, 1H), 7.80 – 7.70 (m, 4H), 7.66 (d, *J* = 8.1 Hz, 1H), 7.59 – 7.44 (m, 1H), 7.36 – 7.19 (m, 7H), 6.10 (t, *J* = 5.4 Hz, 1H), 4.82 (dd, *J* = 14.5, 7.9 Hz, 1H), 3.74 (s, 1H), 3.28 (dd, *J* = 13.5, 6.4 Hz, 1H), 3.22 – 3.03 (m, 3H), 1.49 – 0.92 (m, 20H), 0.86 (t, *J* = 6.9 Hz, 3H). ^{13}C NMR (101 MHz, $CDCl_3$) δ 170.65, 165.36, 149.63, 149.17, 142.34, 141.93, 137.47, 136.92, 136.89, 133.99, 132.55, 131.08, 129.40, 128.72, 128.48, 128.22, 128.10, 127.85, 127.06, 125.31, 123.58, 123.52, 94.47, 92.46, 88.49, 87.71, 55.74, 39.69, 38.90, 31.95, 29.70, 29.68, 29.64, 29.56, 29.40, 29.29, 26.85, 22.73, 14.18. MS-ESI: calculated for $[M+K]^+$ ($C_{42}H_{46}O_2N_4K$): *m/z* 677.33, found: *m/z* 677.21.

F14: ^{1}H NMR (400 MHz, $CDCl_3$) δ 8.80 – 8.65 (m, 2H), 8.04 (d, *J* = 1.6 Hz, 1H), 7.84 – 7.71 (m, 5H), 7.66 (d, *J* = 8.2 Hz, 1H), 7.47 – 7.28 (m, 7H), 5.93 (t, *J* = 5.4 Hz, 1H), 4.81 (dd, *J* = 14.3, 8.1 Hz, 1H), 3.28 – 3.24 (m, 1H), 3.12 (dt, *J* = 5.3, 2.3 Hz, 4H), 1.28 – 1.14 (m, 24H), 0.86 (t, *J* = 6.9 Hz, 3H). ^{13}C NMR (101 MHz, $CDCl_3$) δ 170.61, 165.30, 149.68, 149.19, 142.05, 141.62, 137.87, 137.26, 136.77, 134.02, 132.54, 132.05, 131.12, 129.40, 128.76, 128.30, 128.27, 128.08, 127.81, 127.13, 125.30, 123.87, 123.79, 94.34, 92.28, 88.84, 87.94, 55.68, 46.08, 39.71, 38.93, 31.95, 29.74, 29.72, 29.70, 29.64, 29.55, 29.40, 29.28, 26.84, 22.73, 14.18, 8.67. MS-ESI: calculated for $[M+H]^+$ ($C_{44}H_{51}O_2N_4$): *m/z* 667.40, found: *m/z* 667.83.

F16: ^{1}H NMR (400 MHz, $CDCl_3$) δ 8.80 – 8.61 (m, 2H), 8.04 (d, *J* = 1.6 Hz, 1H), 7.84 – 7.69 (m, 4H), 7.65 (d, *J* = 8.2 Hz, 1H), 7.53 (d, *J* = 7.9 Hz, 1H), 7.41 – 7.21 (m, 7H), 6.02 (t, *J* = 5.4 Hz, 1H), 4.82 (dd, *J* = 14.4, 8.1 Hz, 1H), 3.32 – 3.23 (m, 1H), 3.19 – 3.04 (m, 4H), 1.48 – 1.04 (m, 28H), 0.86 (t, *J* = 6.9 Hz, 3H). ^{13}C NMR (101 MHz, $CDCl_3$) δ 170.68, 165.35, 149.72, 149.21, 142.19, 141.76, 137.67, 137.07, 136.82, 133.96, 132.51, 131.11, 129.40, 128.74, 128.25, 128.22, 128.08, 127.79, 127.10, 125.30, 123.75, 123.68, 94.44, 92.37, 88.65, 87.78, 55.70, 45.93, 39.71, 38.90, 31.96, 29.74, 29.71, 29.70, 29.65, 29.56, 29.40, 29.29, 26.85, 22.73, 14.18, 8.66. MS-ESI: calculated for $[M+H]^+$ ($C_{46}H_{55}O_2N_4$): *m/z* 695.43, found: *m/z* 695.29.

A8: ^{1}H NMR (400 MHz, $CDCl_3$) δ 8.77 – 8.63 (m, 2H), 8.25 (d, *J* = 1.1 Hz, 1H), 7.96 – 7.72 (m, 5H), 7.62 (d, *J* = 7.1 Hz, 1H), 7.51 – 7.35 (m, 2H), 6.68 (s, 1H), 4.72 – 4.64 (m, 1H), 4.38 (s, 1H), 3.22 (dd, *J* = 13.1, 7.0 Hz, 2H), 1.63 – 1.43 (m, 5H), 1.25 (dd, *J* = 12.1, 4.8 Hz, 10H), 0.90 – 0.75 (m, 3H). ^{13}C NMR (101 MHz, $CDCl_3$) δ 172.29, 165.20, 148.55, 147.55, 141.14, 140.30, 139.42, 138.26, 134.36, 132.81, 132.33, 131.58, 128.96, 128.71, 128.66, 127.58, 127.27, 124.72, 124.17, 123.96, 93.27, 90.79, 89.34, 53.48, 50.07, 39.78, 31.81, 29.46, 29.27, 29.25, 26.93, 22.67, 18.59, 14.14. MS-ESI: calculated for $[M+H]^+$ ($C_{32}H_{35}O_2N_4$): *m/z* 507.27, found: *m/z* 507.46.

A10: ^{1}H NMR (400 MHz, $CDCl_3$) δ 8.51 (d, *J* = 4.9 Hz, 2H), 8.12 – 7.92 (m, 2H), 7.74 (dd, *J* = 8.1, 1.5 Hz, 1H), 7.62 – 7.42 (m, 6H), 7.15 (ddd, *J* = 8.9, 4.5, 2.1 Hz, 2H), 4.84 – 4.67 (m, 1H), 3.73 (s, 1H), 3.13 (ddd, *J* = 38.0, 13.2, 5.9 Hz, 2H), 1.60 – 1.25 (m, 6H), 1.26 – 0.94 (m, 12H), 0.72 (t, *J* = 6.9 Hz, 3H). ^{13}C NMR (101 MHz, $CDCl_3$) δ 172.67, 165.62, 149.95, 149.85, 142.73, 136.36, 136.34, 133.86, 132.31, 131.16, 128.00, 127.94, 127.85, 127.62, 125.35, 123.33, 123.26, 94.77, 93.30, 87.04, 49.72, 39.70, 31.74, 29.35, 29.23, 29.18, 26.91, 22.59, 18.66, 14.08. MS-

ESI: calculated for $[M+H]^+$ ($C_{34}H_{39}O_2N_4$): *m/z* 535.31, found: *m/z* 535.19.

I8: ^{1}H NMR (400 MHz, $CDCl_3$) δ 8.63 (s, 2H), 8.03 (s, 1H), 7.78 (d, *J* = 7.8 Hz, 1H), 7.60 (d, *J* = 48.0 Hz, 5H), 7.25 (d, *J* = 5.3 Hz, 2H), 7.09 – 6.84 (m, 1H), 4.53 (d, *J* = 7.3 Hz, 1H), 3.47 (s, 1H), 3.31 (td, *J* = 13.1, 6.6 Hz, 1H), 3.13 (d, *J* = 3.5 Hz, 1H), 2.02 (d, *J* = 7.0 Hz, 1H), 1.65 (ddd, *J* = 13.1, 7.4, 2.9 Hz, 1H), 1.47 (s, 2H), 1.18 (s, 12H), 1.04 – 0.86 (m, 6H), 0.81 (d, *J* = 2.2 Hz, 3H). ^{13}C NMR (101 MHz, $CDCl_3$) δ 171.31, 165.86, 150.02, 149.89, 142.79, 142.71, 136.52, 136.41, 134.16, 132.39, 130.91, 128.14, 128.06, 127.92, 127.66, 125.52, 123.34, 94.78, 93.28, 87.28, 87.21, 58.72, 39.66, 37.35, 31.79, 29.44, 29.24, 29.23, 26.99, 25.31, 22.65, 15.52, 14.12, 11.22. MS-ESI: calculated for $[M+H]^+$ ($C_{35}H_{41}O_2N_4$): *m/z* 549.32, found: *m/z* 549.81.

I10: ^{1}H NMR (400 MHz, $CDCl_3$) δ 8.61 (d, *J* = 4.4 Hz, 2H), 8.01 (d, *J* = 1.5 Hz, 1H), 7.77 (dd, *J* = 8.2, 1.7 Hz, 1H), 7.66 – 7.58 (m, 5H), 7.25 – 7.21 (m, 2H), 7.14 – 7.02 (m, 1H), 4.54 (t, *J* = 8.5 Hz, 1H), 3.31 (dd, *J* = 13.4, 6.4 Hz, 1H), 3.12 (dt, *J* = 8.1, 3.3 Hz, 2H), 2.01 (dd, *J* = 8.3, 6.5 Hz, 1H), 1.65 (ddd, *J* = 13.4, 7.5, 3.2 Hz, 1H), 1.45 (dd, *J* = 14.3, 7.1 Hz, 2H), 1.39 – 1.34 (m, 1H), 1.26 – 1.15 (m, 14H), 0.98 (d, *J* = 6.7 Hz, 3H), 0.90 (t, *J* = 7.3 Hz, 3H), 0.81 (t, *J* = 6.8 Hz, 3H). ^{13}C NMR (101 MHz, $CDCl_3$) δ 171.37, 165.89, 150.07, 149.97, 142.75, 142.72, 136.50, 136.42, 134.17, 132.34, 130.91, 128.11, 128.06, 127.91, 127.65, 125.52, 123.38, 123.34, 94.78, 93.33, 87.28, 58.73, 46.19, 39.66, 37.30, 31.89, 29.58, 29.57, 29.43, 29.33, 29.30, 27.01, 25.31, 22.68, 15.51, 14.14, 11.21, 8.67. MS-ESI: calculated for $[M+H]^+$ ($C_{37}H_{45}O_2N_4$): *m/z* 577.35, found: *m/z* 577.14.

V8: ^{1}H NMR (400 MHz, $CDCl_3$) δ 8.64 (s, 2H), 8.05 (s, 1H), 7.80 (dd, *J* = 8.1, 1.4 Hz, 1H), 7.67 (ddd, *J* = 13.7, 10.4, 3.1 Hz, 5H), 7.40 – 7.26 (m, 2H), 6.84 – 6.64 (m, 1H), 4.52 – 4.36 (m, 1H), 3.41 – 3.02 (m, 3H), 2.23 (dt, *J* = 13.7, 6.8 Hz, 1H), 1.53 – 1.43 (m, 2H), 1.24 (dd, *J* = 15.7, 7.3 Hz, 10H), 1.04 (dd, *J* = 6.5, 4.6 Hz, 6H), 0.82 (td, *J* = 6.7, 1.9 Hz, 3H). ^{13}C NMR (101 MHz, $CDCl_3$) δ 171.08, 165.91, 149.99, 149.85, 142.83, 142.74, 136.55, 136.42, 134.19, 132.47, 130.88, 128.20, 128.05, 127.90, 127.63, 125.57, 123.32, 94.81, 93.30, 87.24, 87.13, 59.56, 39.68, 31.79, 31.47, 29.48, 29.24, 29.23, 26.98, 22.65, 19.39, 18.77, 14.13. MS-ESI: calculated for $[M+H]^+$ ($C_{34}H_{39}O_2N_4$): *m/z* 535.31, found: *m/z* 535.75.

V10: ^{1}H NMR (400 MHz, $CDCl_3$) δ 8.61 (s, 2H), 8.01 (d, *J* = 1.2 Hz, 1H), 7.77 (dd, *J* = 8.1, 1.6

Hz, 1H), 7.64 (dt, *J* = 14.9, 7.8 Hz, 5H), 7.53 (d, *J* = 8.7 Hz, 1H), 7.25 (s, 1H), 7.00 (t, *J* = 5.4 Hz, 1H), 4.52 (t, *J* = 8.3 Hz, 1H), 3.31 (dt, *J* = 13.4, 6.7 Hz, 1H), 3.23 – 3.04 (m, 1H), 2.23 (dd, *J* = 14.0, 6.9 Hz, 1H), 1.41 (ddd, *J* = 20.3, 18.7, 6.9 Hz, 4H), 1.24 – 1.10 (m, 13H), 1.03 (dd, *J* = 6.6, 4.1 Hz, 6H), 0.82 (t, *J* = 6.9 Hz, 3H). ^{13}C NMR (101 MHz, $CDCl_3$) δ 171.26, 166.01, 149.97, 149.83, 142.70, 142.65, 136.62, 136.51, 134.22, 132.40, 130.94, 128.15, 128.08, 127.94, 127.62, 125.54, 123.42, 94.78, 93.30, 87.25, 87.18, 59.63, 54.68, 39.69, 31.90, 31.39, 29.71, 29.64, 29.57, 29.46, 29.38, 29.33, 29.30, 27.00, 22.69, 19.40, 18.83, 18.56, 17.19, 14.15. MS-ESI: calculated for $[M+H]^+$ ($C_{36}H_{43}O_2N_4$): *m/z* 563.34, found: *m/z* 563.61.

L8: ^{1}H NMR (400 MHz, $CDCl_3$) δ 8.51 – 8.40 (m, 2H), 7.97 – 7.89 (m, 2H), 7.74 (dd, *J* = 8.2, 1.7 Hz, 1H), 7.60 – 7.49 (m, 4H), 7.45 (d, *J* = 8.1 Hz, 1H), 7.32 (t, *J* = 5.4 Hz, 1H), 7.15 (tdd, *J* = 4.8, 2.9, 1.7 Hz, 2H), 4.61 (td, *J* = 8.6, 5.4 Hz, 1H), 3.63 (s, 1H), 2.98 (dd, *J* = 13.1, 5.8 Hz, 1H), 1.80 – 1.58 (m, 3H), 1.37 – 1.31 (m, 2H), 1.12 – 1.01 (m, 10H), 0.82 (dd, *J* = 8.2, 6.3 Hz, 6H), 0.67 (t, *J* = 6.9 Hz, 3H). ^{13}C NMR (101 MHz, $CDCl_3$) δ 172.67, 165.77, 149.90, 149.74, 142.49, 142.48, 136.62, 136.53, 133.79, 132.20, 131.16, 127.98, 127.96, 127.82, 127.78, 125.15, 123.48, 123.43, 94.66, 93.12, 87.12, 86.99, 53.11, 46.60, 41.12, 39.57, 31.68, 29.25, 29.15, 29.13, 26.86, 22.54, 14.05, 8.89. MS-ESI: calculated for $[M+H]^+$ ($C_{35}H_{41}O_2N_4$): *m/z* 549.32, found: *m/z* 549.78.

L10: ^{1}H NMR (400 MHz, $CDCl_3$) δ 8.69 (dd, *J* = 13.1, 4.1 Hz, 2H), 8.15 (s, 1H), 7.94 – 7.73 (m, 5H), 7.68 (d, *J* = 8.1 Hz, 1H), 7.37 (dd, *J* = 18.7, 14.2 Hz, 2H), 6.67 (s, 1H), 4.67 (d, *J* = 7.8 Hz, 1H), 4.35 (s, 1H), 3.32 – 3.09 (m, 2H), 1.78 (d, *J* = 2.4 Hz, 3H), 1.57 – 1.42 (m, 2H), 1.29 – 1.20 (m, 13H), 0.98 (t, *J* = 6.1 Hz, 6H), 0.85 (t, *J* = 6.9 Hz, 3H). ^{13}C NMR (101 MHz, $CDCl_3$) δ 172.07, 165.69, 149.81, 149.12, 142.52, 141.91, 137.49, 136.72, 134.01, 132.52, 131.03, 128.12, 128.08, 125.21, 123.64, 123.49, 94.67, 92.45, 88.55, 87.40, 52.78, 41.38, 39.73, 31.92, 29.59, 29.44, 29.35, 29.31, 26.94, 24.98, 22.99, 22.71, 22.24, 14.17, 1.06. MS-ESI: calculated for $[M+H]^+$ ($C_{37}H_{45}O_2N_4$): *m/z* 577.35, found: *m/z* 577.48.

3: 4-Iodobenzoic acid (248 mg, 1.0 mmol), **NH2-Phe-C8** (276 mg, 1.0 mmol) and BOP (486 mg, 1.1 mmol) were dissolved in 10 mL CH_2Cl_2/DMF (8:2, v:v) to which diisopropylamine (0.39 ml, 2.2 mmol) was added. The reaction mixture was stirred for 10 hours at room temperature. Solvent was removed in *vacuo* and the crude product was purified by flash column chromatography (MeOH:CH_2Cl_2 = 1:70, v:v) to afford the pure product **3** as a white solid. Yield: 415 mg, 82%.

^{1}H NMR (400 MHz, $CDCl_3$) δ 7.83 – 7.70 (m, 2H), 7.51 – 7.39 (m, 2H), 7.34 – 7.22 (m, 5H), 7.11 (d, *J* = 6.8 Hz, 1H), 5.74 (s, 1H), 4.76 (td, *J* = 8.2, 5.9 Hz, 1H), 3.33 – 3.00 (m, 4H), 1.79 (s, 1H), 1.36 – 1.05 (m, 11H), 0.87 (t, *J* = 7.0 Hz, 3H). ^{13}C NMR (101 MHz, $CDCl_3$) δ 170.50, 166.32, 137.83, 136.69, 133.15, 129.36, 128.78, 128.69, 127.17, 98.95, 55.34, 39.68, 38.98, 31.81, 29.25, 29.21, 29.18, 26.80, 22.68, 14.15. MS-ESI: calculated for $[M+H]^+$ ($C_{24}H_{32}O_2N_2$): *m/z* 507.15, found: *m/z* 507.09.

sF8: In a 100 mL round-bottom flask charged with **3** (506 mg, 1 mmol), 2-ethynylpyridine (103 mg, 1 mmol), $PdCl_2(PPh_3)_2$ (35 mg, 10 mol%) and CuI (3.8 mg, 5 mol%) were dissolved in NEt_3 (30 mL). The reaction mixture was degassed through three freeze-pump-thaw cycles and heated to 50 °C under a nitrogen atmosphere and held there for 20 h. The resulting suspension was filtered off and the residue was purified by flash column chromatography (MeOH:CH_2Cl_2 = 1:50, v:v) to afford the pure compound s**F8** as a pale yellow solid. Yield: 337 mg, 70%. ^{1}H NMR (400 MHz, $CDCl_3$) δ 7.72 (d, *J* = 6.2 Hz, 3H), 7.61 (s, 2H), 7.47 (d, *J* = 7.6 Hz, 2H), 7.35 – 7.15 (m, 6H), 6.42 (s, 1H), 4.90 (d, *J* = 6.9 Hz, 1H), 3.35 – 2.97 (m, 4H), 1.37 – 1.04 (m, 13H), 0.85 (t, *J* = 6.9 Hz, 3H). ^{13}C NMR (101 MHz, $CDCl_3$) δ 170.85, 166.38, 136.86, 133.83, 132.06, 129.42, 128.64, 127.29, 127.00, 88.53, 55.40, 39.64, 38.93, 31.82, 29.28, 29.25, 29.20, 26.86, 22.68, 14.15. MS-ESI: calculated for $[M+H]^+$ ($C_{31}H_{35}O_2N_3$): *m/z* 481.27, found: *m/z* 481.12.

4: Fmoc-Phe-OH (387 mg, 1.0 mmol), **NH2-Phe-C8** (276 mg, 1.0 mmol) and BOP (486 mg, 1.1 mmol) were dissolved in 10 mL CH_2Cl_2/DMF (8:2, v:v) to which diisopropylamine (0.39 ml, 2.2 mmol) was added. The reaction mixture was stirred for 10 hours at room temperature. Solvent was removed in *vacuo* and the crude product was purified by flash column chromatography (MeOH:CH_2Cl_2 = 1:60, v:v) to afford the pure product **4** as a white solid. Yield: 433 mg, 67%. ^{1}H NMR (400 MHz, $CDCl_3$) δ 7.77 (d, *J* = 7.5 Hz, 2H), 7.50 (t, *J* = 7.3 Hz, 2H), 7.41 (t, *J* = 7.5 Hz, 2H), 7.33 – 7.26 (m, 5H), 7.25 – 7.12 (m, 5H), 7.09 (d, *J* = 7.0 Hz, 2H), 6.52 (d, *J* = 6.5 Hz, 1H), 5.74 (s, 1H), 5.25 (d, *J* = 6.1 Hz, 1H), 4.55 (d, *J* = 6.4 Hz, 1H), 4.39 (dd, *J* = 10.4, 6.9 Hz, 2H), 4.27 – 4.18 (m, 1H), 4.14 (t, *J* = 6.9 Hz, 1H), 3.15 – 2.88 (m, 6H), 1.83 (s, 2H), 1.29 – 1.12 (m, 10H), 0.87 (t, *J* = 7.0 Hz, 3H). ^{13}C NMR (101 MHz, $CDCl_3$) δ 170.61, 169.96, 156.10, 143.64, 141.32, 136.43, 136.00, 129.26, 128.87, 128.69, 127.85, 127.30, 127.14, 127.08, 125.07, 124.99, 120.08, 67.22, 56.28, 54.49, 47.04, 39.70, 38.21, 38.11, 31.83, 29.23, 29.21, 26.82, 22.68, 14.16. MS-ESI: calculated for $[M+H]^+$ ($C_{41}H_{48}O_4N_3$): *m/z* 646.36, found: *m/z* 646.24.

5: To a solution of **4** (2.58 g, 4 mmol) in $CHCl_3$ (20 mL) was added piperidine (2.0 mL), and reaction was allowed to stir at room temperature for 12 h. The solvent was then removed in *vacuo* and the crude product was purified by flash column chromatography (MeOH:CH_2Cl_2 = 1:20, v:v) to yield product **NH2-Phe-Phe-C8**. Fmoc-Phe-OH (387 mg, 1.0 mmol), **NH2-Phe-Phe-C8** (423 mg, 1.0 mmol) and BOP (486 mg, 1.1 mmol) were dissolved in 10 mL CH_2Cl_2/DMF (8:2, v:v) to which diisopropylamine (0.39 ml, 2.2 mmol) was added. The reaction mixture was stirred for 10 hours at room temperature. Solvent was removed in *vacuo* and the crude product was dissolved in MeOH (30 mL), which was recrystallized from acetonitrile to yield the pure product **5** as a white solid. Yield: 492 mg, 62%. ^{1}H NMR (400 MHz, DMSO) δ 8.21 (d, *J* = 8.2 Hz, 1H), 8.09 (d, *J* = 8.1 Hz, 1H), 7.90 – 7.78 (m, 3H), 7.59 (d, *J* = 8.4 Hz, 2H), 7.45 – 7.35 (m, 2H), 7.29 – 7.10 (m, 14H), 4.60 – 4.42 (m, 2H), 4.24 – 4.04 (m, 3H), 3.07 – 2.63 (m, 9H), 1.40 – 0.99 (m, 12H), 0.84 (t, *J* = 6.9 Hz, 3H). ^{13}C NMR (101 MHz, DMSO) δ 171.81, 170.94, 170.67, 162.78, 156.13, 144.22, 144.15, 141.11, 141.10, 138.61, 138.01, 137.93, 129.74, 129.66, 129.62, 128.53, 128.45, 128.43, 128.09, 127.53, 126.73, 126.67, 125.81, 125.72, 120.56, 66.12, 56.52, 54.49, 54.21, 46.98, 31.75, 29.41, 29.22, 29.15, 26.76, 22.60, 14.46. MS-ESI: calculated for $[M+H]^+$ ($C_{50}H_{57}O_5N_4$): *m/z* 793.43, found: *m/z* 793.18.

F28: **2** (324 mg, 1.0 mmol), **NH2-Phe-Phe-C8** (423mg, 1.0 mmol) and BOP (486 mg, 1.1 mmol) were dissolved in 10 mL CH_2Cl_2/DMF (8:2, v:v) to which diisopropylamine (0.39 ml, 2.2 mmol) was added. The reaction mixture was stirred for 10 hours at room temperature. Solvent was removed in *vacuo* and the crude product was purified by flash column chromatography (MeOH:CH_2Cl_2 = 1:50, v:v) to afford the pure product **F28** as a yellow solid. Yield: 438 mg, 60%. ^{1}H NMR (400 MHz, DMSO) δ 8.87 (d, *J* = 8.2 Hz, 1H), 8.68 (s, 2H), 8.24 (d, *J* = 8.2 Hz, 1H), 8.16 (d, *J* = 1.5 Hz, 1H), 8.02 – 7.73 (m, 6H), 7.54 – 7.40 (m, 2H), 7.37 – 7.05 (m, 8H), 4.72 (ddd, *J* = 10.6, 8.3, 4.5 Hz, 1H), 4.47 (td, *J* = 8.4, 5.8 Hz, 1H), 3.60 (s, 2H), 3.09 – 2.77 (m, 5H), 2.51 (d, *J* = 9.3 Hz, 2H), 1.44 – 0.99 (m, 12H), 0.82 (t, *J* = 6.8 Hz, 3H). ^{13}C NMR (101 MHz, DMSO) δ 171.33, 170.80, 165.04, 150.88, 142.30, 142.22, 138.68, 138.19, 137.53, 134.80, 132.76, 131.37, 129.68, 129.57, 129.01, 128.55, 128.51, 128.45, 128.31, 127.24, 126.73, 124.74, 124.54, 95.40, 94.06, 86.60, 55.55, 55.42, 54.65, 37.31, 36.95, 36.91, 31.76, 29.42, 29.23, 29.17, 26.78, 22.60, 14.45. MS-ESI: calculated for $[M+H]^+$ ($C_{47}H_{48}O_3N_5$): *m/z* 730.38, found: *m/z* 730.26.

F38: To a solution of **5** (3.17 g, 4 mmol) in $CHCl_3$ (20 mL) was added piperidine (2.0 mL), and

reaction was allowed to stir at room temperature for 12 h. The solvent was then removed in *vacuo* and the crude product was purified by flash column chromatography (MeOH:CH_2Cl_2 = 1:20, v:v) to yield product **NH2-Phe-Phe-Phe-C8**. **2** (324 mg, 1.0 mmol), **NH2-Phe-Phe-Phe-C8** (571 mg, 1.0 mmol) and BOP (486 mg, 1.1 mmol) were dissolved in 10 mL CH_2Cl_2/DMF (8:2, v:v) to which diisopropylamine (0.39 ml, 2.2 mmol) was added. The reaction mixture was stirred for 10 hours at room temperature. Solvent was removed in *vacuo* and the crude product was purified by flash column chromatography (MeOH:CH_2Cl_2 = 1:50, v:v) to afford the pure product **F38** as a yellow solid. Yield: 465 mg, 53%. ^{1}H NMR (400 MHz, DMSO) δ 8.86 (d, *J* = 8.4 Hz, 2H), 8.68 (ddd, *J* = 3.9, 3.4, 2.4 Hz, 2H), 8.23 – 8.11 (m, 3H), 7.95 – 7.76 (m, 6H), 7.48 (ddd, *J* = 7.6, 4.8, 1.3 Hz, 3H), 7.29 – 7.14 (m, 10H), 4.80 – 4.63 (m, 2H), 4.60 – 4.36 (m, 4H), 3.12 – 2.72 (m, 9H), 1.44 – 1.02 (m, 12H), 0.83 (t, *J* = 6.9 Hz, 3H). ^{13}C NMR (101 MHz, DMSO) δ 171.46, 170.90, 170.70, 164.94, 150.91, 142.33, 142.25, 138.75, 138.05, 138.01, 137.49, 134.79, 132.74, 131.34, 129.74, 129.62, 129.54, 129.00, 128.54, 128.44, 128.28, 127.20, 126.73, 124.71, 124.52, 95.42, 94.08, 86.54, 55.25, 54.49, 54.39, 31.75, 29.41, 29.22, 29.14, 26.77, 22.59, 14.45. MS-ESI: calculated for $[M+H]^+$ ($C_{56}H_{57}O_4N_6$): *m/z* 877.44, found: *m/z* 877.62.

7: **6** (1.33 g, 5.00 mmol), 1-octanol (0.78 ml, 5.00 mmol), EDC (1.15 g, 6.00 mmol) and DMAP (1.22 g, 10.0 mmol) were dissolved in CH_2Cl_2/DMF (25 mL:5 mL). The reaction mixture was stirred for 24 h at room temperature. Solvent was removed *in vacuo* and the crude product was dissolved in CH_2Cl_2 (30 mL), and washed with water (2 x 40 mL) the crude product was purified by flash column chromatography (Hexane:EA = 8:1, v:v) to give the target compound **7** as a white solid. Yield: 1.70 g, 90%. ^{1}H NMR (400 MHz, $CDCl_3$) δ 7.31 – 7.26 (m, 2H), 7.24 (dd, *J* = 5.2, 1.9 Hz, 1H), 7.13 (d, *J* = 6.8 Hz, 2H), 4.98 (d, *J* = 8.1 Hz, 1H), 4.57 (dd, *J* = 14.1, 6.1 Hz, 1H), 4.12 – 4.03 (m, 2H), 3.13 – 3.02 (m, 2H), 1.60 – 1.55 (m, 2H), 1.42 (s, 9H), 1.27 (s, 10H), 0.88 (d, *J* = 7.1 Hz, 3H). ^{13}C NMR (101 MHz, $CDCl_3$) δ 172.03, 155.11, 136.11, 129.37, 128.53, 127.00, 65.58, 54.46, 38.47, 31.81, 29.20, 29.18, 28.49, 28.33, 25.85, 22.68, 14.14. MS-ESI: calculated for $[M+Na]^+$ ($C_{22}H_{35}O_4NNa$): *m/z* 400.28, found: *m/z* 400.37.

8: Compound **7** (1.00 g, 2.66 mmol) was dissolved in CH_2Cl_2 (20 mL), with an installation of N_2 balloon on top of the round bottom flask. This solution was cooled to 0 ºC using an ice bath. TFA (10 mL, 26.6 mmol) was slowly added to the solution. After that the reaction was allowed to stir at room temperature for 12 h. Then the reaction mixture was neutralized using saturated aqueous solution of $NaHCO_3$ in the 0 ºC ice bath. The product was extracted with CH_2Cl_2 (4 x 50 mL).

Combination of the organic layer and drying over anhydrous Na_2SO_4 gave the pure product **8** as a light yellow oil, which was directly used in the next step without further purification. Yield: 0.68 g, 92%.

F8-esters: **2** (324 mg, 1.00 mmol), **8** (277 mg, 1.00 mmol) and BOP (486 mg, 1.10 mmol) were dissolved in CH_2Cl_2/DMF (8 mL:2 mL) to which N,N-diisopropylethylamine (0.39 ml, 2.20 mmol) was added. The reaction mixture was stirred for 24 h at room temperature. Solvent was removed *in vacuo*, and the crude product was dissolved in CH_2Cl_2 (30 mL) and washed with water (2 x 40 mL). The crude product was then purified by flash column chromatography (MeOH:CH_2Cl_2 = 1:200, v:v) to give the target compound **F8-eter** as a dark brown solid. Yield: 496 mg, 85%. ^{1}H NMR (400 MHz, $CDCl_3$) δ 8.69 – 8.63 (m, 2H), 8.01 (d, *J* = 1.4 Hz, 1H), 7.77 – 7.67 (m, 6H), 7.32 – 7.24 (m, 5H), 7.17 – 7.13 (m, 2H), 6.76 (d, *J* = 7.5 Hz, 1H), 5.06 (dd, *J* = 13.3, 5.8 Hz, 1H), 4.19 – 4.08 (m, 2H), 3.26 (qd, *J* = 13.9, 5.8 Hz, 2H), 1.67 – 1.58 (m, 2H), 1.27 (dd, *J* = 15.1, 6.3 Hz, 10H), 0.87 (t, *J* = 6.9 Hz, 3H). ^{13}C NMR (101 MHz, $CDCl_3$) δ 170.50, 164.17, 148.91, 148.86, 141.67, 141.64, 135.54, 135.51, 134.72, 132.89, 131.54, 129.71, 128.30, 127.63, 127.28, 127.03, 126.84, 126.38, 126.20, 124.63, 122.37, 122.30, 93.72, 92.30, 86.16, 64.92, 52.78, 36.89, 30.74, 28.14, 27.42, 24.81, 21.62, 13.11. MS-ESI: calculated for $[M+Na]^+$ ($C_{38}H_{37}O_3N_3Na$): *m/z* 606.28, found: *m/z* 606.46.

Proton transport study using HPTS assay and EC_{50} measurements using Hill analysis. Egg yolk L-α-phosphatidylcholine (EYPC, 1 ml, 25 mg/mL in $CHCl_3$, Avanti Polar Lipids, USA) solvents were removed under reduced pressure at room temperature. After drying the resulting film under high vacuum overnight at room temperature, the film was hydrated with 4-(2-hydroxyethyl)-1-piperazine-ethane sulfonic acid (HEPES) buffer solution (1.0 mL, 10 mM HEPES, 100 mM NaCl, pH 7.0) containing a pH-sensitive dye 8-hydrox-ypyrene-1,3,6-trisulfonic acid (HPTS, 1 mM) in thermostatic shaker-incubator at 37 °C for 2 h to give a milky suspension. The mixture was then subjected to 10 freeze-thaw cycles: freezing in liquid N_2 for 1 min and heating at 55 °C for 2 min. The vesicle suspension was extruded through polycarbonate membrane (0.1 μm) to produce a homogeneous suspension of large unilamellar vesicles (LUVs) of about 100 nm in diameter with HPTS encapsulated in the LUVs. The unencapsulated HPTS dye was separated from the LUVs by using size exclusion chromatography (stationary phase: Sephadex G-50, GE Healthcare, USA, mobile phase: HEPES buffer with 100 Mm NaCl at pH 7.0), and diluted with the mobile phase to yield 13 mL of 2.5 mM lipid stock solution. The HPTS-

containing LUV suspension (25 μL, 2.5 mM of lipid in 10 mM HEPES buffer containing 100 mM NaCl at pH 7.0) was added to a HEPES buffer solution (1.93 mL, 10 mM HEPES, 100 mM NaCl at pH 8.0) to create a pH gradient for ion transport study. A solution of channel molecules in DMSO (20 μL) was then injected into the suspension under gentle stirring. Upon the addition of channels, the emission of HPTS was immediately monitored at 510 nm with excitations at both 460 and 403 nm recorded simultaneously for 300 s using fluorescence spectrophotometer (Hitachi, Model F-7100, Japan) after which time an aqueous solution of Triton X-100 (20 μL, 20% v/v) was immediately added to achieve the maximum change in dye fluorescence emission. The final transport trace was obtained as a ratiometric value of I_{460}/I_{403}, and normalized based on the ratiometric value of I_{460}/I_{403} after addition of triton. The fractional changes R_H^+ was calculated for each curve using the normalized value of I_{460}/I_{403} at 300 s before the addition of triton, with ratiometric value of I_{460}/I_{403} at t = 0 s as 0% and that of I_{460}/I_{403} at t = 300 s after addition of triton as 100%. For determination of EC_{50} values, the ratiometric value of I_{460}/I_{403} at 300 s, after subtracting background intensity at t = 300, was normalized based on the ratiometric value of I_{460}/I_{403} after addition of triton. Fitting these normalized fractional transmembrane activities vs. channel concentrations using the Hill equation: $Y = 1/(1+ (EC_{50}/[C])^n)$ gave the Hill coefficient n and EC_{50} values.

Preparation of cholesterol-containing LUVs. EYPC (1 ml, 25 mg/mL in $CHCl_3$) and cholesterol (6.3 mg) were dissolved in $CHCl_3$ (10 mL). The mixed solvents were removed under reduced pressure at room temperature. After drying the resulting film under high vacuum overnight at room temperature, the film was hydrated with HEPES buffer solution (1.0 mL, 10 mM HEPES, 100 mM NaCl, pH 7.0) containing a pH-sensitive dye HPTS (1 mM) in thermostatic shaker-incubator at 37 °C for 2 h to give a milky suspension. The mixture was then subjected to 10 freeze-thaw cycles: freezing in liquid N_2 for 1 min and heating at 55 °C for 2 min. The vesicle suspension was extruded through polycarbonate membrane (0.1 μm) to produce a homogeneous suspension of LUVs of ~100 nm in diameter with HPTS encapsulated inside. The unencapsulated HPTS dye was separated from the LUVs by using size exclusion chromatography (stationary phase: Sephadex G-50, mobile phase: HEPES buffer with 100 Mm NaCl), and diluted with the mobile phase to yield 13 mL of 2.5 mM lipid stock solution.

The HPTS assay for cation selectivity. Method 1: The HPTS-containing LUV suspension (25 μL, 2.5 mM of lipid in 10 mM HEPES buffer containing 100 mM NaCl at pH 7.0) was added to

a HEPES buffer solution (1.93 mL, 10 mM HEPES, 100 mM MCl at pH 8.0, where M^+= Li^+, Na^+, K^+, Rb^+, and Cs^+) to create a pH gradient for ion transport study. A solution of monopeptide molecule **F14** at a final concentration of 5 μM in DMSO was then injected into the suspension under gentle stirring. **Method 2:** The HPTS-containing LUV suspension (25 μL, 2.5 mM of lipid in 10 mM HEPES buffer at pH 7.0) was added to a HEPES buffer solution (1.93 mL, 10 mM HEPES, 200 mM Na_2SO_4 at pH 7.0, where M^+ = Li^+, Na^+, K^+, Rb^+, Cs^+ and Mg^{2+}) to create a metal ion gradient for ion transport study. A solution of monopeptide molecule **F14** at concentrations of 5 and 10 μM in DMSO was then injected into the suspension under gentle stirring. **Method 3:** The HPTS-containing LUV suspension (25 μL, 2.5 mM of lipid in 10 mM HEPES buffer at pH 7.0) was added to a HEPES buffer solution (1.93 mL, 10 mM HEPES, 200 mM $CaCl_2$, $MgCl_2$ or NaCl at pH 7.0) to concurrently create gradients in pH and metal ion for ion transport study. A solution of monopeptide molecule **F14** at 5 μM in DMSO was then injected into the suspension under gentle stirring.

The HPTS assay for anion selectivity. Method 1: The SPQ-containing LUV suspension (25 μL, 200 mM $NaNO_3$) was added to a NaCl solution (1.93 mL, 200 mM NaCl) to create anion concentration gradients for chloride transport study. A solution of **F14** or **IL8** at a final concentration of 5 μM in DMSO was then injected into the suspension under gentle stirring. **Method 2:** The HPTS-containing LUV suspension (25 μL, 2.5 mM of lipid in 10 mM HEPES buffer containing 50 mM Na_2SO_4 at pH 7.0) was added to a HEPES buffer solution (1.93 mL, 10 mM HEPES, 50 mM Na_2SO_4 at pH 8.0) to create a pH gradient for ion transport study. A solution of monopeptide molecule **F14** at final concentrations of 5 and 10 μM in DMSO was then injected into the suspension under gentle stirring.

Water transport experiment. DOPC (1-palmitoyl-2-oleoyl-sn-glycero-3-phospho- choline, 0.24 ml, 25 mg/mL in $CHCl_3$, Avanti Polar Lipids, USA) and channel samples (**F14** or gA in chloroform) were mixed at lipid:channel molar ratios of 500:1 and 168:1, respectively, in micro-tubes (2 ml). The solvent was removed by N_2 flow and the resulting film was dried under high vacuum overnight. HEPES buffer (10 mM HEPES, 100 mM NaCl, pH = 7.0, 1.0 mL) was then added, followed by vortexing the solution for 30 s and then ten cycles of sonication (37 kHz, power 100, 70 °C, 2.5 min) in order to maximize the extent of channel molecules incorporated in the membrane. A glass spatula was used if necessary to make sure the residue was fully detached from the surface of the micro-tube. The mixture was further subjected to 10 freeze-

thaw cycles (freezing in liquid N_2 for 1 min, and heating in 55 °C water bath for 2 min), and extruded at 80 °C for 15 times. The LUVs thus obtained contained 6 mg/mL of lipids, were stored in 4 °C fridge before use, and diluted six times with HEPES buffer to make 1 mg/mL of LUV for stopped flow measurement. The size of LUV (120 nm) was characterized by dynamic light scattering (Zetasizer Nano, Malvern Instruments Ltd., UK). The water permeability measurements were conducted on a stopped-flow instrument (Chirascan Circular Dichroism Spectrometer, Applied Photophysics, UK). Exposure of vesicles to three types of hypertonic osmolytes (Sucrose 0.3 M, 10 mM HEPES, 100 mM NaCl, pH = 7; 10 mM HEPES, 250 mM NaCl, pH = 7; or 10 mM HEPES, 100 mM NaCl, 150 mM KCl, pH = 7) resulted in the shrinkage of the vesicles due to an outwardly directed osmotic gradient. The abrupt decrease of the vesicle size leads to an increase in light scattering intensity at 90° angle based on the Rayleigh-Gans theory. The changes of light scattering intensity caused by vesicle shrinkage were recorded at a wavelength of 577 nm.

Membrane integrity using carboxyfluorescein assay. 25 μL of the LUV suspension containing 500 mM carboxyfluorescein dye, 100 mM NaCl and 10 mM HEPES buffer at pH = 7.5 was added to a HEPES buffer solution (1.93 mL, 10 mM HEPES, 100 mM NaCl, pH 7.5) to create a concentration gradient of CF dye for CF transport study. A solution of **F14** (5 or 10 μM) or natural pore-forming peptide Melittin (25, 125 or 250 nM) in DMSO was then injected into the suspension under gentle stirring. Upon the addition of pore-forming monopeptide molecules, the emission of carboxyfluorescein was immediately monitored at 517 nm with excitations at 492 nm for 300 s using fluorescence spectrophotometer (Hitachi, Model F-7100, Japan) after which time an aqueous solution of Triton X-100 (20 μL, 20% v/v) was immediately added. The final transport trace was obtained by normalizing the fluorescence intensity using the equation of $I_f = [(I_t - I_0)/(I_1 - I_0)]$, where I_f = fractional emission intensity, I_t = fluorescence intensity at time t, I_1 = fluorescence intensity after addition of Triton X-100, and I_0 = initial fluorescence intensity.

Determination of pKa using NMR spectroscopy

The equilibrium between a heterocyclic base (B) and its conjugate acid (BH^+), such as pyridine (eq 1), will shift depending on the pH of the solution. The dissociation constant for the pyridinium cation is given by equation 2. This equation can be manipulated, using logarithms, to obtain an expression that relates pKa of the pyridinium cation to solution pH and the concentration ratio of the two species (See equation 3).

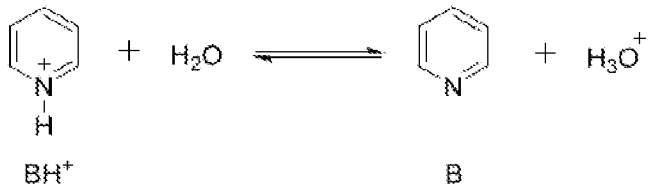

(1)

$$K_a = \frac{[H_3O^+][B]}{[BH^+]} \quad (2)$$

$$pK_a = pH + \log\frac{[BH^+]}{[B]} \quad (3)$$

The NMR shift of the pyridinium ring hydrogens is dependent on the relative concentrations of BH+ or B. If the solution is at a low pH and the species is 100% protonated (BH^+), it will have a chemical shift of υ_{BH+}. If the solution is at a high pH and the species is 100% deprotonted (B), it will have a chemical shift of υ_B. If the solution is at a pH where both species are present, it will have a chemical shift of υ. The chemical shift of υ is related to the chemical shift of the protonated and deprotonated forms by equation 4,

$$\nu = \nu_{BH^+} x_{BH^+} + \nu_B x_B \quad (4)$$

where υ is the observed chemical shift at the specified pH, and x_{BH+} and x_B are the mole fraction of the two species at the same specified pH. However, in order to determine the pKa of the pyridinium cation of interest, x_{BH+} and x_B must be calculated using the chemical shifts of the compound. This is accomplished by using equations 5 and 6. Equation 5 uses the chemical shift of a specific ring proton to determine the mole fraction of the deprotonated species (x_B) and equation 6 can be used to determine the mole fraction of the protonated species (x_{BH+}) since the sum of the two fractions must equal one.

$$x_B = \frac{\text{chemical shift at low pH - observed chemical shift}}{\text{chemical shift at low pH -chemical shift at high pH}} \quad (5)$$

$$x_{BH^+} + x_B = 1 \quad (6)$$

After the mole fraction of the two forms has been determined, the pKa can be estimated using equation 7. Equation 7 is similar to equation 3 except that concentrations of the two species have been replaced by mole fractions.

$$pK_a = pH + \log\frac{x_{BH^+}}{x_B} \quad (7)$$

Recording NMR sample spectra over a wide range of pH values: The pH probe is inserted into the test tube with the sample and the pH is recorded. Next, a portion of the sample is placed in a NMR tube and a spectrum is collected for that specific pH value. The sample in the NMR tube is then returned to the test tube containing the sample and the sample pH is adjusted with either HCl or KOH. When the solution has reached the desired pH, a portion of the sample is again placed in a NMR tube and a spectrum collected. This procedure is repeated until the spectra are collected for the desired number of pH values. The chemical shift of the peaks can then be plotted against the pH to derive the pKa (Figure 6).

Molecular dynamics simulations. Membrane builder in CHARM-GUI is used to build the initial structure. The protocol comprises six steps as described by Jo et al (J. Comput. Chem. 2008, 29, 1859-1865) which are sequentially performed in the following order: objects reading, objects orientation, system size determination, building lipid bilayer, assembling lipid bilayer and system equilibrium. In this work, the H-bonded structure, consisting of six molecules of **F8**, is placed in the center of the membrane made up of 128 POPC molecules. The membrane is then placed in a box of 70Å x 70 Å in width and 74 Å in height. 4794 water molecules are placed on the top side and bottom side of the membrane (2397 each side). Counter KCl ions were added to produce an ion concentration of 0.15 M. The simulation used the CHARMM36 (C36) force filed for lipids, CHARMM General Force Field (CGenFF) for the repeating unit of **F8** and the CHARMM TIP3P water model. The periodic boundary condition (PBC) were employed and the particle mesh Ewald (PME) method was used for long-range electrostatic interactions. The simulation time step was set to 2 fs in conjunction with the SHAKE algorithm to constrain the covalent bonds involving hydrogen atoms. The constructed system is first relaxed through molecular mechanics (MM) minimization of 20000 steps, then heated to 303.15 K using 50 ps NPT molecular dynamics (MD) simulations, and finally equilibrated using 200 ps NPT MD simulations. During MD simulations, the pressure was maintained at 1 bar. After equilibration steps, the production run of simulation was performed for 20 ns and the structure at the 20^{th} ns trajectory was used for analyzing stability of H-boned structure.

Cell lines. The human cancer cell lines (7786-O, A-431, A-498, A549, BT-474, DU145, HUH7, H69, H69AR, HCT116, HeLa, HepG2, PC-3, SH-SY5Y, U-87 MG, PC-9 and MCF-7) were purchased from ATCC (U.S.A.). Cancer cell lines A2780 and A2780cis were obtained from Sigma. The drug-resistant cell lines (PC-9/GR and MCF-7/LCC2) were provided by Professor Cheguo Cai (Medical Research Institute, Wuhan University, Wuhan, Hubei, China 430071) and Professor Zhesheng Chen (Department of Pharmaceutical Sciences, College of Pharmacy and Health Sciences, St. John's University, Queens, NY 11439), respectively. 786-O, PC-3, H69, A2780, H69AR and A549 were maintained in RPMI 1640 medium supplemented with 10% FBS. A-431, BT-474, DU145, HUH7, HCT116, HeLa, HepG2, SH-SY5Y, U-87MG, PC-9, PC-9/GR, MCF-7 and MCF-7/LCC2 cells were cultured in DMEM medium supplemented with 10% FBS. A-498 and A2780cis were cultured in the medium according to manufacturer's instruction. All cells were maintained at 37 °C in a humidified atmosphere containing 5% CO_2, and passaged with trypsin-EDTA (Life Technology) every 5–7 days.

***In vitro* anticancer study.** The cytotoxicity of channel compounds against various cancer cell lines was studied by CellTiter-Glo® Cell Viability Assay. The cells were seeded onto 96-well plates at 10,000 cells per well and incubated overnight. Channel compounds were prepared in DMSO as a stock solution and diluted with the growth medium at defined pHs (adjusted using 1M HCl to pH 6.8 and 7.4) to give final concentrations ranging from 0.01 to 100 μM. The media in the wells were replaced with 100 μL of the pre-prepared samples. Cisplatin or Tamoxifen were employed as positive and comparative controls in each experiment. The plates were then returned to the incubator and maintained in 5% CO_2 at 37°C for 48 h. 100 μL CellTiter-Glo solution was then added. The plates were incubated at room temperature for 10 min to stabilize the signal, and luminescence was measured with a microplate reader (Cytation 5, Biotek Instruments Inc., Canada). The cell viability was expressed as the ratio of the number of viable cells with treatment to that without treatment. The experiment was repeated three times independently. The results are shown in Figures

***In vivo* therapeutic efficacy of F8 in HCT116 xenograft nude mice.** The HCT116 xenograft nude mice model was constructed by injecting 1×10^6 cells to the right flank of BALB/c nude mice (6 weeks old). When the tumor volume reached 100 mm^3 after inoculation, the mice were randomly divided into 4 groups, 8 mice in each group. The mice in each group were injected intra-tumor with PBS, control vehicle, or **F8** at a dose of 20 mg/kg or 40 mg/kg (20% DMSO,

10% Tween 80, 70% PBS) once every 2 or 3 days for 20 days. During the treatment period, the tumor volume and body weight of the nude mice were measured. The tumor volume was calculated by the following formula: tumor volume = $l \times (w/2)^2$, where l and w are the length and width of the tumor. After the mice were sacrificed, the mouse tissues were separated and processed for histological analysis at Histopathology Unit (Biopolis Shared Facilities, Singapore). All animal experimental procedures were approved and performed following the guidelines of the National Advisory Committee on Laboratory Animal Research (NACLAR). The blood samples of mice were collected for hematological analysis.

Histological analysis of mice tissues. For histological analysis, the tissues were fixed with 3.7% formaldehyde, embedded with paraffin and sectioned. Subsequently, the tissues were stained with hematoxylin and eosin for histological observation under an optical microscope.

Hematological analysis of nude mice bearing HCT116 xenograft. The plasma was collected by centrifuging the blood samples at 3000 rpm. The plasma was then subjected to hematological analysis to determine biochemical indexes of blood urea, creatinine (CREA), alanine aminotransferase (ALT), asparatate aminotransferase (AST), total bilirubin (TBIL), chloride, potassium and sodium concentrations in blood of the mice.

Statistical analysis Data are expressed as mean ± standard deviation (s.d.). Statistical significance between two groups was determined by the unpaired Student's t-test. Results for more than two experimental groups were evaluated by one-way ANOVA to specify differences between groups. $P < 0.05$ was considered significantly different.

Table 3: Blood biochemistry analysis results[a]

Toxicity Test Results

F8 Concentration	0 mg/kg	20 mg/kg	40 mg/kg
Nephrotoxicity			
Creatinine (μmol/L)	< 9	< 9	< 9
Urea (mmol/L)	5.3 ± 1.0	5.5 ± 0.6	6.5 ± 0.5
Hepatotoxicity			
ALT (U/L)	34.0 ± 3.7	39.1 ± 17.3	30.4 ± 6.6
AST (U/L)	100.4 ± 12.8	103.4 ± 24.1	97.5 ± 41.8
TBIL (μmol/L)	≤ 4	≤ 4	≤ 3
Electrolytes			
Chloride (mmol/L)	117.5 ± 1.8	116.9 ± 1.5	119.4 ± 2.2
Potassium (mmol/L)	4.6 ± 0.4	4.7 ± 0.3	4.6 ± 0.1
Sodium (mmol/L)	150.4 ± 2.1	150.6 ± 1.5	150.9 ± 1.0
Sodium/Potassium	32.8 ± 2.9	32.0 ± 1.9	33.0 ± 1.1

[a] The nephrotoxicity (blood urea, creatinine), hepatotoxicity (ALT, AST, TBIL), and electrolytes (Na, K, etc.) were measured from the blood samples collected from the mice at the end of the 20-day treatments of **F8**.

***In vitro* hemolytic activity measurement:** Fresh mouse red blood cells (RBCs) were diluted 25 folds with PBS buffer to give an RBC stock suspension (4 V% blood cells). A 100 μL aliquot of RBC stock was added to a 96-well plate containing 100 μL stock solutions of proton channel **F8** at various concentrations (a serial of 2-fold dilution in PBS that contains 1% DMSO to improve solubility of **F8** in buffer). After 24h incubation at 37 °C, the contents of each well was pipetted into a micro-centrifuge tube and then centrifuged at 2000 rpm for 5 min. Hemolytic activity was determined as a function of hemoglobin release by measuring OD576 of 100 μL of the supernatant. A control solution that contains only PSB was used as a reference for 0% hemolysis. 100% hemolysis was measured by adding 0.5% Triton-X to the RBCs. The hemolytic activity was then calculated using the following equation:

$$\%\ Hemolysis = \frac{OD576\ (\boldsymbol{F8}) - OD576\ (PBS)}{OD576\ (Triton - X) - OD576\ (PBS)} X\ 100$$

CLAIMS

1. A compound of Formula (I), or a salt, solvate, stereoisomer and prodrug thereof for forming a proton channel in a lipid membrane:

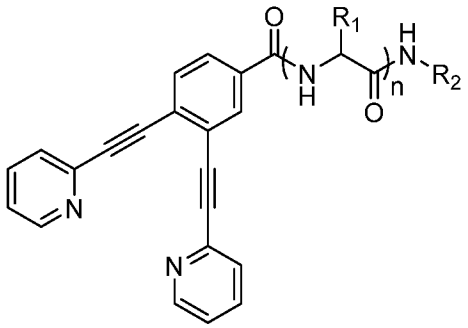

(I)

wherein R_1 is optionally substituted alkyl, optionally substituted alkenyl or optionally substituted alkynyl, optionally substituted arylalkyl, optionally substituted heteroarylalkyl, optionally substituted aryl, optionally substituted heteroaryl;

R_2 is an optionally substituted alkyl, optionally substituted alkenyl or optionally substituted alkynyl; and

n is an integer selected from 1 to 5.

2. The compound of claim 1, wherein R_1 is optionally substituted alkyl, optionally substituted arylalkyl or optionally substituted heteroarylalkyl.

3. The compound according to claim 1 or 2, wherein R_2 is optionally substituted C_5-C_{18} alkyl.

4. The compound according to any one of claims 1 to 3, wherein n is 1.

5. The compound according to any one of claims 1 to 4, the compounds of Formula (I) are selected from:

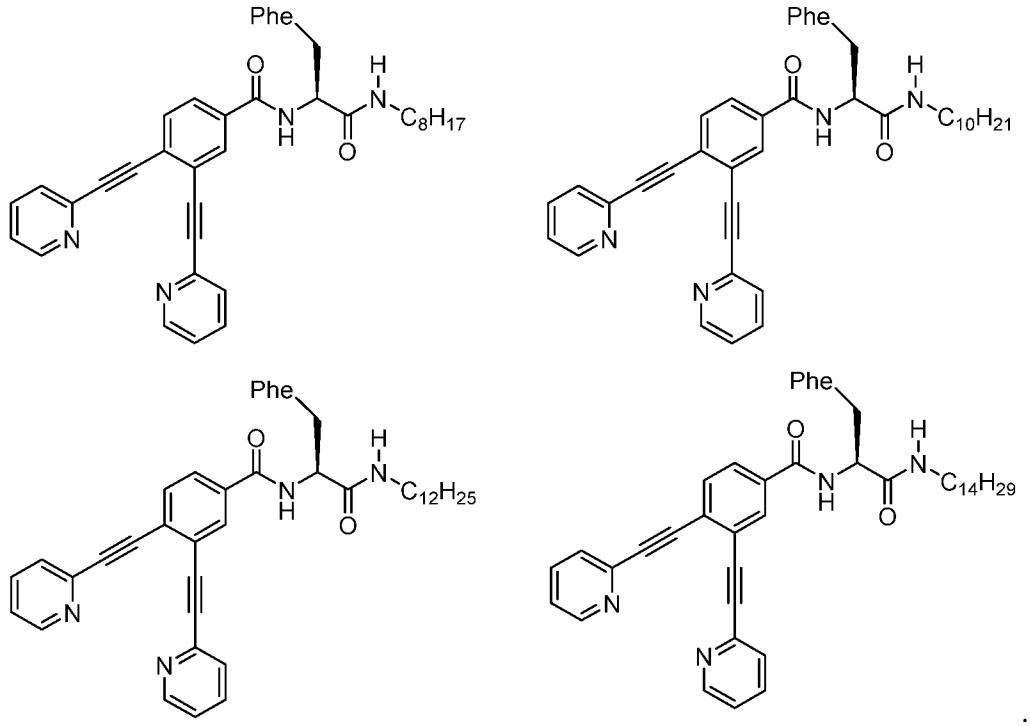

6. An assembly of two or more compounds of Formula (I) or a salt, solvate, stereoisomer and prodrug thereof, wherein the assembly of compounds is capable of forming a proton channel in a lipid membrane.

7. The assembly according to claim 6, comprising at least 6 compounds of Formula (I).

8. The assembly according to claim 6 or 7, formed via H-bonds.

9. A combination comprising:

a) a lipid membrane; and

b) an assembly of two or more compounds of Formula (I) or a salt, solvate, stereoisomer and prodrug thereof;

wherein the assembly of compounds is capable of forming a proton channel in the lipid membrane.

10. The combination according to claim 9, wherein the lipid membrane is a phospholipid bilayer.

11. A method of forming a proton channel in a lipid membrane, including the step of contacting the lipid membrane with two or more compounds of Formula (I) or a salt, solvate, stereoisomer and prodrug thereof.

12. A method of modulating a flow of protons through a lipid membrane, including the steps of:

a) providing a proton channel, the proton channel comprising an assembly of two or more compounds of Formula (I) or a salt, solvate, stereoisomer and prodrug thereof; and

b) imposing a proton gradient or membrane potential across the lipid membrane.

13. A pharmaceutical composition comprising an effective amount of a compound of Formula (I) or a pharmaceutically acceptable salt, solvate or prodrug thereof.

14. A method of treating cancer, comprising administering a therapeutically effective amount of compound of Formula (I) or a pharmaceutically acceptable salt, solvate or prodrug thereof to a subject in need, for a sufficient time and under conditions to treat the subject.

15. The method according to claim 14, wherein the cancer is selected from breast cancer, cervix adenocarcinoma, colorectal carcinoma, epidermoid carcinoma, glioblastoma, hepatocellular carcinoma, kidney carcinoma, lung cancer, neuroblastoma, ovarian carcinoma, prostate carcinoma, prostate adenocarcinoma, renal cell adenocarcinoma and small cell lung carcinoma.

16. A compound of Formula (I) or a pharmaceutically acceptable salt, solvate or prodrug thereof for use as a medicament in treating cancer in a subject in need thereof.

17. The compound for use according to claim 14, wherein the cancer is selected from breast cancer, cervix adenocarcinoma, colorectal carcinoma, epidermoid carcinoma, Glioblastoma, hepatocellular carcinoma, kidney carcinoma, lung cancer, neuroblastoma, ovarian carcinoma, prostate carcinoma, prostate adenocarcinoma, renal cell adenocarcinoma and small cell lung carcinoma.

18. Use of a therapeutically effective amount of a compound of Formula (I) or a pharmaceutically acceptable salt, solvate or prodrug thereof in the manufacture of a medicament for treating cancer in a subject in need thereof.

19. The use according to claim 18, wherein the cancer is selected from breast cancer, cervix adenocarcinoma, colorectal carcinoma, epidermoid carcinoma, Glioblastoma, hepatocellular carcinoma, kidney carcinoma, lung cancer, neuroblastoma, ovarian carcinoma, prostate carcinoma, prostate adenocarcinoma, renal cell adenocarcinoma and small cell lung carcinoma.

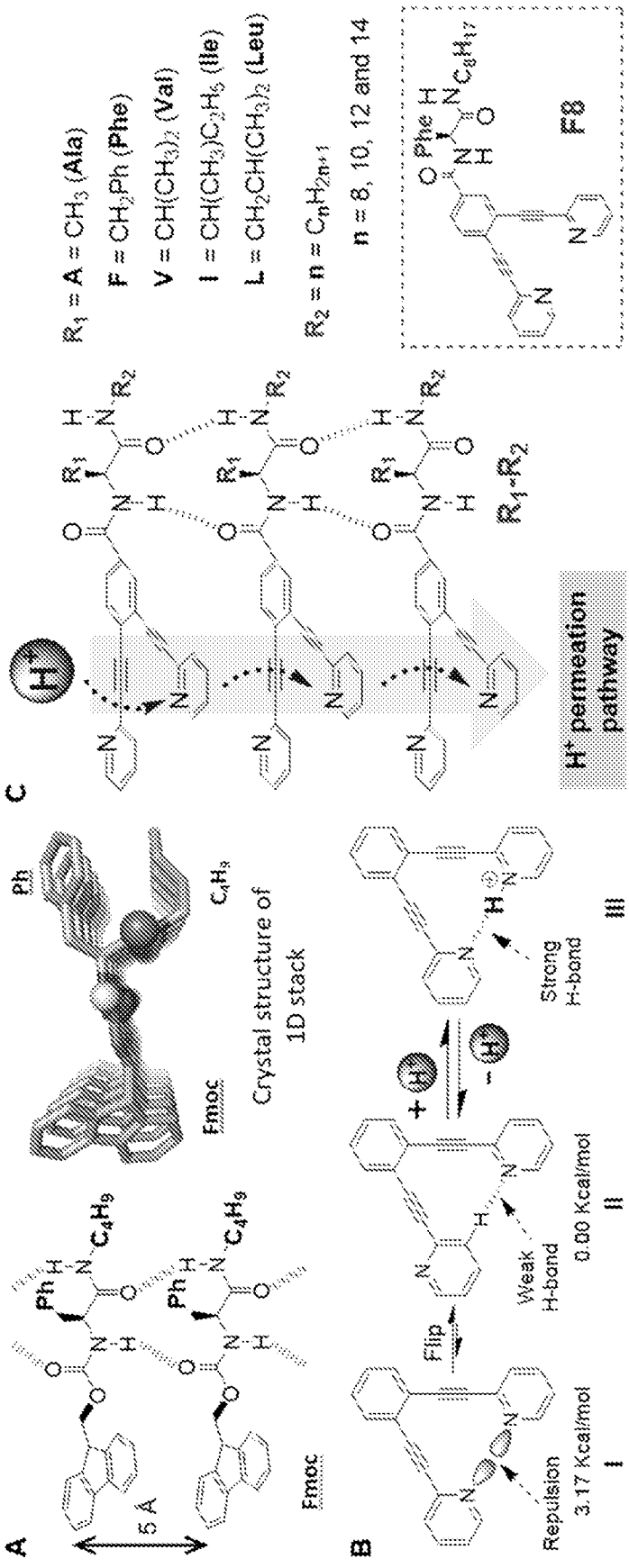
A
5 Å
Fmoc
Ph
C_4H_9
Fmoc
Crystal structure of
1D stack
B
Repulsion
3.17 Kcal/mol
I
Flip
Weak
H-bond
0.00 Kcal/mol
II
+ H+
- H+
Strong
H-bond
III
C
H+
R_1-R_2
H+ permeation
pathway
R_1 = A = CH_3 (Ala)
F = CH_2Ph (Phe)
V = $CH(CH_3)_2$ (Val)
I = $CH(CH_3)C_2H_5$ (Ile)
L = $CH_2CH(CH_3)_2$ (Leu)
R_2 = n = C_nH_{2n+1}
n = 8, 10, 12 and 14
Phe
F8

Figure 1

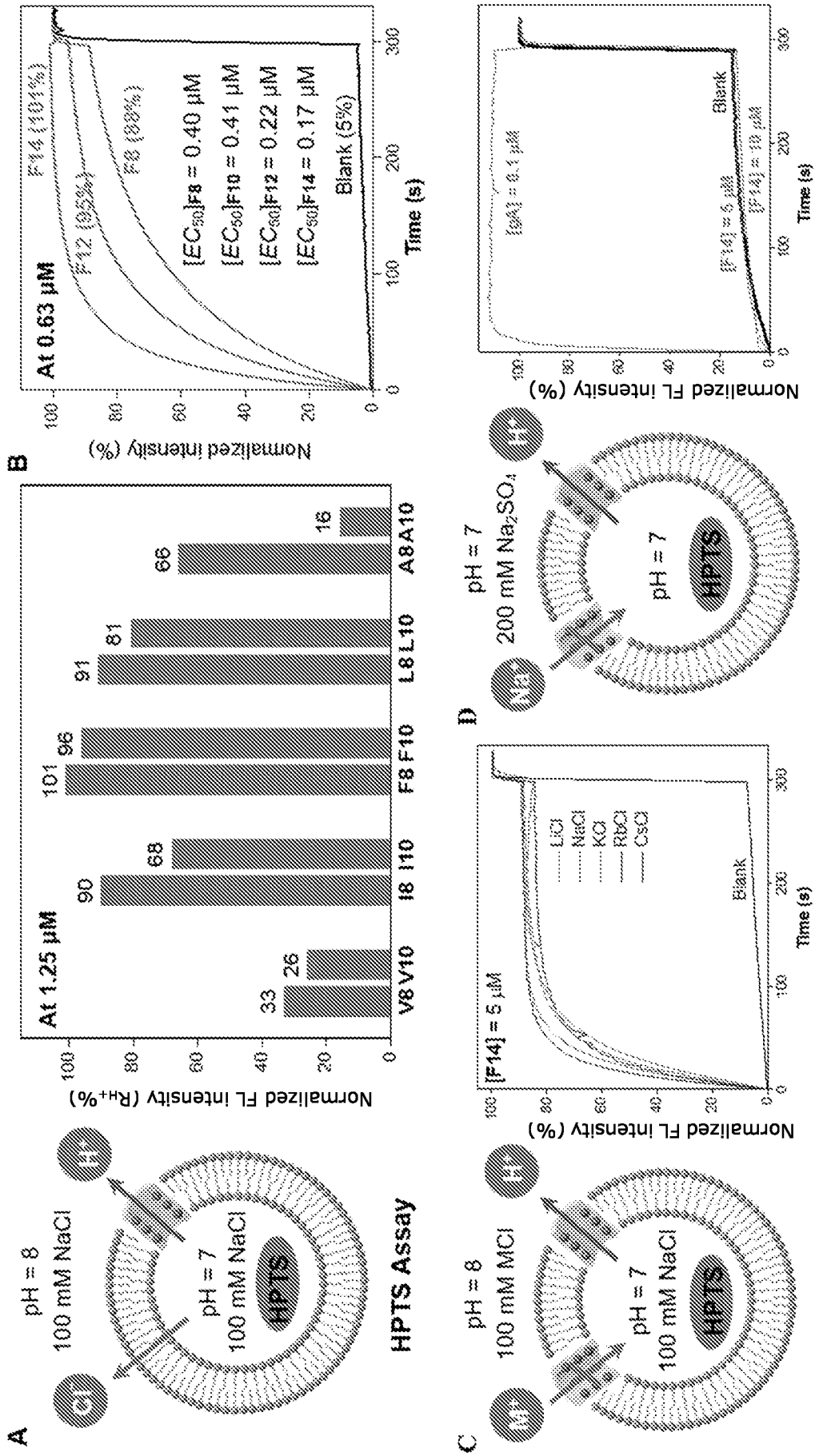

Figure 2(a)-(d) (continued)

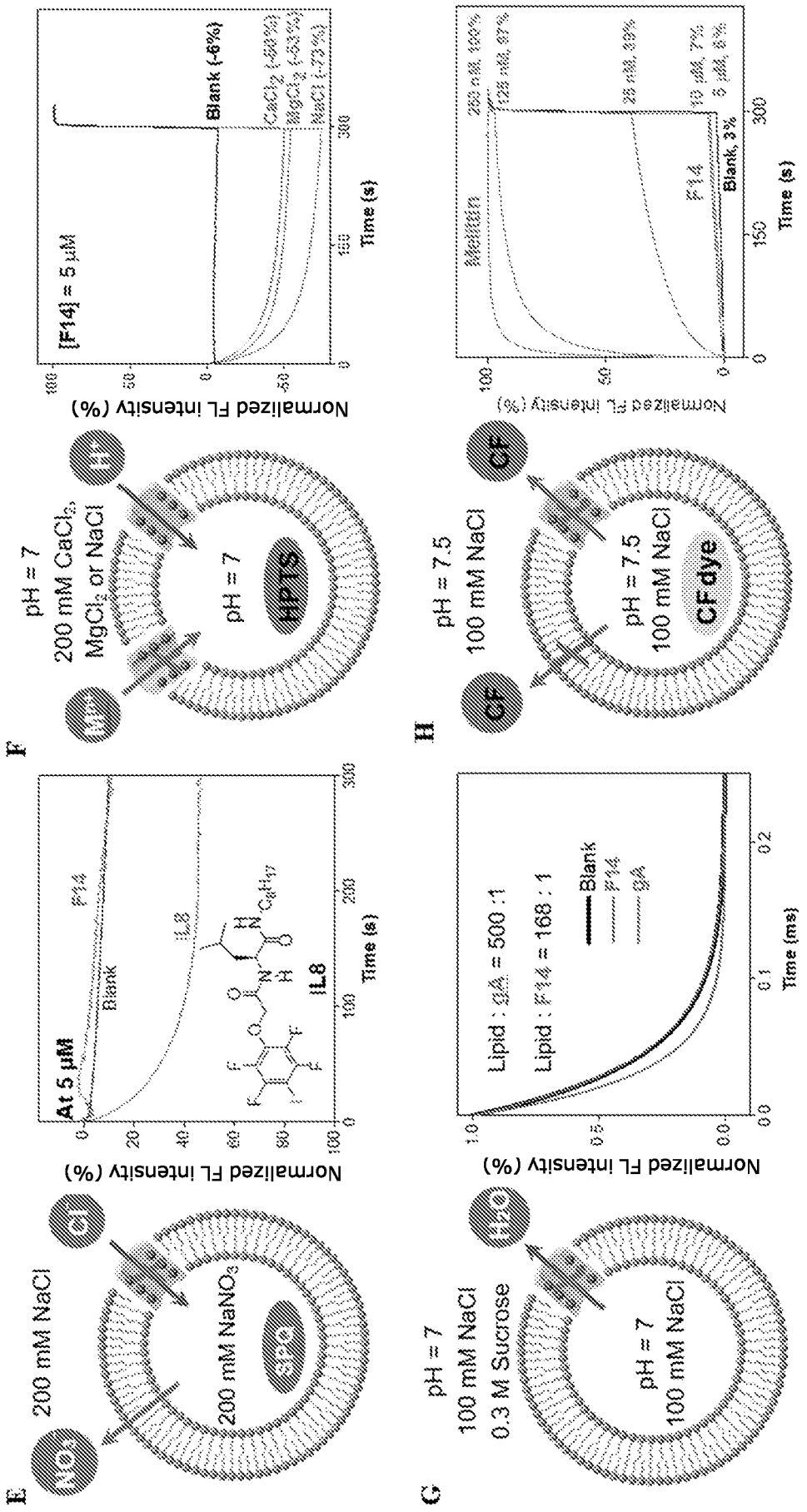

Figure 2(e)-(h) (end)

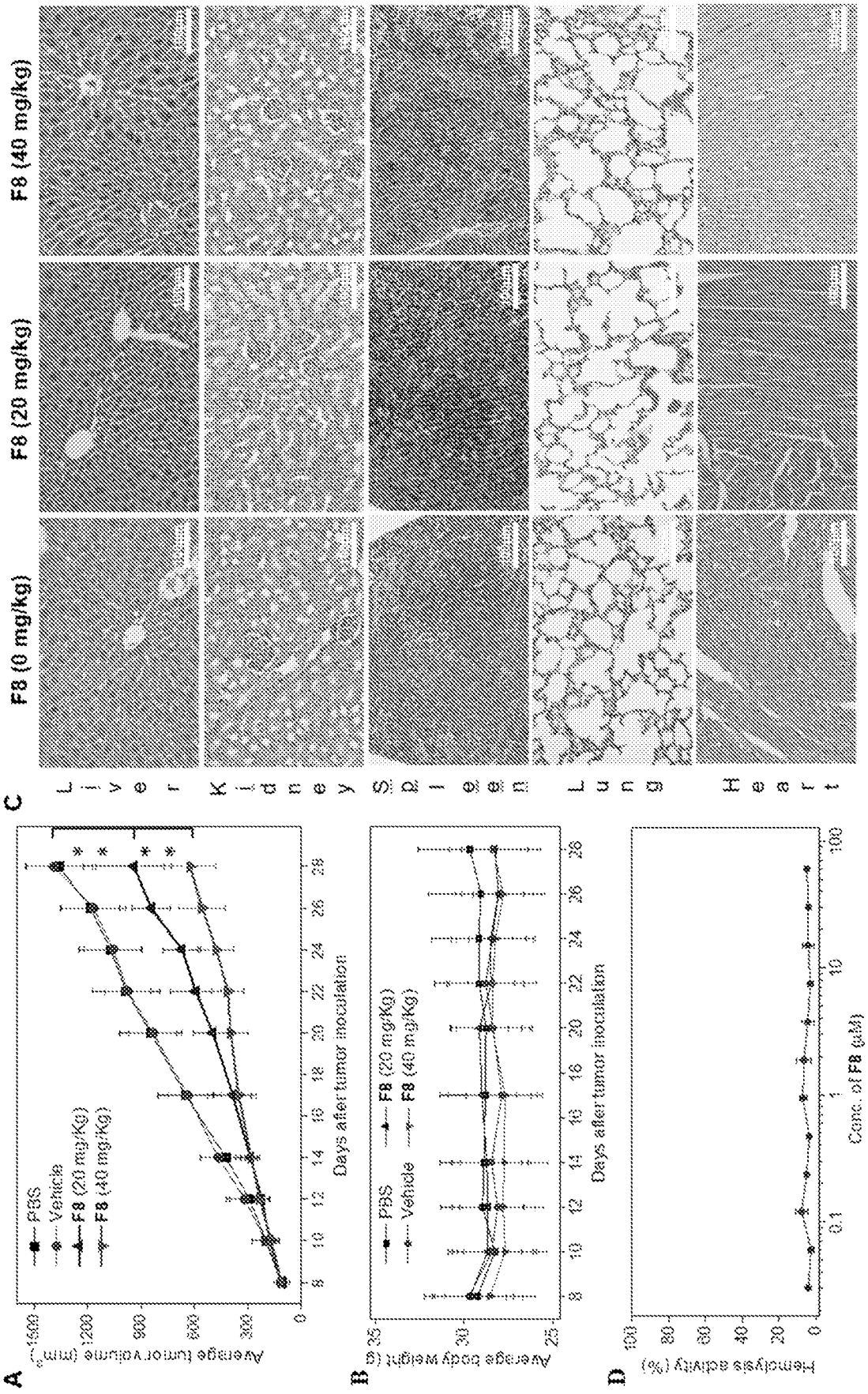
C
F8 (0 mg/kg)
F8 (20 mg/kg)
F8 (40 mg/kg)
Liver
Kidney
Spleen
Lung
Heart
A
Average tumor volume (mm³)
PBS
Vehicle
F8 (20 mg/Kg)
F8 (40 mg/Kg)
Days after tumor inoculation
B
Average body weight (g)
PBS
Vehicle
F8 (20 mg/Kg)
F8 (40 mg/Kg)
Days after tumor inoculation
D
Hemolysis activity (%)
Conc. of F8 (μM)

Figure 3

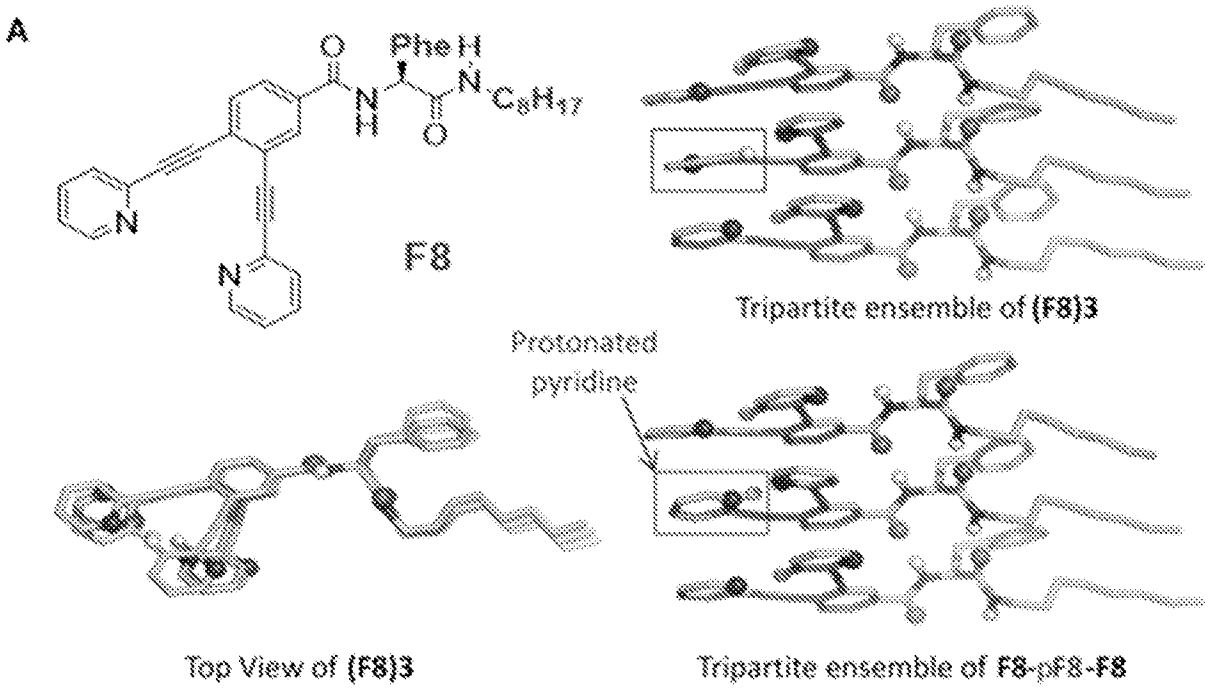
A
Phe
H
N
C_8H_{17}
O
N
H
O
N
N
F8
Tripartite ensemble of (F8)3
Protonated pyridine
Top View of (F8)3
Tripartite ensemble of F8-pF8-F8

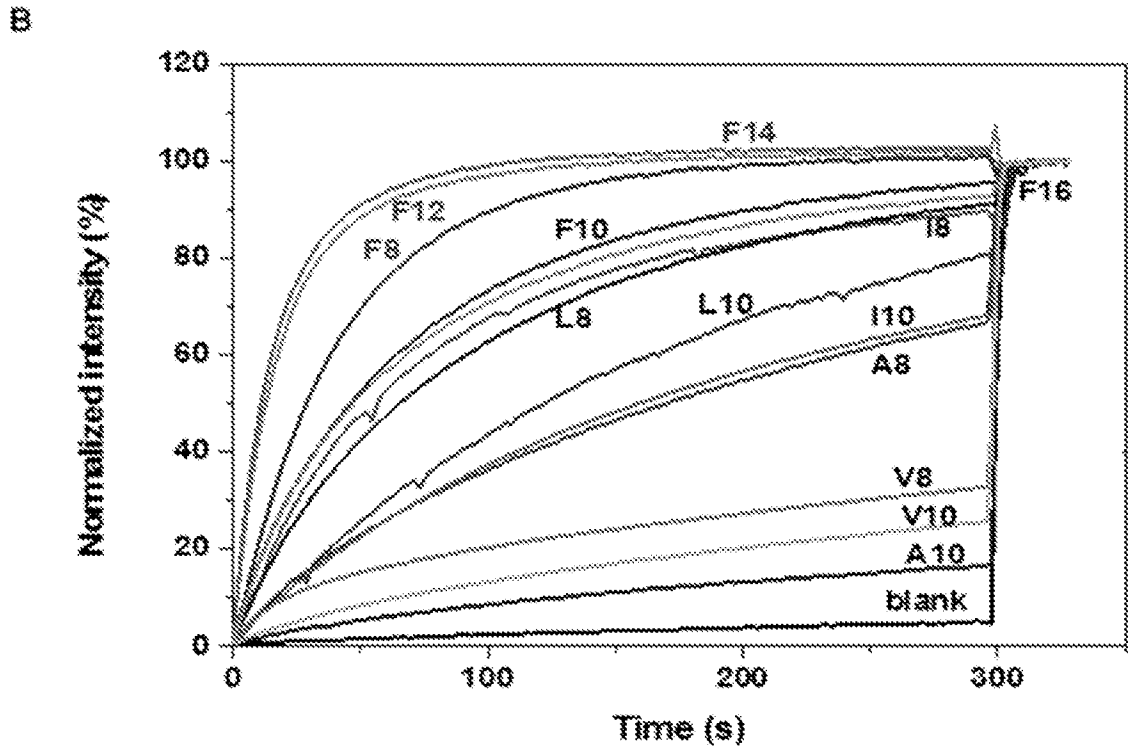
B
Normalized intensity (%)
Time (s)
0
20
40
60
80
100
120
0
100
200
300
F14
F16
F12
F8
F10
I8
L8
L10
I10
A8
V8
V10
A10
blank

Figure 4

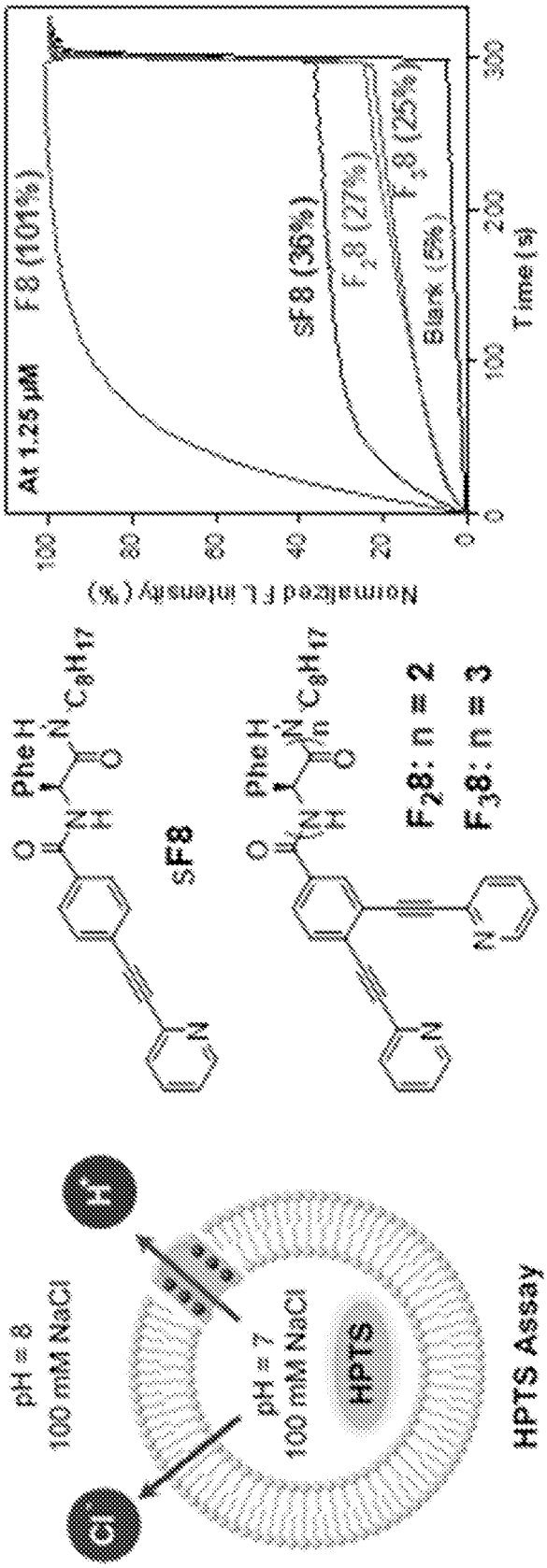
At 1.25 μM
F8 (101%)
sF8 (36%)
F28 (27%)
F38 (25%)
Blank (6%)
Normalized F.L. Intensity (%)
Time (s)
sF8
F28: n = 2
F38: n = 3
pH = 8
100 mM NaCl
pH = 7
100 mM NaCl
HPTS
HPTS Assay

Figure 5

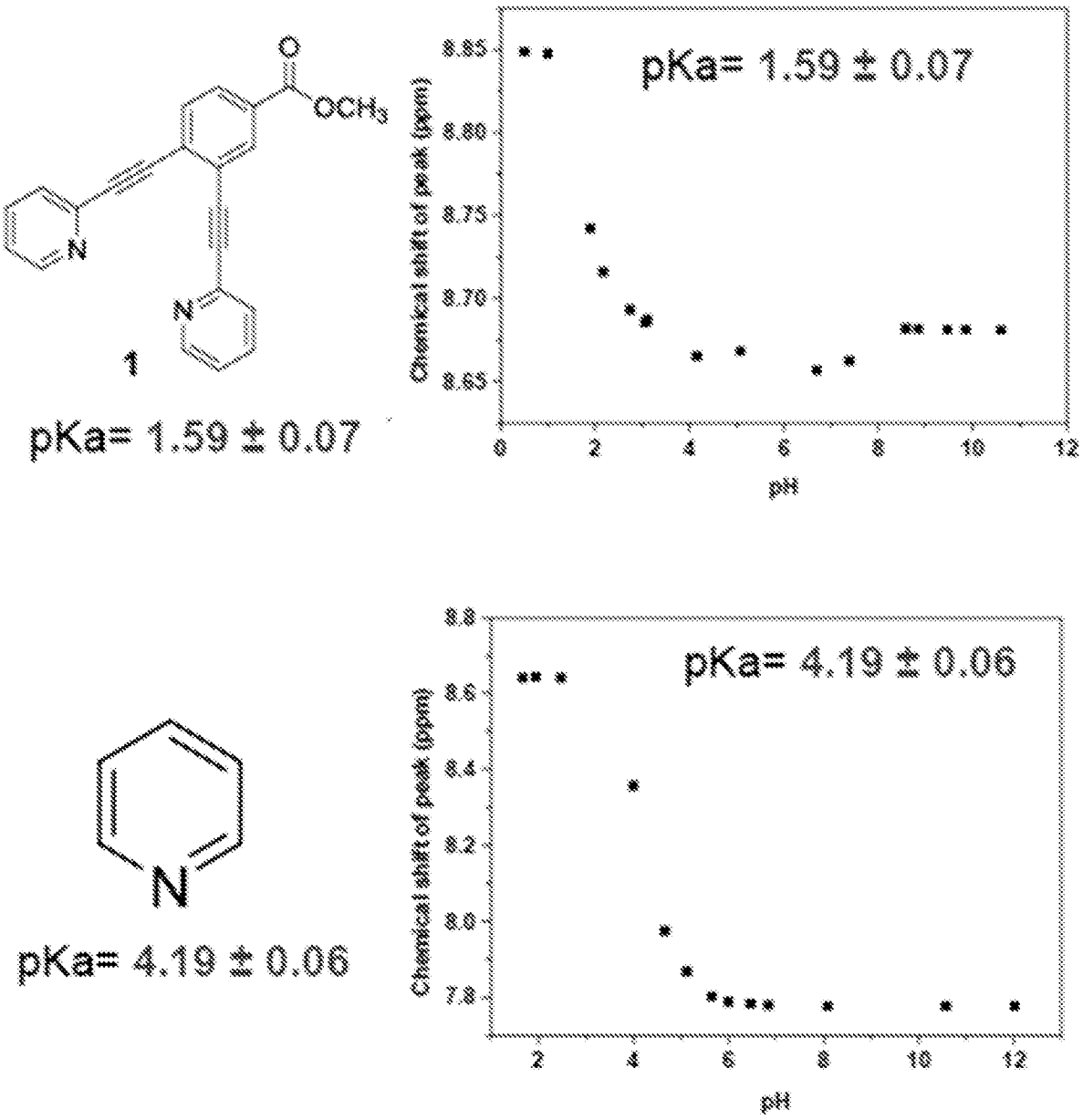
O
OCH3
N
N
1
pKa= 1.59 ± 0.07
Chemical shift of peak (ppm)
8.85
8.80
8.75
8.70
8.65
pKa= 1.59 ± 0.07
0
2
4
6
8
10
12
pH
N
pKa= 4.19 ± 0.06
Chemical shift of peak (ppm)
8.8
8.6
8.4
8.2
8.0
7.8
pKa= 4.19 ± 0.06
2
4
6
8
10
12
pH

Figure 6

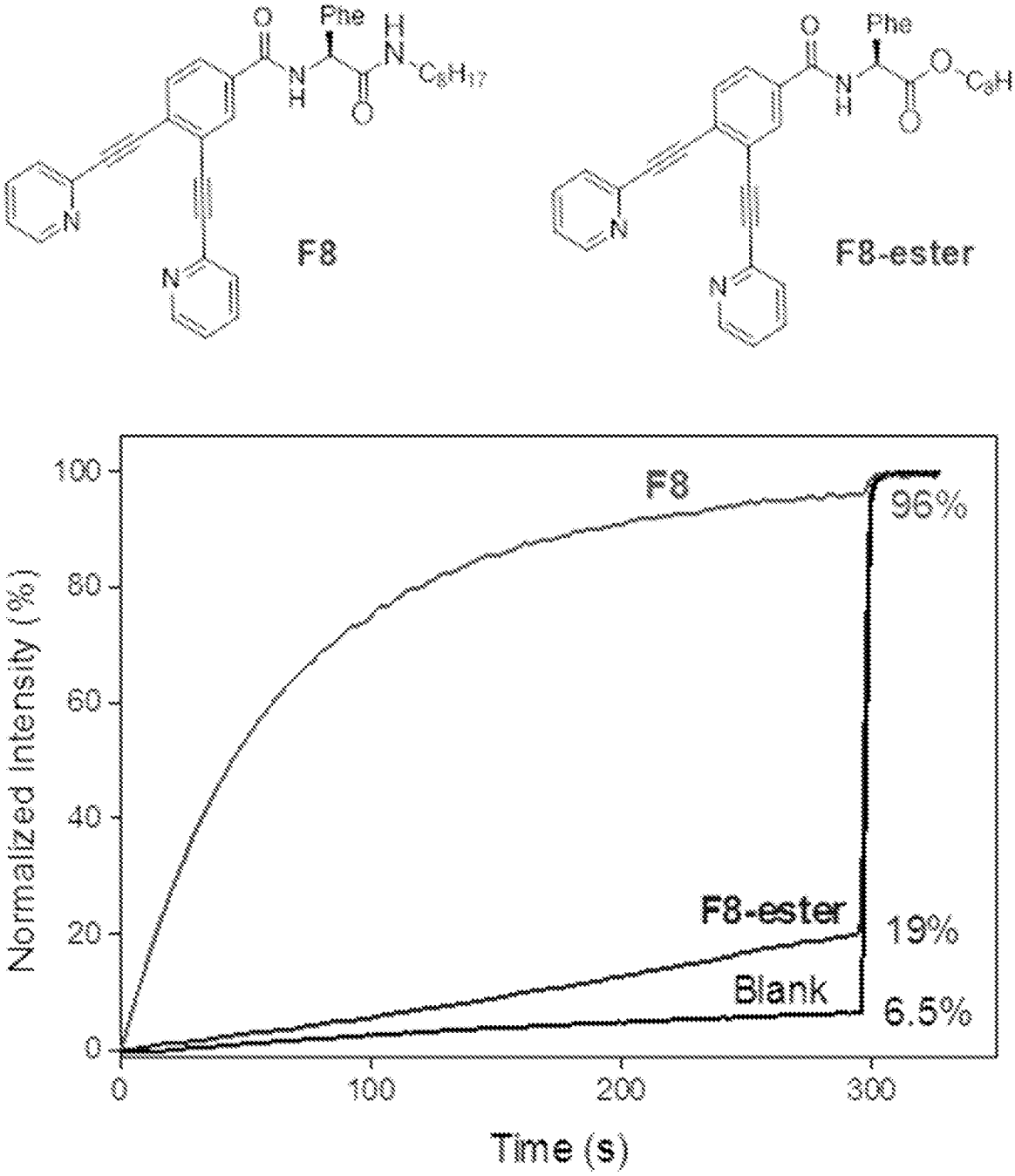
Phe
F8
Phe
F8-ester
F8
96%
F8-ester
19%
Blank
6.5%
Normalized Intensity (%)
Time (s)
0
20
40
60
80
100
0
100
200
300

Figure 7

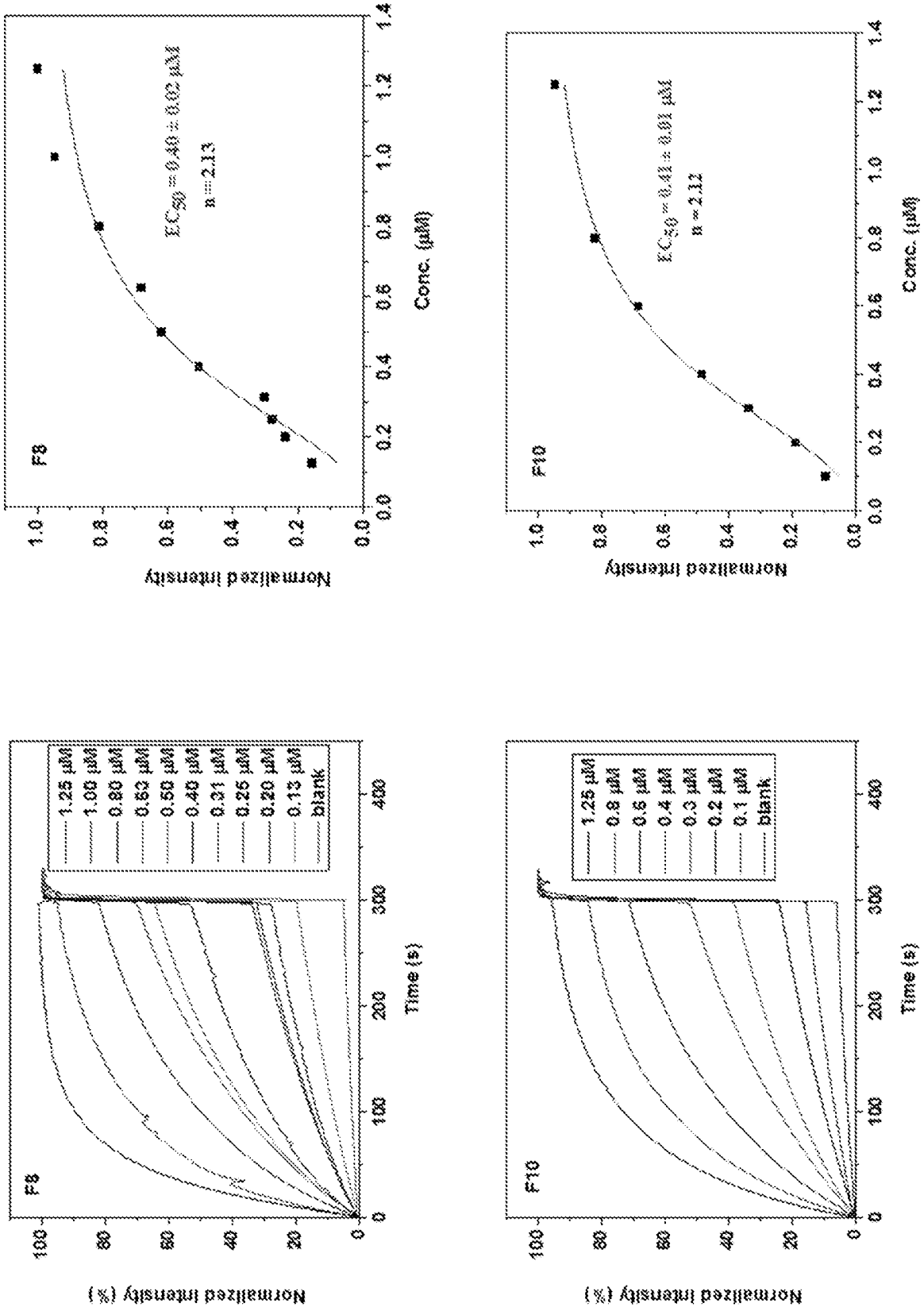

Figure 8 (continued)

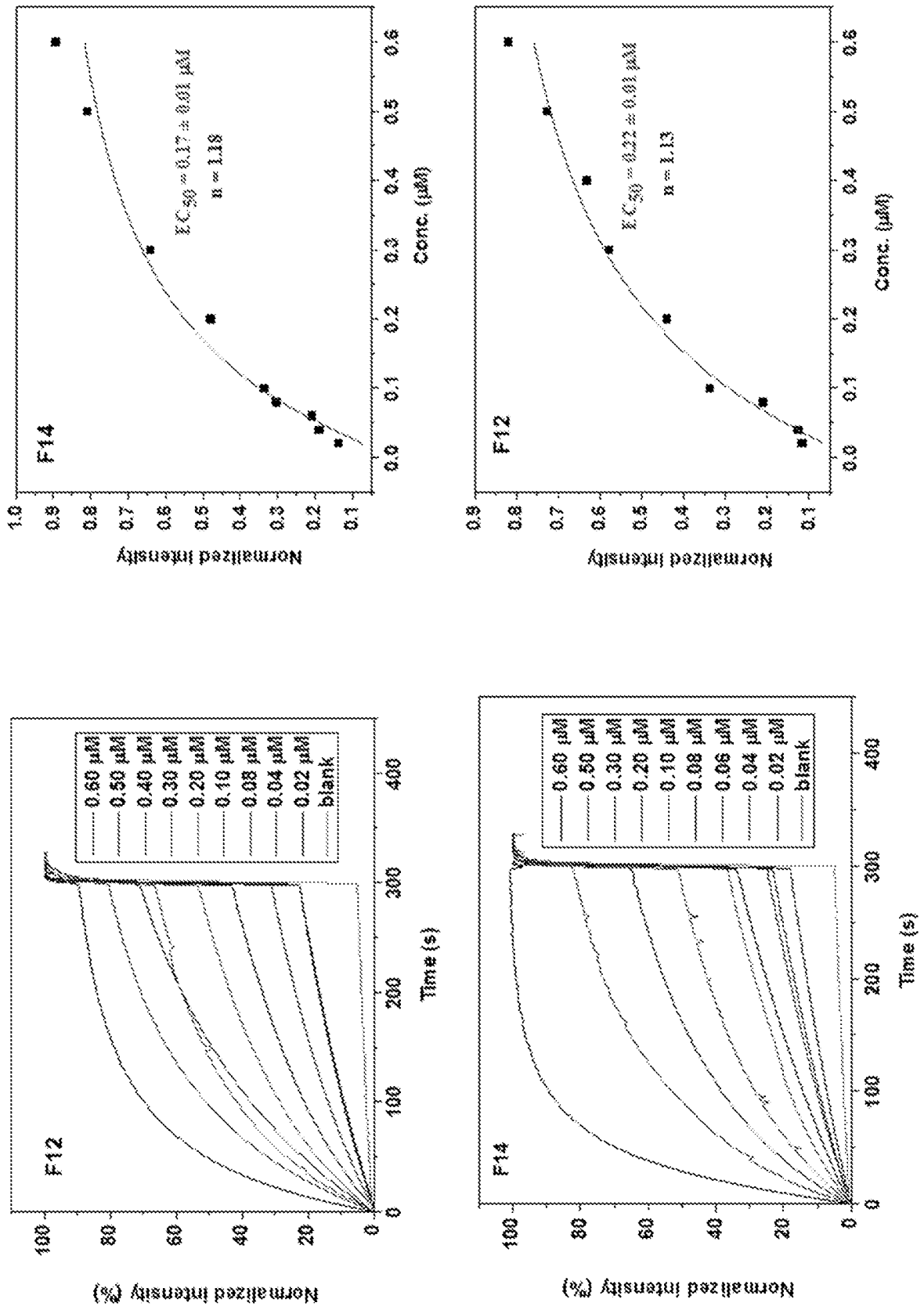
F14
EC_{50} = 0.17 ± 0.01 μM
n = 1.18
Normalized intensity
Conc. (μM)
F12
EC_{50} = 0.22 ± 0.01 μM
n = 1.13
Normalized intensity
Conc. (μM)
F12
0.60 μM
0.50 μM
0.40 μM
0.30 μM
0.20 μM
0.10 μM
0.08 μM
0.04 μM
0.02 μM
blank
Normalized intensity (%)
Time (s)
F14
0.60 μM
0.50 μM
0.30 μM
0.20 μM
0.10 μM
0.08 μM
0.06 μM
0.04 μM
0.02 μM
blank
Normalized intensity (%)
Time (s)

Figure 8 (end)

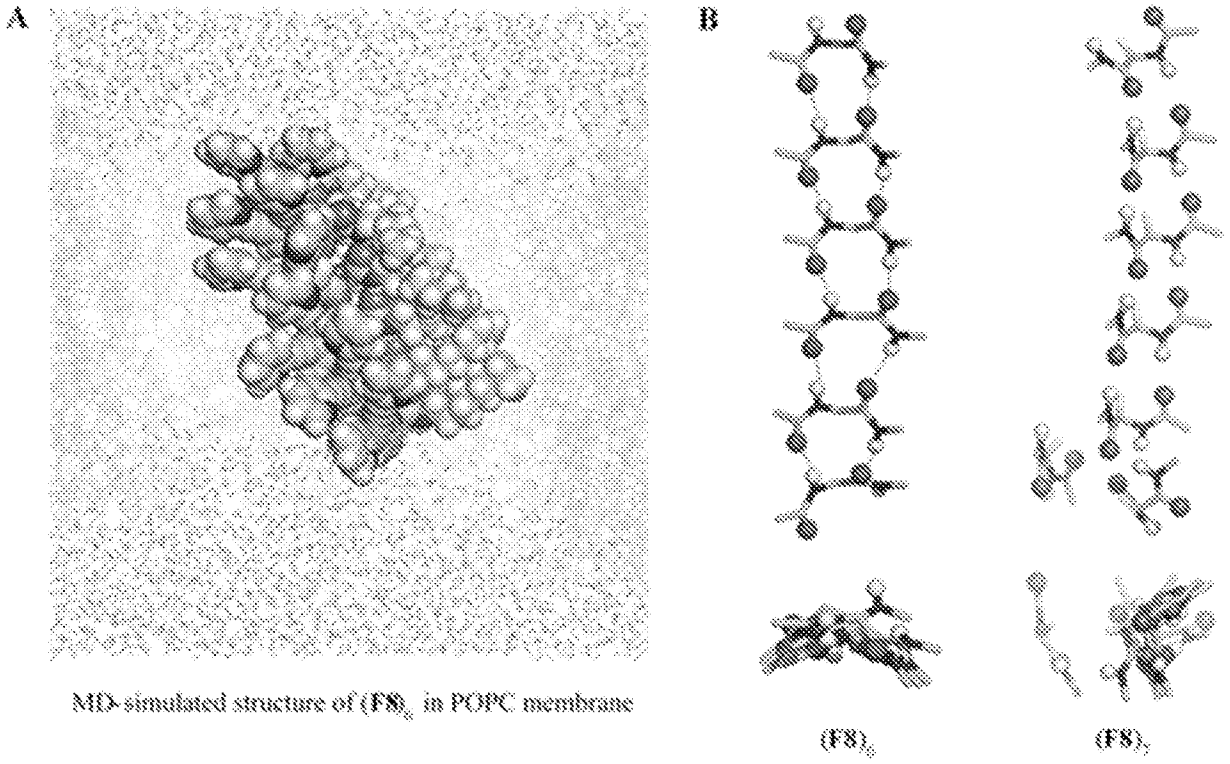
A
B
MD-simulated structure of (F8)8 in POPC membrane
(F8)8
(F8)7
C
Pt groups
Bifurcated pyridine groups
C8H17 groups
Top view of MD-simulated structure of (F8)8 in POPC membrane

Figure 9

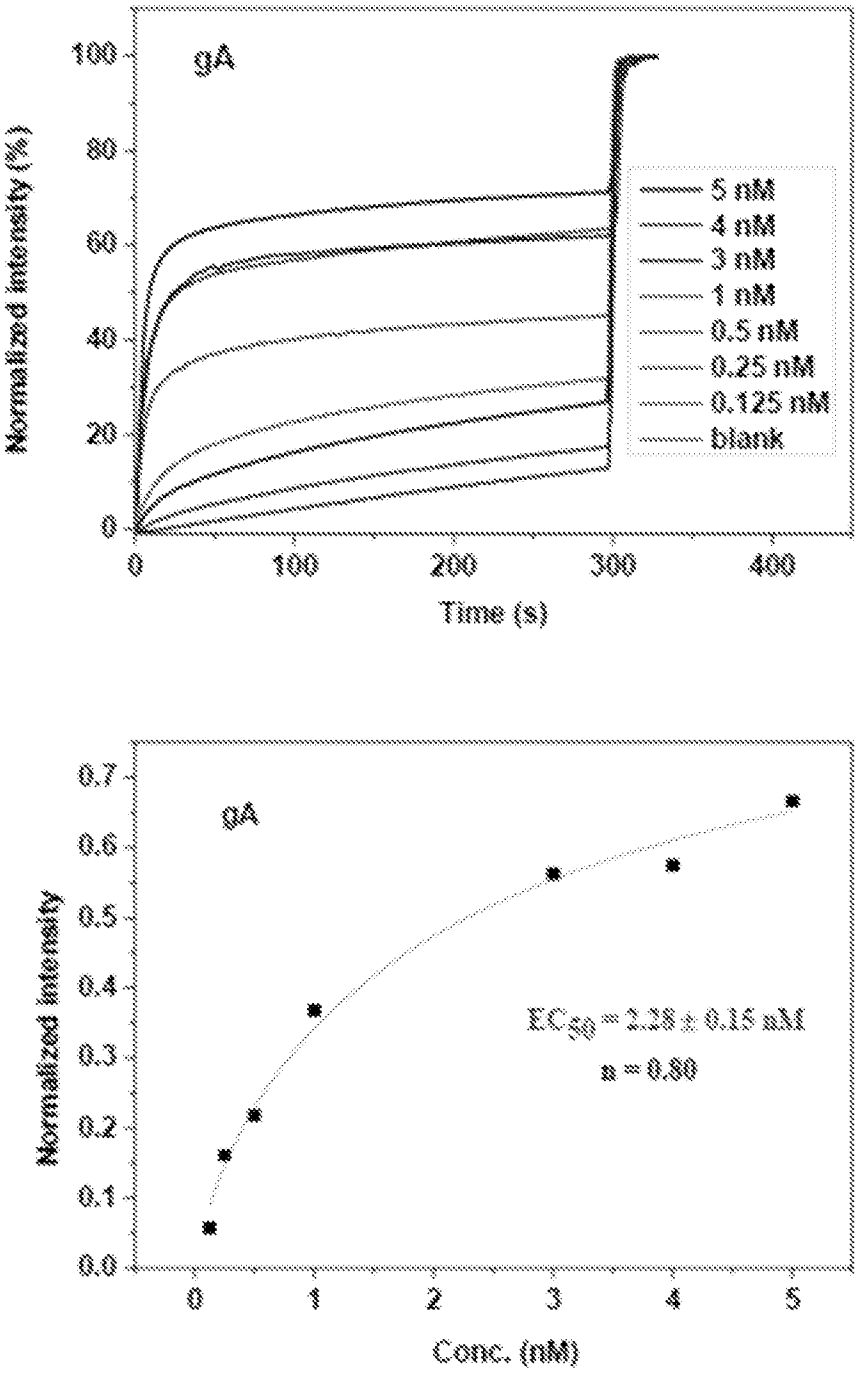
gA
Normalized intensity (%)
Time (s)
5 nM
4 nM
3 nM
1 nM
0.5 nM
0.25 nM
0.125 nM
blank
gA
Normalized intensity
Conc. (nM)
EC50 = 2.28 ± 0.15 nM
n = 0.80

Figure 10

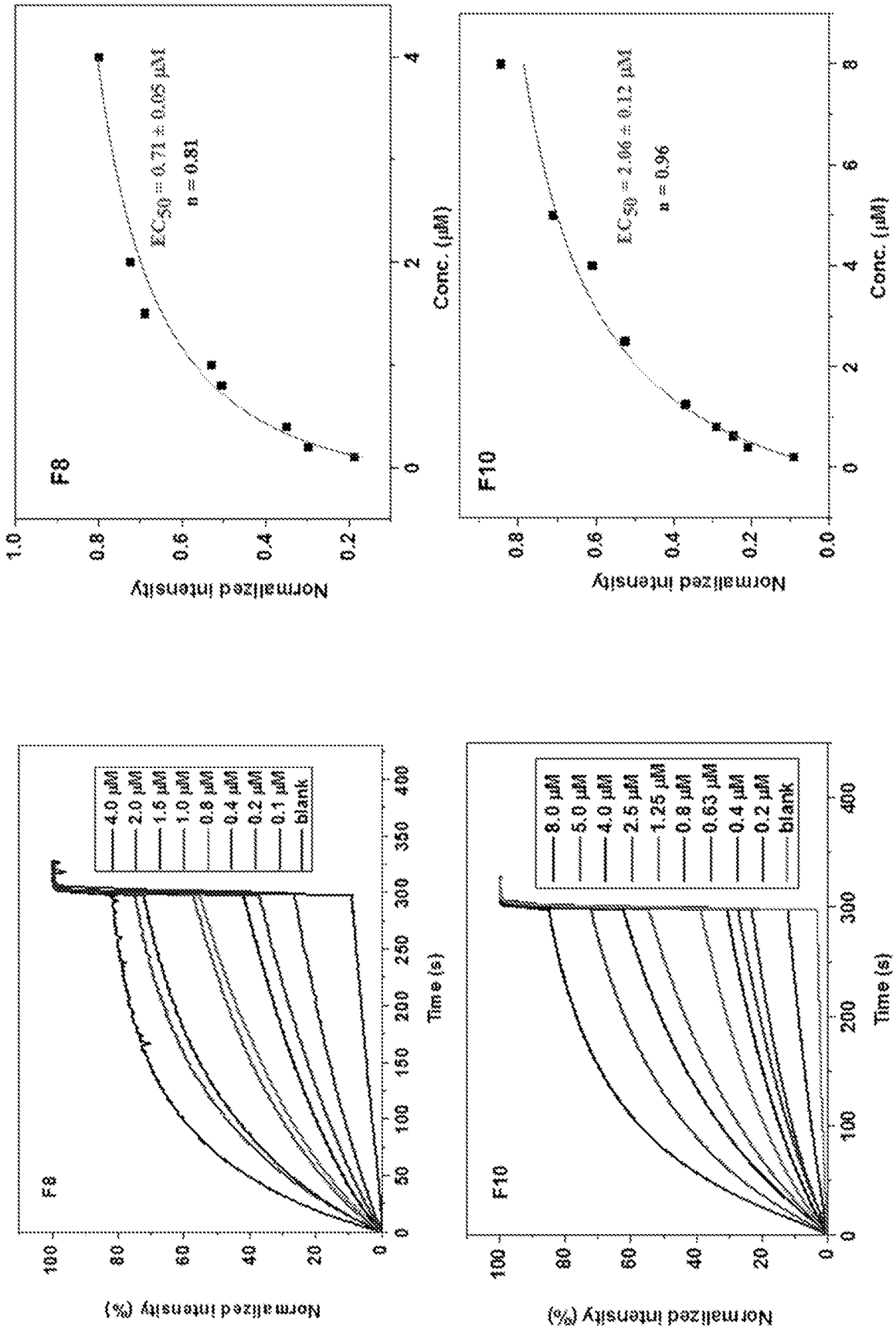

Figure 11 (continued)

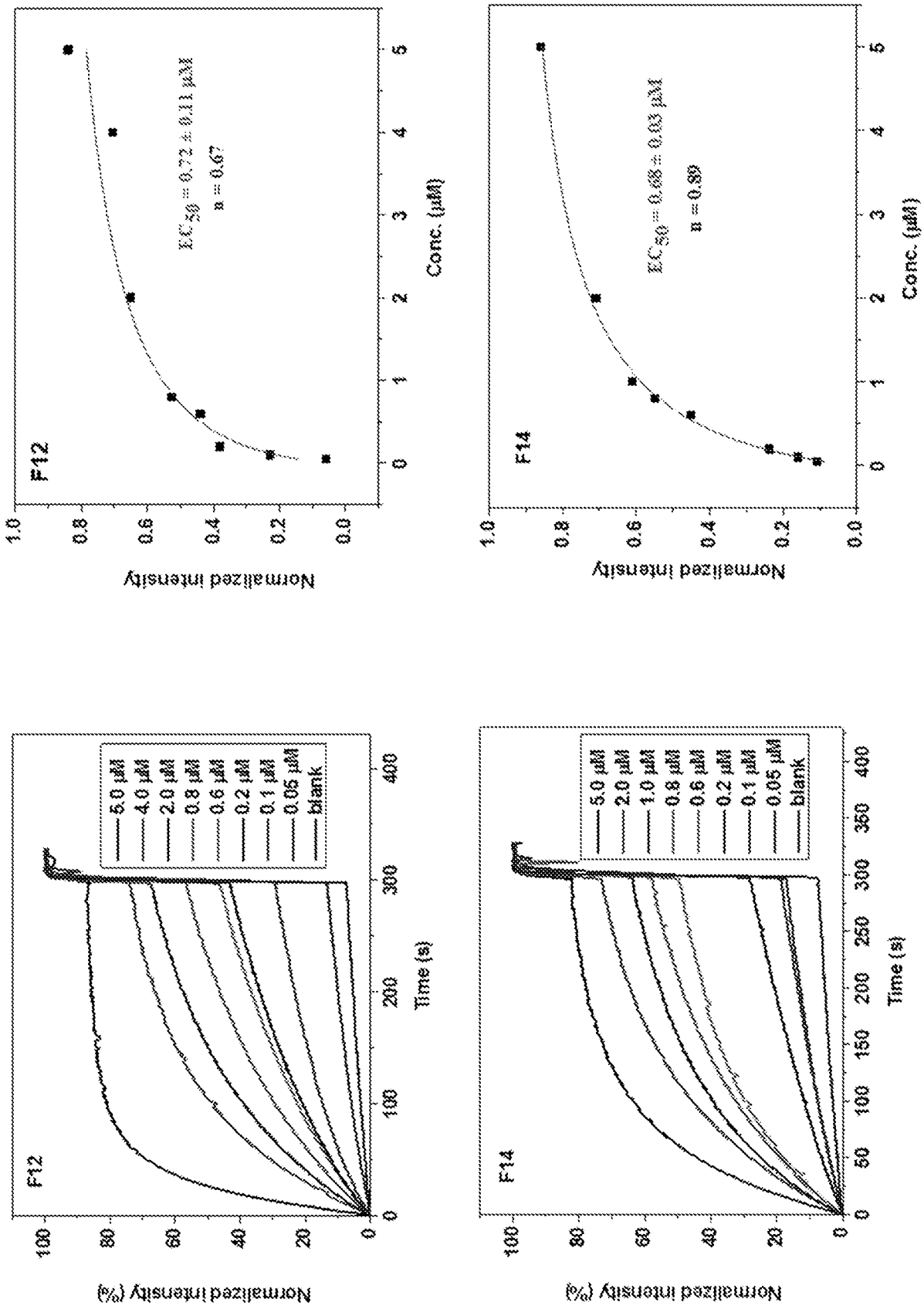

Figure 11 (end)

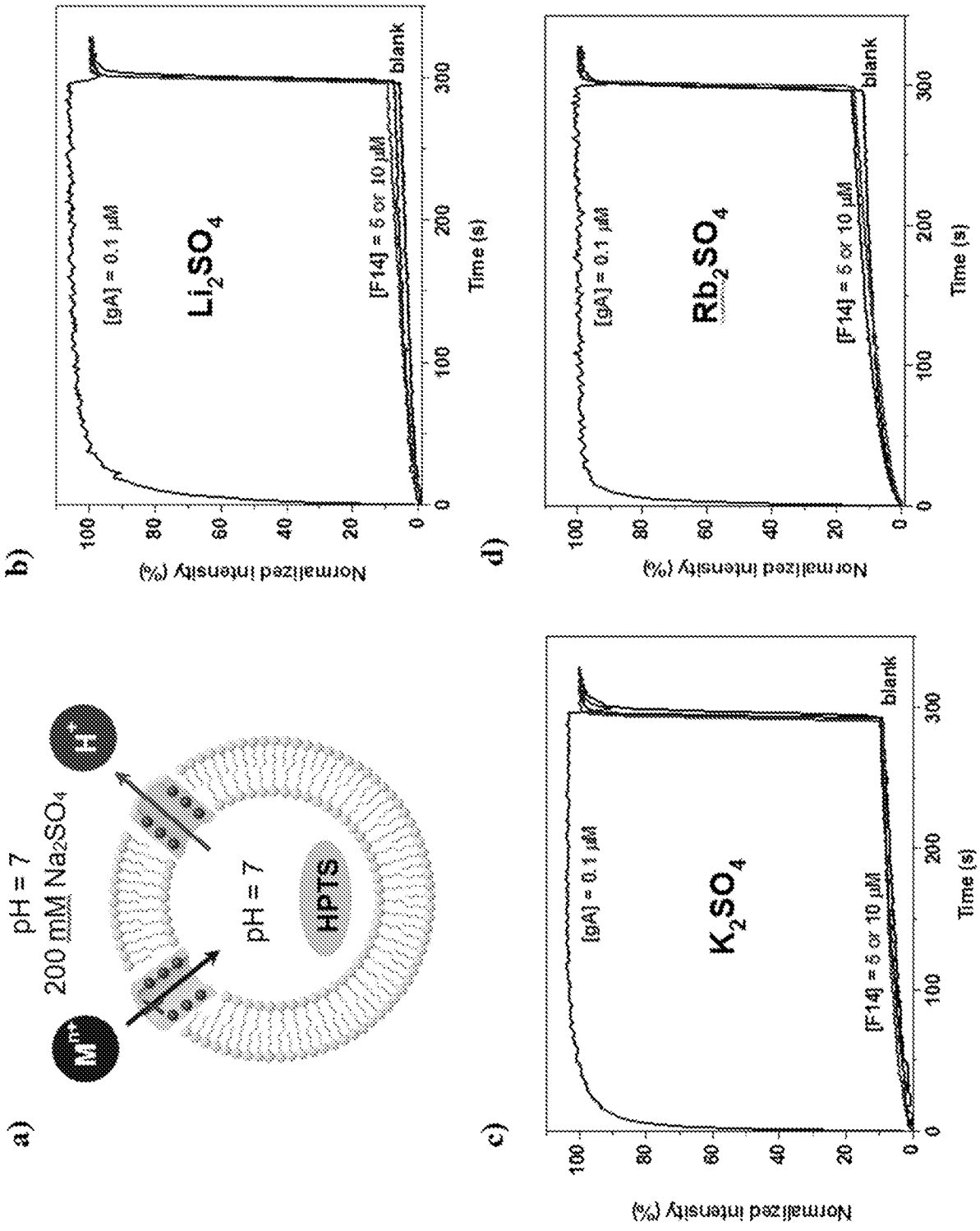

Figure 12 (continued)

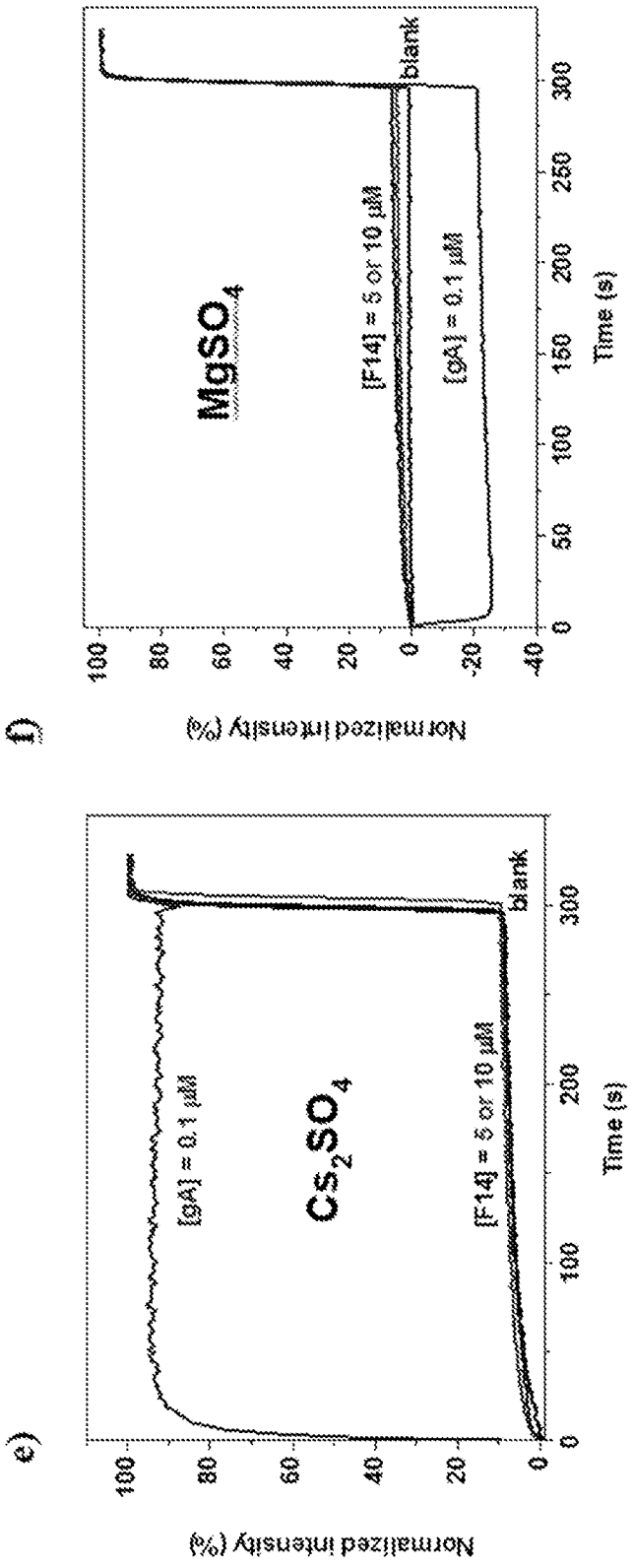

Figure 12 (end)

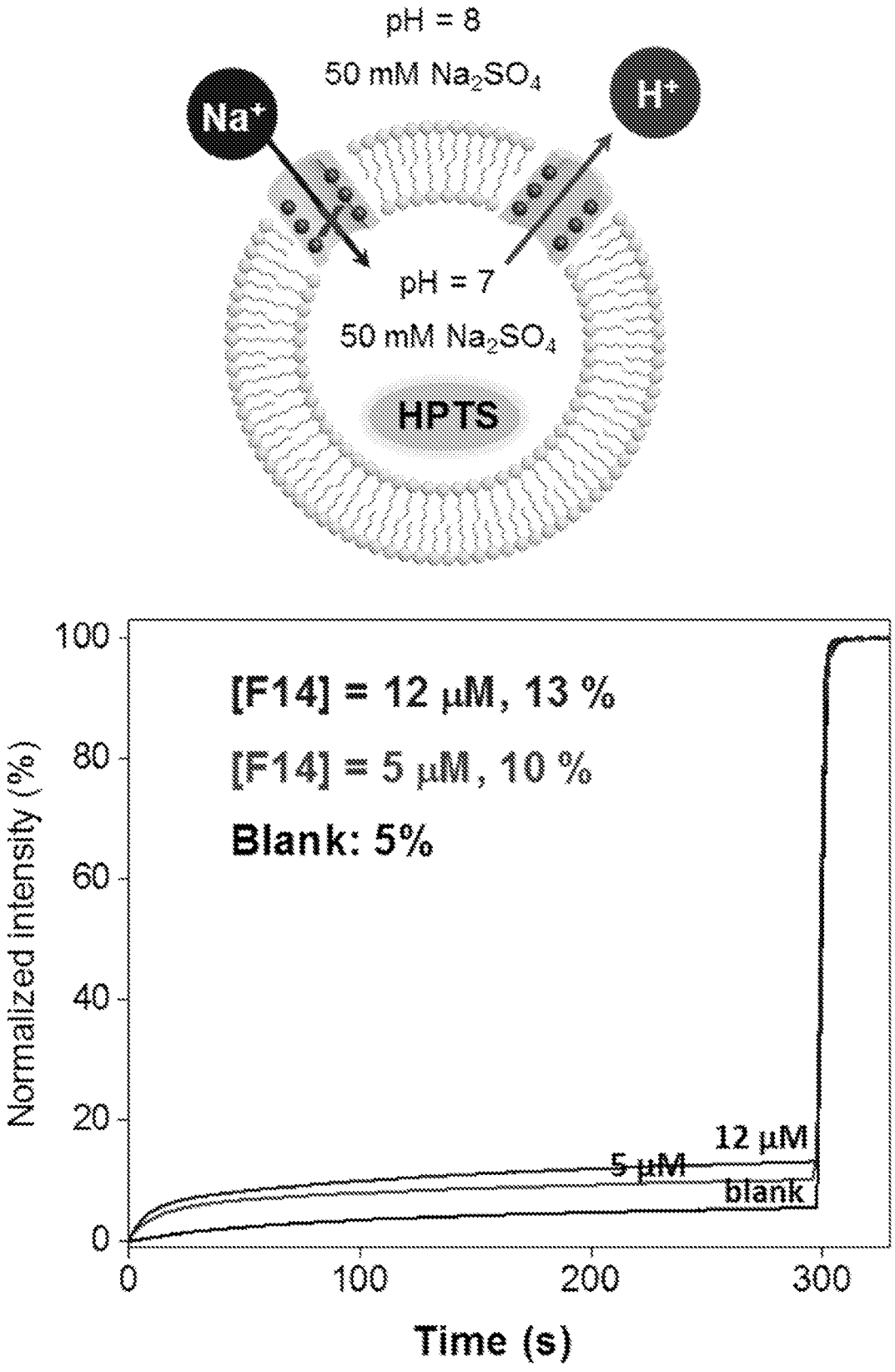
pH = 8
50 mM Na_2SO_4
Na^+
H^+
pH = 7
50 mM Na_2SO_4
HPTS
[F14] = 12 μM, 13 %
[F14] = 5 μM, 10 %
Blank: 5%
Normalized intensity (%)
100
80
60
40
20
0
12 μM
5 μM
blank
0
100
200
300
Time (s)

Figure 13

INTERNATIONAL SEARCH REPORT

International application No.
PCT/SG2020/050040

A. CLASSIFICATION OF SUBJECT MATTER

See Supplemental Box

According to International Patent Classification (IPC)

B. FIELDS SEARCHED

Minimum documentation searched (classification system followed by classification symbols)

C07D, C07K, A61K

Documentation searched other than minimum documentation to the extent that such documents are included in the fields searched

Electronic data base consulted during the international search (name of data base and, where practicable, search terms used)

CAPLUS, EMBASE, MEDLINE, BIOSIS: structural search based on claim 1, proton channel, hydrogen bond, self-assembly, cancer, and like terms

C. DOCUMENTS CONSIDERED TO BE RELEVANT

Category*	Citation of document, with indication, where appropriate, of the relevant passages	Relevant to claim No.
A	REN C., ET AL., A halogen bond-mediated highly active artificial chloride channel with high anticancer activity. *Chemical Science*, 15 March 2018, Vol. 9, No. 17, pages 4044-4051 [Retrieved on 2020-02-21] <DOI: 10.1039/C8SC00602D> Fig. 1	1-19
A	REN C., ET AL., Combinatorial Evolution of Fast-Conducting Highly Selective K^+-Channels via Modularly Tunable Directional Assembly of Crown Ethers. *Journal of the American Chemical Society*, 24 August 2017, Vol. 139, No. 36, pages 12338-12341 [Retrieved on 2020-02-21] <DOI: 10.1021/JACS.7B04335> Fig. 1	1-19
A	US 2005/0004212 A1 (WU M.-J., ET AL.) 6 January 2005 Compound 38, Table 3	--

☒ Further documents are listed in the continuation of Box C. ☒ See patent family annex.

*Special categories of cited documents:

"A" document defining the general state of the art which is not considered to be of particular relevance

"D" document cited by the applicant in the international application

"E" earlier application or patent but published on or after the international filing date

"L" document which may throw doubts on priority claim(s) or which is cited to establish the publication date of another citation or other special reason (as specified)

"O" document referring to an oral disclosure, use, exhibition or other means

"P" document published prior to the international filing date but later than the priority date claimed

"T" later document published after the international filing date or priority date and not in conflict with the application but cited to understand the principle or theory underlying the invention

"X" document of particular relevance; the claimed invention cannot be considered novel or cannot be considered to involve an inventive step when the document is taken alone

"Y" document of particular relevance; the claimed invention cannot be considered to involve an inventive step when the document is combined with one or more other such documents, such combination being obvious to a person skilled in the art

"&" document member of the same patent family

Date of the actual completion of the international search	Date of mailing of the international search report
14/02/2020 *(day/month/year)*	*09/03/2020* *(day/month/year)*

Name and mailing address of the ISA/SG

IPOS INTELLECTUAL PROPERTY OFFICE OF SINGAPORE

Intellectual Property Office of Singapore
1 Paya Lebar Link, #11-03
PLQ 1, Paya Lebar Quarter
Singapore 408533

Email: pct@ipos.gov.sg

Authorized officer

Cao Ye (Dr)

IPOS Customer Service Tel. No.: (+65) 6339 8616

INTERNATIONAL SEARCH REPORT

International application No.
PCT/SG2020/050040

C (Continuation). DOCUMENTS CONSIDERED TO BE RELEVANT

Category*	Citation of document, with indication, where appropriate, of the relevant passages	Relevant to claim No.
A	BOSCH E., ET AL., Synthesis of a New Tetrapyridyl Ligand and the Characterization of Three Distinct Metal- and Hydrogen-Bonding Conformations. *Crystal Growth & Design*, 23 January 2003, Vol. 3, No. 2, pages 263-266 [Retrieved on 2020-02-21] <DOI: 10.1021/CG0255974> Whole document	--
A	WANG Z., ET AL., Multidirectional proton-conducting membrane based on sulfonated big π-conjugated monomer into block copoly(ether sulfone)s. *Polymer*, 21 November 2018, Vol. 160, pages 138-147 [Retrieved on 2020-02-21] <DOI: 10.1016/J.POLYMER.2018.11.033> Fig. 1	--

INTERNATIONAL SEARCH REPORT

International application No.
PCT/SG2020/050040

Supplemental Box
(Classification of Subject Matter)

Int. Cl.
C07D 213/56 (2006.01)
C07K 5/06 (2006.01)
C07K 5/08 (2006.01)
A61K 31/4402 (2006.01)
A61K 38/05 (2006.01)
A61K 38/06 (2006.01)
A61P 35/00 (2006.01)

INTERNATIONAL SEARCH REPORT
Information on patent family members

International application No.
PCT/SG2020/050040

Note: This Annex lists known patent family members relating to the patent documents cited in this International Search Report. This Authority is in no way liable for these particulars which are merely given for the purpose of information.

Patent document cited in search report	Publication date	Patent family member(s)	Publication date
US 2005/0004212 A1	06/01/2005	NONE	